Understanding salinity tolerance of a bread wheat landrace Mocho de Espiga Branca

Chana
M.Sc. Plant Science

A thesis submitted for the degree of
Doctor of Philosophy

Faculty of Sciences
School of Agriculture, Food and Wine
The University of Adelaide

THE UNIVERSITY of ADELAIDE

November 2019

Table of Contents

Table of Contents ..... **i**
List of Figures ..... **iii**
List of Tables ..... **v**
List of Abbreviations ..... **vi**
List of Publications ..... **ix**
List of Conference Presentations ..... **ix**
List of Awards ..... **x**
Abstract ..... **xi**
Declaration ..... **xiii**
Acknowledgements ..... **xiv**
Chapter 1 - Literature review and research aims **1**
Literature review 2
Research aims 13
References 14
Chapter 2 - *TaHKT1;5-D*: Switching a T to C makes bread wheat salty **23**
Abstract 29
Introduction 30
Results 32
Discussion 37
Online Methods 41
Data availability statement 51
Acknowledgments 51
Author Contributions 52
Competing Interest 52
References 53
Figures 58
Supplementary Figures 66
Supplementary Tables 71
Chapter 3 - Identifying the genetic control of salinity tolerance in a bread wheat landrace Mocho de Espiga Branca **75**
Abstract 80
Introduction 81
Materials and Methods 83
Results 88
Discussion 93

Conflict of Interest 98
Author Contributions 98
Acknowledgments 98
References 99
Figures 109
Tables 112
Supplementary Figures 124
Supplementary Tables 130
Appendix Files 130
Chapter 4 - Understanding the role of five known compatible solutes in salinity tolerance of a bread wheat landrace Mocho de Espiga Branca 131
Abstract 135
Introduction 136
Materials and methods 138
Results 143
Discussion 147
Acknowledgments 152
Author Contributions 152
References 153
Figures 157
Tables 161
Supplementary Figures 163
Chapter 5 - General discussion 165
Review of thesis aims 166
Summary of the main findings 167
Implications of thesis findings 167
Future directions 174
Concluding remarks 176
References 177

List of Figures

Chapter 1 - Literature review and research aims……..……..... 1

Figure 1: Salinity impacts on the growth rate of a cereal plant……. 3

Figure 2: Several known transporters or channels putatively involved in Na^+ transport in the shoot or root in the glycophytic plants..... 8

Figure 3: Salinity tolerance of various plant species..... 11

Chapter 2 - *TaHKT1;5-D*: Switching a T to C makes bread wheat salty……... 23

Fig. 1: Salinity tolerance and 4th leaf Na^+ concentration of Mocho de Espiga Branca relative to 72 bread wheat diversity lines and Gladius and Scout…….....…… 58

Fig. 2: Na^+ concentration in the 4th leaf blade, sheath, and roots of Mocho de Espiga Branca, Gladius and Scout in hydroponics…….....…… 59

Fig. 3: A SNP in Mocho de Espiga Branca *TaHKT1;5-D* results in a L190P amino acid residue variation in the Na^+ transporter TaHKT1;5-D……..…….. 60

Fig. 4: The physiological characterisation of L190P variation in TaHKT1;5-D and the evaluation of the xylem sap Na^+ concentration in Mocho de Espiga Branca…….…. 62

Fig. 5: Ion fluxes measured at the root elongation zone after removal from 100 mM NaCl……..…….…… 64

Fig. 6: Ion transport model for Mocho de Espiga Branca and Gladius plants under NaCl stress……..... 65

Supplementary Fig. 1: Plant biomass and salinity tolerance of plants in relation to their 4th leaf Na^+ concentration in Mocho de Espiga Branca and Gladius and Scout in a hydroponic system with 0, 150 and 200 mM NaCl concentrations……. 66

Supplementary Fig. 2: K^+ and Cl^- concentrations in the 4th leaf blade, sheath, and roots of Mocho de Espiga Branca, Gladius and Scout in a hydroponic system…… 67

Supplementary Fig. 3: Expression of *TaHKT1;5-D* in the root tissue and CAPS marker tsl2SALTY-4D genotyping of Mocho de Espiga Branca, Gladius and Scout……..... 68

Supplementary Fig. 4: Xylem sap K^+ and Cl^- concentration of Mocho de Espiga Branca and Gladius under 0 and 150 mM NaCl concentrations…….. 69

Supplementary Fig. 5: Ion fluxes measured at root mature zone after a sudden exposure to 100 mM NaCl concentration……... 70

Chapter 3 - Identifying the genetic control of salinity tolerance in a bread wheat landrace Mocho de Espiga Branca……..... 75

Figure 1: Visual representation of the genetic linkage map of the F_2 Mocho de Espiga Branca × Gladius population showing the chromosomes and the genetic distance (cM)……. 109

Figure 2: QTL positions detected in composite interval mapping for salinity tolerance traits in the Mocho de Espiga Branca × Gladius F_2 population…… 110
Figure 3: Frequency distribution of the F_2 population for the salinity tolerance sub-traits…….. 111
Supplementary Figure 1: Plant growth response before and after 150 mM NaCl treatment……...…… 124
Supplementary Figure 2: The genotyping of Mocho de Espiga Branca × Gladius F_2 population using the tsl2SALTY-4D marker and the allele segregation for the 4th leaf Na^+ concentration....…….…. 126
Supplementary Figure 3: Frequency distribution of the F_2 population of Mocho de Espiga Branca × Gladius for the 4th leaf ion concentrations (mM)…… 127
Supplementary Figure 4: Frequency distribution of the F_2 population for the smoothed projected shoot area (PSA), smoothed absolute growth rate (AGR) and smoothed relative growth rate (RGR)……. 128
Chapter 4 - Understanding the role of five known compatible solutes in salinity tissue tolerance of Mocho de Espiga Branca……..131
Figure 1: Shoot and root biomass of Mocho de Espiga Branca, Gladius and Scout at 0 and 150 mM NaCl....…… 157
Figure 2: Ion concentrations of the 4th leaf and root from Mocho de Espiga Branca, Gladius and Scout at 0 and 150 mM NaCl……. 158
Figure 3: The 4th leaf organic solutes concentration in Mocho de Espiga Branca, Gladius and Scout at 0 and 150 mM NaCl....……... 159
Figure 4: Osmolality of the 4th leaf sap in Mocho de Espiga Branca, Gladius and Scout at 0 and 150 mM NaCl....…….…….. 160
Supplementary Figure 1: Separation of a mixed standard solution containing glycine betaine, proline, sucrose, fructose, glucose, sorbitol and mannitol....…… 163

List of Tables

Chapter 2 - *TaHKT1;5-D*: Switching a T to C makes bread wheat salty…….. 23

Supplementary Table 1: Screening of 75 bread wheat lines for salinity tolerance…….. 71

Supplementary Table 2: Genotyping of Mocho de Espiga Branca, Gladius, Scout and 68 bread wheat diversity lines for the SNP (T/C) resulting in TaHKT1;5-D L190P variation using the CAPS marker tsl2SALTY-4D designed for the SNP…….. 73

Supplementary Table 3: Primers used for *TaHKT1;5-D* coding sequence amplification and sequencing……..…. 74

Chapter 3 - Identifying the genetic control of salinity tolerance in a bread wheat landrace Mocho de Espiga Branca…… 75

Table 1: Summary table of the genetic linkage map constructed for the Mocho de Espiga Branca × Gladius F_2 population……..... 112

Table 2: The mean ± SEM of the parents Mocho de Espiga Branca and Gladius, and range of the F_2 population (min-max) for plant growth and 4th leaf ion concentration……..... 113

Table 3: QTL detected for plant growth and 4th leaf ion concentration in the Mocho de Espiga Branca × Gladius F_2 population using composite interval mapping with 1000 permutation at $p \leq 0.05$…….. 114

Table 4: Significant marker ($p \leq 0.001$) intervals detected for plant growth and 4th leaf ion concentration in the Mocho de Espiga Branca × Gladius F_2 population using single marker analysis…….…. 115

Table 5: List of potential candidate genes (gene ID and gene name) for each QTL detected in CIM……... 116

Table 6: List of potential candidate genes (gene ID and gene name) within the significant marker ($p \leq 0.001$) intervals detected in SMA……... 119

Supplementary Table 1: The mean ± SEM of the parent Mocho de Espiga Branca and Gladius, and the range of the F_2 population (min-max) for 4th leaf ion concentration……. 130

Chapter 4 - Understanding the role of five known compatible solutes in salinity tissue tolerance of Mocho de Espiga Branca……..131

Table 1: Osmotic potential (ψ_π) of leaf sap and the selected solutes at 0 and 150 mM NaCl treatment……..… 161

Table 2: Estimated contributions of the selected solute to the leaf sap $\psi_{\pi\text{-sap}}$ at 0 and 150 mM NaCl……... 162

List of Abbreviations

3'	three prime, of nucleic acid sequence
5'	five prime, of nucleic acid sequence
~	approximately
°C	degree Celsius
Å	Angstrom
ACPFG	Australian Centre for Plant Functional Genomics
AGR	absolute growth rate
AGRF	Australian Genome Research Facility
ANOVA	analysis of variance
APPF	Australian Plant Phenomics Facility
ARC	Australian Research Council
ATP	adenosine triphosphate
bp	base pairs, of nucleic acid
BSM	basal salt medium
CAPS	cleaved amplified polymorphic sequence
CBL	calcineurin B-like protein
cDNA	complementary deoxyribonucleic acid
CDPK	calcium dependent protein kinase
CHX	cation proton antiporter
CIM	composite interval mapping
CIPK	CBL-interacting protein kinase
CLC-c	chloride channel C
cm	centimetre(s)
cM	centimorgan
CRISPR	clustered regularly interspaced short palindromic repeats
CSIRO	Commonwealth Scientific and Industrial Research Organisation
CSS	Chromosome Survey Sequence
cv.	cultivar
d	day(s)
DAP	days after planting
DAWN	Diversity Among Wheat Genome
df	degrees of freedom
DH	doubled haploid
DNA	deoxyribonucleic acid
dS	deciSiemens
DW	dry weight
ECe	electrical conductivity of a soil extract
EDTA	ethylenediaminetetraacetic acid
EDX	energy-dispersive X-ray microanalysis
EMS	ethyl methane sulphonate
F_2	second filial generation
FAO	Food and Agricultural Organization of the United Nations
FAOSTAT	Food and Agricultural Organization of the United Nations Statistics
FW	Fresh weight
g	gram(s)
g/g	gram per gram
GBS	genotyping by sequencing
GC-MS	gas chromatography–mass spectrometry
gDNA	genomic deoxyribonucleic acid
GFP	green fluorescent protein
GL mix	Goldilocks soil mix
GMO	genetically modified organisms

GRDC	Grain Research and Development Corporation
GWAS	Genome Wide Association study
h	hour(s)
H^+-ATPase	proton-pumping pyrophosphatase
ha	hectare
HKT	High-Affinity Potassium Transporter
HPLC	High-Performance Liquid Chromatography
IWGSC	International Wheat Genome Sequencing Consortium
K	degree Kelvin
KASP™	Kompetitive Allele Specific PCR
kg	kilograms(s)
L	litre(s)
LC-MS	Liquid Chromatography–Mass Spectrometry
LOD	Logarithm of odds
M	molar(s)
mg	milligram(s)
MIFE	Microelectrode Ion Flux Estimation
min	minute(s)
MIPS	Munich Information Center for Protein Sequences (MIPS)
mL	millilitre(s)
mm	millimetre(s)
mM	milliMolar(s)
mmol	millimole(s)
mOsmol/kg	milliosmoles per kilogram
MPa	megaPascal(s)
mV	millivolt
MΩ	megaohm
n	sample size
Nax	sodium exclusion loci
NCRIS	National Collaborative Research Infrastructure Strategy
NGS	Next Generation Sequencing
NHX	sodium hydrogen exchanger
NILs	near isogenic lines
nm	nanometre(s)
nmol	nanomole(s)
OST	osmotic tolerance
p	probability
PCA	perchloric acid
PCR	polymerase chain reaction
PDA	photodiode array detector
pH	power of hydrogen
PM	plasma membrane
POTAGE	PopSeq Ordered *Triticum aestivum* Gene Expression
PSA	projected shoot area
QTL	quantitative trait loci
RFP	red fluorescent protein
RGB	red-green-blue
RGR	relative growth rate
Rht	reduced height loci
RILs	recombinant inbred lines
RNA	ribonucleic acid
RNAi	ribonucleic acid interference
RO	reverse osmosis
ROS	reactive oxygen species

s	second(s)
SA	South Australia
SAHMRI	South Australian Health and Medical Research Institute
SEM	standard error of the mean
SKOR	potassium outwardly rectifying channel
SMA	single marker analysis
SNP	single nucleotide polymorphism
t	tonne(s)
T_3	3rd progeny of primary transformant
TALEN	transcription activator-like effector-based nucleases
TEVC	two-electrode voltage clamping
TILLING	Targeting Induced Local Lesions IN Genomes
TPA	The Plant Accelerator
TUE	transpiration use efficiency
µg	microgram(s)
µL	microlitre(s)
µM	micromolar(s)
µmol	micromole(s)
UC mix	University of California soil mix (1:1 peat:sand)
UV	ultraviolet light
V	volt
v/v	volume per volume
w/v	weight per volume
w/w	weight per weight
ψ_π	osmotic potential

List of Publications

Borjigin C, Schilling RK, Bose J, Hrmova M, Qiu J, Wege S, Situmorang A, Brien C, Berger B, Gilliham M, Pearson AS and Roy SJ. *TaHKT1;5-D*: Switching a T to C makes bread wheat salty. Submitted to Nature Plants.

List of Conference Presentations

Poster Presentations

Borjigin C, Schilling RK, Qiu J, Bose J, Sanchez-Ferrero JC, Eckermann PJ, Watson-Haigh NS, Baumann U, Pearson AS and Roy SJ. 6th - 7th June 2018. Understanding sodium tissue tolerance in a bread wheat landrace Mocho de Espiga Branca. Poster presentation at the Gordon Research Conference on Salt and Water Stress in Plants, Waterville Valley, NH, USA

Borjigin C, Schilling RK, Qiu J, Bose J, Sanchez-Ferrero JC, Eckermann PJ, Watson-Haigh NS, Baumann U, Pearson AS and Roy SJ. 3rd June 2018. Understanding sodium tissue tolerance in a bread wheat landrace Mocho de Espiga Branca. Poster presentation at the Gordon Research Seminar on Salt and Water Stress in Plants, Waterville Valley, NH, USA

Borjigin C, Schilling RK, Pearson AS and Roy SJ. 4th October 2017. Identification of novel loci and genes for salinity tissue tolerance in a bread wheat landrace Mocho de Espiga Branca. Poster presentation at ComBio2017, Adelaide Convention Centre, Adelaide, Australia

List of Awards

The Plant Nutrition Trust Travel Award (2018)

Awarded to promising students and early-career scientists working in the area of plant mineral nutrition, soil fertility, fertiliser and soil amendment technologies and other related topics in agronomy and plant breeding to conduct a study-tour or to attend a conference or such other activities to the stated objectives

Research Travel Scholarship (2018)

Awarded to student enrolled in a higher degree by research program at the University of Adelaide to support research travel both in Australia and overseas for current HDR students.

Global Learning Travel Grant (2018)

Awarded to students at the University of Adelaide to complete a short program overseas, including an internship which is contributing to the requirements of the students' degree.

ASPS Student Poster Award (2017)

Awarded by the Australian Society of Plant Scientists (ASPS) to the poster titled Identification of novel loci and genes for salinity tissue tolerance in a bread wheat landrace Mocho de Espiga Branca presented at ComBio2017 conference held at Adelaide Convention Centre, Adelaide, Australia.

Abstract

Salinity is one of the major abiotic stresses severely affecting cereal crop yields worldwide. Improving salinity tolerance of the most widely cultivated cereal, bread wheat (*Triticum aestivum* L.), is essential to increase grain yields on saline agricultural lands. Shoot sodium (Na^+) exclusion is often reported as a major salinity tolerance mechanism in bread wheat. This process enables plants to reduce root-to-shoot Na^+ transport by retrieving Na^+ from the xylem and prevent toxic concentrations of Na^+ from accumulating in the shoot. However, a Portuguese bread wheat landrace Mocho de Espiga Branca was recently identified with up to 10× higher leaf Na^+ concentrations and yet maintained similar salinity tolerance compared to other bread wheat cultivars.

The first focus of this PhD study was to understand how Mocho de Espiga Branca accumulates high concentrations of Na^+ in the leaf compared to Gladius and Scout under salinity. DNA sequencing of a major Na^+ exclusion gene *TaHKT1;5-D* revealed that a naturally occurring single nucleotide substitution resulted in a L190P amino acid residue change. This variation was found to disrupt the capability of TaHKT1;5-D to retrieve Na^+ from the xylem and hence causing the high leaf Na^+ accumulation in Mocho de Espiga Branca. A CAPS marker was developed to enable plant breeders to select for this allele in bread wheat.

The second focus of this study was to identify novel genetic loci linked to salinity tolerance of Mocho de Espiga Branca. 19 salinity tolerance sub-traits were phenotyped in an F_2 population derived from Mocho de Espiga Branca and Gladius for quantitative trait loci (QTL) analysis. Genomic regions significantly associated with salinity tolerance were detected on chromosomes 1A, 1D, 4A, 4B and 5A for the sub-traits of plant growth, and on chromosome 2A, 2B, 4D and 5D for Na^+, potassium (K^+) and chloride (Cl^-) accumulation. A number of candidate genes that encode proteins associated with plant salinity tolerance were identified. These include Na^+/H^+ antiporters, K^+ channels, Na^+/calcium (Ca^{2+}) transporter, H^+-ATPase, calcineurin B-like proteins (CBLs) and CBL-interacting protein kinases (CIPKs).

The third focus of this study was to investigate whether any difference(s) in accumulation of five known compatible solutes (glycine betaine, proline, sucrose, glucose and fructose) associated with osmotic adjustment were present in Mocho de Espiga Branca compared to Gladius and Scout under salinity. The concentrations of the detected compatible solutes in Mocho de Espiga Branca were found to respond similarly compared to Gladius and Scout in response to salinity, suggesting these organic solutes are not contributing to the ability of

Mocho de Espiga Branca to maintain growth while accumulating high concentration of leaf Na^+ salinity.

Overall, in this PhD study, a SNP linked to impairment of the Na^+ transporter TaHKT1;5-D was identified and shown to be responsible for the increased shoot Na^+ concentration in Mocho de Espiga Branca. The findings highlight the importance of other mechanisms that are independent from Na^+ exclusion in salinity tolerance of bread wheat and the need to investigate these further in the future.

Declaration

I certify that this work contains no material which has been accepted for the award of any other degree or diploma in my name, in any university or other tertiary institution and, to the best of my knowledge and belief, contains no material previously published or written by another person, except where due reference has been made in the text. In addition, I certify that no part of this work will, in the future, be used in a submission in my name, for any other degree or diploma in any university or other tertiary institution without the prior approval of the University of Adelaide and where applicable, any partner institution responsible for the joint-award of this degree.

I acknowledge that copyright of published works contained within this thesis resides with the copyright holder(s) of those works.

I also give permission for the digital version of my thesis to be made available on the web, via the University's digital research repository, the Library Search and also through web search engines, unless permission has been granted by the University to restrict access for a period of time.

Chana

Signature: _ _ Date: 15/11/2019

Acknowledgements

First and foremost, I would like to express the deepest appreciation to my supervisors Associate Professor. Stuart Roy, Dr. Allison Pearson and Dr. Rhiannon Schilling for being fantastic supervisors, and for all their continued guidance, advice, input, encouragement and support throughout my PhD. I would like to thank my independent advisor Dr. Caitlin Byrt for her advice and help during my candidature. I would also like to thank Professor Timothy Colmer at the University of Western Australia and Professor Matthew Gilliham for their constructive advice towards my experimental designs.

I would like to acknowledge the financial support of a postgraduate scholarship jointly offered by the University of Adelaide and the China Scholarship Council (CSC). I would like to thank the Grain Research and Development Corporation (GRDC) and the International Wheat Yield Partnership (IWYP) for funding this PhD project, and the University of Adelaide, the Australian Centre for Plant Functional Genomics (ACPFG), the Australian Plant Phenomics Facility (APPF) and the University of Western Australia for providing research facilities and resources to carry out my PhD study. I would like to thank the Research Travel Scholarship and the Global Learning Travel Grant at the University of Adelaide and The Plant Nutrition Trust for offering travel grants to attend conferences.

My sincere thanks go to all wonderful people who have provided endless help and support throughout my PhD. Thank you to all past and present members of the Salt Focus Group, Ms. Melissa Pickering, Ms. Jodie Kretschmer, Ms. Laura short, Ms. Christine Tritterman, Mr. William Heaslip, Dr. Muhammad Ahsan Asif, Dr. Daniel Menadue, Dr. Yogendra Kalenahalli and Dr. Takashi Okada. Thank you all for your support and friendship.

Finally, I would like to thank my husband Enhemend and my family and friends for their unconditional love and support throughout my PhD candidature.

Chapter 1 - Literature review and research aims

Literature review

Salinity is a major abiotic stress

Soil salinity is a major abiotic stress reducing cereal crop growth and yield (Flowers 2004; Colmer *et al.* 2005; Munns and Tester 2008; Roy *et al.* 2014; Munns and Gilliham 2015; Hanin *et al.* 2016; Ismail and Horie 2017; Negrão *et al.* 2017; Munns *et al.* 2019a; Tyerman *et al.* 2019). Soil with an electrical conductivity (EC_e) of 4 dS/m (or 40 mM of NaCl) is generally considered saline (United States Salinity Laboratory Staff 1954; Munns and Tester 2008; Wicke *et al.* 2011; Munns *et al.* 2019a). More than 800 million hectares (ha) of the total land is salt-affected, which includes 45 million ha of irrigated and 32 million ha of dryland agricultural land (FAO 2019a). In Australia, the estimated land affected by salt is approximately 5.7 million ha with 16% of the total dryland agricultural region affected by groundwater induced salinity and estimated to cost $300 million per year (Rengasamy 2002). This area of salt affected land is predicted to triple by the year 2050 due to land clearing for agricultural purposes, low-quality water irrigation and inadequate drainage after irrigation (Rengasamy 2002).

Impact of salinity on cereal plants

Plants can be divided into two groups based on their tolerance to salinity (1) halophytes: plants that require salt for optimal growth and (2) glycophytes: plants that are sensitive to salinity (Greenway and Munns 1980; Flowers and Colmer 2008; Shabala and Mackay 2011; Shabala 2013). Halophytes often require salt to maintain their growth, whereas glycophytes are likely to have reduced growth and yield when exposed to salt (Flowers and Colmer 2008; Plett and Møller 2010; Shabala and Mackay 2011; Shabala 2013). Most cereals, such as bread wheat (*Triticum aestivum* L.), barley (*Hordeum vulgare* L.) and rice (*Oryza sativa* L.), are glycophytes and the impact of salinity on the growth of these cereal plants is known to occur in two distinct phases: shoot-ion independent phase (also referred to as osmotic stress); and shoot-ion dependant phase (also referred to as ionic stress) (Figure 1) (Munns and Tester 2008; Roy et al. 2014; Alqahtani et al. 2019).

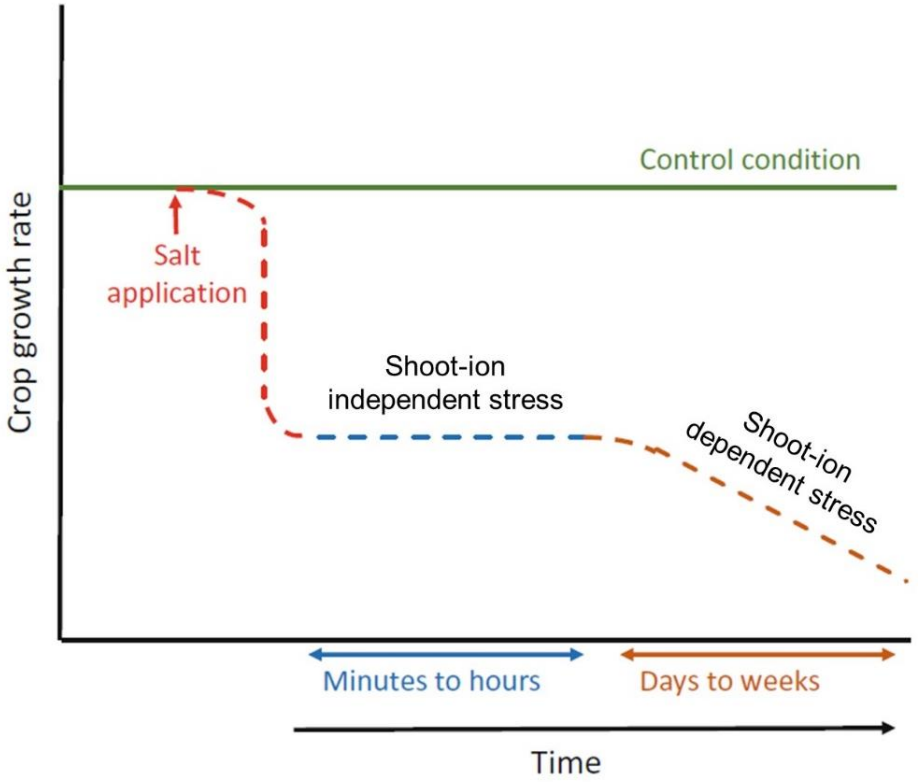

Figure 1: Salinity impacts on the growth rate of a cereal plant. An immediate reduction in plant growth rate occurs just after salt application as a result of shoot-ion independent stress (minutes to hours). Over time, Na^+ and Cl^- accumulate in the shoot resulting in a further reduction in growth rate because of the increasing effect of shoot-ion dependent stress (days to weeks). Adapted from Alqahtani et al. (2019).

Shoot-ion independent stress (osmotic stress)

Shoot-ion independent stress occurs as soon as the plant roots are exposed to salinity, and is hypothesized to result in an immediate reduction in shoot growth (Figure 1) (Munns and Tester 2008). This initial reduction in growth is partially due to the inability of a plant to maintain water uptake at the roots rather than because of the accumulation of Na^+ and Cl^- in the shoot (Munns 2002; Munns and Tester 2008).

The sudden exposure to salinity restricts the ability of plant roots to uptake water due to the negative soil water potential resulting from the presence of salt in the soil (Munns 2002). As a consequence, the major effects of salt in cereal plants is a reduction in total leaf area, number of tillers, and a decrease in photosynthesis and transpiration rates (Fricke and Peters 2002; Munns and Tester 2008; Roy *et al.* 2014; Shabala *et al.* 2015; Hanin *et al.* 2016; Ismail and Horie 2017; Munns *et al.* 2019a). The reduction in shoot growth rate is likely to be regulated by long distance sensing and signalling processes via plant hormones, reactive oxygen species (ROS), Ca^{2+} waves or electrical signalling (Munns and Tester 2008; Dodd *et al.* 2010; Kudla *et al.* 2010; Mittler *et al.* 2011; Suzuki *et al.* 2012; Roy *et al.* 2014; Shabala *et al.* 2015; Hanin *et al.* 2016; Steinhorst and Kudla 2019).

An osmotically stressed plant will close stomates due to reduced water uptake, resulting in a limited CO_2 availability for photosynthesis (Munns and Tester 2008). The insufficient CO_2 supply results in reduced carbon fixation in photosynthetic processes which leads to an elevated level of light energy being present in leaves (Logan 2008). This excessive energy reacts with oxygen containing molecules to produce high energy forms of oxygen, known as ROS, which can damage plant DNA and protein (Apel and Hirt 2004; Foyer and Noctor 2005; Logan 2008; Munns and Tester 2008).

Shoot-ion dependent stress (ionic stress)

Shoot-ion dependent stress has a slow onset and occurs when Na^+ and Cl^- concentrations accumulate to toxic levels in older leaves of the plant during prolonged exposure to salinity (from days to months) (Munns and Tester 2008). Ionic stress results in further decrease in plant growth rate and causes premature leaf senescence (Figure 1) (Munns 2002; Colmer *et al.* 2005; Munns and Tester 2008; Roy *et al.* 2014; Hanin *et al.* 2016; Munns *et al.* 2016). Premature senescence generally occurs first in older leaves as Na^+ is moved to the mature leaves to maintain lower Na^+ concentrations in the younger, growing leaves (Munns and Tester 2008). If

senescence of the older leaves occurs at a faster rate than the production of the new leaves, the growth of the new leaves is affected due to shortage of carbohydrate supply from the older leaves to the new emerging leaves (Munns and Tester 2008).

Under ionic stress, high levels of Na^+ in the apoplast results in cell dehydration, whereas in the cytoplasm it competes with K^+ that binds to many enzymes essential for cellular function and results in K^+ leakage from the cell (Tester and Davenport 2003; Shabala and Cuin 2008; Munns *et al.* 2016; Rubio *et al.* 2019). A high concentration of Na^+ in plant cells also affects photosynthetic components including chlorophyll and carotenoids, and in turn reduces the photosynthetic rate. (Davenport *et al.* 2005; Munns and Tester 2008; Hanin *et al.* 2016; Wu 2018). Salinity stress symptoms become more evident in the shoot-ion dependent phase, and the degree of damage to the plant is related to the duration in which the plant is exposed to salinity and how well the plant can tolerate this stress (Munns and Tester 2008).

Salinity tolerance mechanisms in cereal plants

Salinity tolerance is a complex trait which involves many different components and is controlled by multiple physiological pathways. In general, salinity tolerance mechanisms can be grouped into two categories: osmotic tolerance and ionic tolerance with various sub-traits (Munns and Tester 2008; Alqahtani *et al.* 2019).

Osmotic tolerance

Cereal plants use osmotic tolerance mechanisms to maintain shoot growth and stomatal conductance when roots are osmotically stressed following exposure to saline environments. Plants that are more tolerant to osmotic stress have greater leaf growth and stomatal conductance (Munns and Tester 2008; Negrão *et al.* 2017). While the mechanisms behind this tolerance remain largely unknown, it may involve maintaining carbon fixation and other long-

term plant hormonal sensing or signalling procedures (Munns and Tester 2008; Roy *et al.* 2014; Isayenkov and Maathuis 2019).

Osmotic tolerance in plants varies within species (Sirault *et al.* 2009; Furbank and Tester 2011; Tilbrook *et al.* 2017). The estimation of osmotic tolerance in plants can be performed by measuring stomatal conductance or growth rate of individual plants under salt stress (Furbank and Tester 2011; Negrão *et al.* 2017). Stomatal conductance can be indirectly estimated for example by measuring the canopy temperature using an infrared imaging, and plants that are more tolerant to osmotic stress have lower leaf temperature and increased stomatal conductance (Furbank and Tester 2011; Negrão *et al.* 2017; Sirault *et al.* 2009). In the past, measuring plant growth rate has been difficult as it required destructive methods and a large number of plants (Furbank and Tester 2011). The development of high-throughput phenotyping facilities, such as The Plant Accelerator® (TPA), makes it possible to track the growth of a single plant over time using a digital imaging system (Golzarian *et al.* 2011; Honsdorf *et al.* 2014; Al-Tamimi *et al.* 2016; Tilbrook *et al.* 2017; Asif *et al.* 2018). At the TPA, plant growing conditions such as soil water content and growing temperature can be controlled by a fully automated system, and high resolution red-green-blue (RGB) images that are recorded from the top and side of each plant which can be used to estimate plant growth rate (Honsdorf *et al.* 2014; Al-Tamimi *et al.* 2016; Tilbrook *et al.* 2017; Asif *et al.* 2018).

Ionic tolerance

Ionic tolerance mechanisms in cereal plants are responsible for maintaining growth under shoot-ion dependent salinity stress. There are two components in ionic tolerance mechanisms: ion exclusion and tissue tolerance (Munns and Tester 2008; Alqahtani *et al.* 2019).

Ion exclusion

Ion exclusion is thought to be an important salinity tolerance mechanism to prevent Na^+ and Cl^- accumulating to toxic concentrations in the shoot of many plants (Munns and Tester 2008). The importance of ion exclusion in overall plant salinity tolerance has been reported in many cereal plants including rice (Lee *et al.* 2003; Diedhiou and Golldack 2006), durum wheat (Munns and James 2003; Lindsay *et al.* 2004), bread wheat (Ashraf and Khanum 1997; Gorham *et al.* 1997) and barley (Forster 2001; Garthwaite *et al.* 2005). Under salt stress, Na^+ and Cl^- enter the plant root and are transported up to the shoot in the transpiration stream (Figure 2) (Munns and Tester 2008; Plett and Møller 2010; Alqahtani *et al.* 2019). To avoid accumulation of toxic levels of Na^+ and Cl^- in the shoot, plants exclude these ions by reducing initial uptake from the soil into the roots. This is achieved by increasing efflux of ions back to the soil, minimizing loading of ions into the xylem at the root, maximizing the retrieval of ions from the root xylem, and mediating Na^+ and Cl^- concentrations in root xylem and transpiration stream (Munns *et al.* 2006).

Ionic tissue tolerance

Plants that maintain growth with high leaf Na^+ and Cl^- concentrations under salt stress mainly rely on tissue tolerance (Flowers and Colmer 2008; Munns and Tester 2008; Shabala and Mackay 2011; Adolf *et al.* 2013; Flowers and Colmer 2015; Munns *et al.* 2016). Tissue tolerance enables plants to avoid damage from toxic levels of Na^+ and Cl^- accumulated in shoot by compartmentalizing these ions into the vacuole to reduce toxic Na^+ and Cl^- concentrations in the cytosol which is essential for the plant to maintain many metabolic processes (Flowers and Colmer 2008; Munns and Tester 2008; Flowers and Colmer 2015; Flowers *et al.* 2015; Munns *et al.* 2016; Munns *et al.* 2019b). Organic solutes that are compatible with metabolic activities, such as sucrose, proline and glycine betaine, are required in the cytosol to balance the osmotic pressure of the Na^+ and Cl^- ions sequestrated into the vacuole (Munns and Tester 2008; Munns *et al.* 2016; Munns *et al.* 2019b). In general, halophytes can effectively sequester

Na^+ and Cl^- in the vacuole to maintain growth under salinity and similar characteristics exist in some glycophyte species, such as barley (Colmer *et al.* 2005; Flowers and Colmer 2008; Flowers *et al.* 2015).

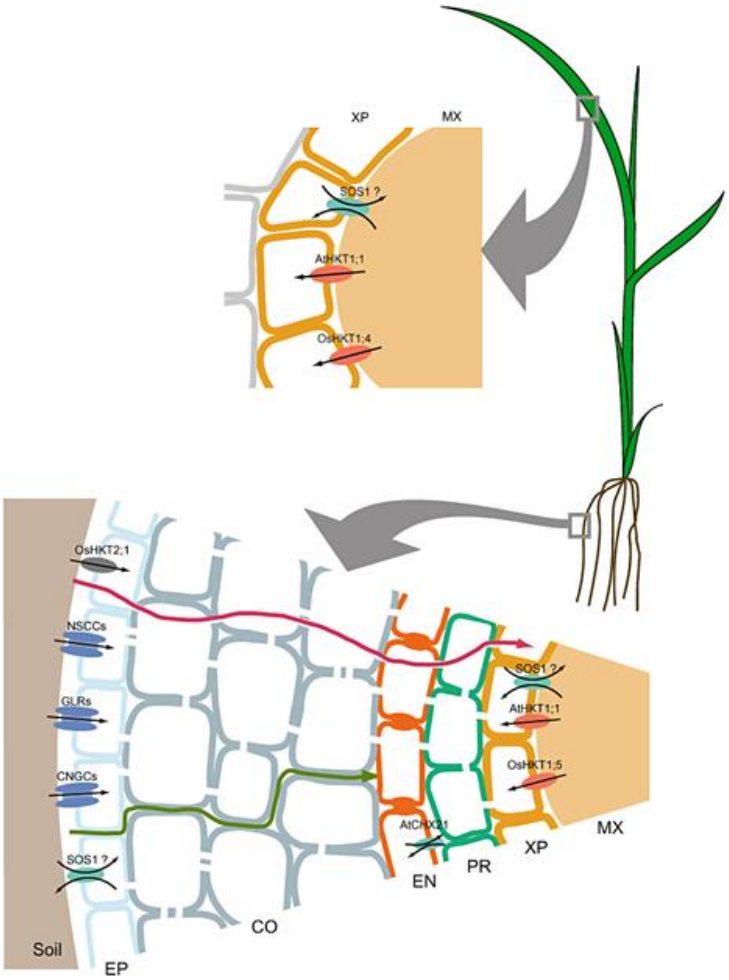

Figure 2: Several known transporters or channels putatively involved in Na^+ transport in the shoot or root in the glycophytic plants. Transporters responsible for Na^+ retrieval from the metaxylem to the xylem parenchyma of the shoot and root include the high affinity potassium transporters (HKT) family members (AtHKT1;1 and OsHKT1;4) and a Na^+/H^+ antiporter (SOS1). The OsHKT2;1, non selective cation channels (NSCCs), glutamate receptors (GLRs) and cyclic-nucleotide gated channels (CNGCs) are the proteins putatively invloved in Na^+ influx from soil to the epidermis. Epidermis = EP; cortex = CO; endodermis = EN; pericycle = PR; xylem parenchyma = XP; and metaxylem = MX. The green arrow indicated the apoplastic influx pathway for Na^+ and the red arrow indicated the symplastic radial transport of Na^+. The figure is from a review paper by Plett and Møller(2010).

Wheat is an important cereal plant

Bread wheat is unique among all cereal plants due to its agronomic adaptability, high productivity and nutritional value (Wrigley 2009). It is cultivated across a large area of land in the world and is well adapted to different latitudes and climates ranging from 67° N in Scandinavia and Russia to 45° S in Argentina (Shewry 2009). The world annual production of wheat is over 600 million tonnes and it is the most traded cereal around the globe (FAO 2019b). Bread wheat is one of the main sources of calories in the human diet due to its high nutritional value (Wrigley 2009). It contains a high amount of energy including starch and other essential nutrients such as proteins, vitamins, minerals, dietary fibres, and its unique properties of gluten protein makes it a suitable material for many food products (Shewry 2009; Wrigley 2009).

Bread wheat is a hexaploid containing three genomes, AA, BB and DD, being a natural hybrid of the diploid (*Aegilops tauschii*) wheat with the genome DD and tetraploid (*Triticum turgidum*) wheat with genome AABB which originated from south-eastern Turkey (Shewry 2009). With sufficient water, nutrient supply and disease management, wheat can achieve yields greater than 10 t/ha (Shewry 2009). However, the current global average of wheat productivity per ha is only 3.5 tonnes, and in Australia, the average yield of wheat is much less at 2.2 t/ha (FAO 2019b). The limitations on yield are due to many factors including abiotic stress such as salinity (Flowers 2004; Colmer *et al.* 2005; Munns *et al.* 2006; Roy *et al.* 2011; Munns and Gilliham 2015; Hanin *et al.* 2016). Therefore, improving bread wheat tolerance to salinity would be important in minimising the gap between potential wheat productivity and actual yield.

Salinity tolerance of wheat

Na^+ exclusion is often reported as a major salinity tolerance mechanism in wheat (Colmer *et al.* 2005; Munns *et al.* 2006; Genc *et al.* 2010; Roy *et al.* 2014; Hanin *et al.* 2016; Ismail and Horie 2017). Durum wheat (*Triticum turgidum*) is typically more sensitive to salinity among the cereals (Figure 3) and accumulates high levels of Na^+ in the leaf under saline conditions, most

likely due to not having the ability to sufficiently reduce root-to-shoot Na^+ transport (Munns *et al.* 2003; Davenport *et al.* 2005; Munns *et al.* 2006; Munns and Tester 2008). However, a durum wheat landrace L149 was found to contain major Na^+ exclusion loci *Nax1* and *Nax2* on the chromosome 2A and 5A, respectively, which originated from a wheat relative *Triticum monococcum* L. (Munns *et al.* 2003; Lindsay *et al.* 2004; James *et al.* 2006). The candidate gene underlying the *Nax2* locus has been identified as being *TmHKT1;5-A*, which encodes a Na^+-selective transporter protein (Byrt *et al.* 2007). TmHKT1;5-A is localised on the plasma membrane of root stele cells and functions to retrieve Na^+ from the xylem and thus reduce the amount of Na^+ transported to the shoot (Munns *et al.* 2012). Introducing the *Nax2* locus (*TmHKT1;5-A*) into a commercial durum wheat (var. Tamaroi) significantly reduced the leaf Na^+ accumulation and lines with the *Nax2* locus were found to contribute a 25% improvement in grain yield in a highly saline field compared to near isogenic lines without this locus (James *et al.* 2011; James *et al.* 2012; Munns *et al.* 2012).

Bread wheat is generally more tolerant to salinity than durum wheat (Figure 2) and has a naturally existing Na^+ exclusion locus *Kna1* which is on chromosome 4D (Dubcovsky *et al.* 1996). *TaHKT1;5-D*, the ortholog of *TmHKT1;5-A*, was identified to be the candidate gene underlying the *Kna1* locus and has been shown to play an important role in Na^+ unloading from the xylem at the root and hence limiting shoot Na^+ accumulation (Byrt *et al.* 2007; Byrt *et al.* 2014). Although shoot Na^+ exclusion has been shown to have a positive correlation with improved plant growth and yield in bread wheat under saline conditions (Chhipa and Lal 1995; Ashraf and O'leary 1996; Ashraf and Khanum 1997; Genc *et al.* 2010), the relationship does not always exist across all genotypes (Ashraf and McNeilly 1988; El-Hendawy *et al.* 2005; Genc *et al.* 2007; Genc *et al.* 2013; Genc *et al.* 2019). Due to this inconsistency in correlation between shoot Na^+ exclusion and plant biomass or yield, it is likely that other important mechanisms are also contributing to the plants ability to tolerate salt. These mechanisms could include maintenance of ion homeostasis and osmotic adjustment or tolerance to toxic ion

accumulation in plant tissues (Munns and Tester 2008; Shabala and Cuin 2008; Munns *et al.* 2016; Ismail and Horie 2017; Munns *et al.* 2019b). Identifying and introducing beneficial alleles controlling these traits into the elite bread wheat cultivars has the potential to enhance the salinity tolerance of bread wheat.

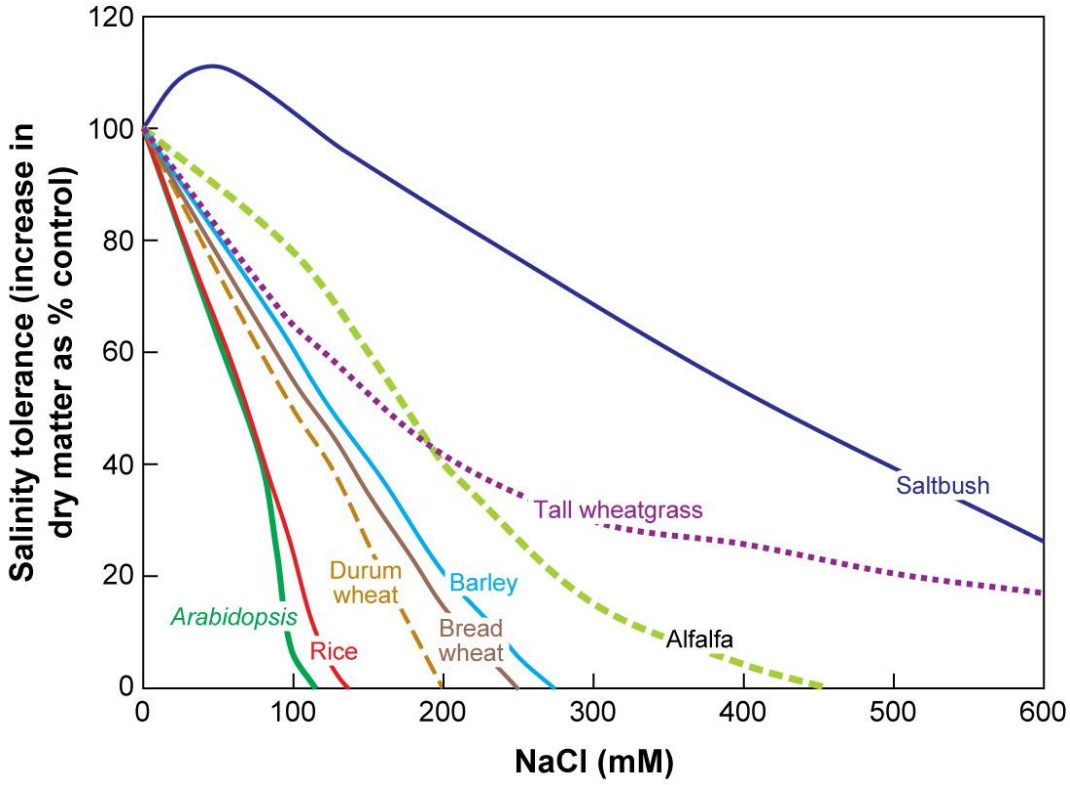

Figure 3: Salinity tolerance of various plant species. The salinity tolerance is shown as increases in shoot dry matter after growth in hydroponics or soil mixture containing NaCl for at least three weeks relative to plant growth at control treatment. Data are for Arabidopsis (*Arabidopsis thaliana*), rice (*Oryza sativa*), durum wheat (*Triticum turgidum* ssp durum), bread wheat (*Triticum aestivum*), barley (*Hordeum vulgare*), tall wheatgrass (*Thinopyrum ponticum*, syn. *Agropyron elongatum*), alfalfa (*Medicago sativa*) and saltbush (*Atriplex amnicola*). The figure is from a review paper by Munns and Tester (2008).

While most cultivated elite cereal crops have limited genetic diversity due to the long-term selection for key traits such as yield and grain quality, considerable genetic variation exists in landraces, early domesticates and wild relatives of those plants (Feuillet et al. 2008). Although introducing beneficial alleles from landraces or wild relatives to the elite cereal cultivars is time consuming and has a risk to introduce undesirable traits along with the beneficial traits, successful transfers has previously been reported in bread wheat (Kerber and Dyck 1973; Feuillet et al. 2008; Olson et al. 2010; Rouse et al. 2011; Olson et al. 2013). For instance, introgression of stem rust resistance genes such as *Sr22* from the *Triticum boeoticum* Boiss. and *Triticum monococcum* L. (Kerber and Dyck 1973), and *Sr33, Sr45 and Sr46* from the D genome donor of bread wheat, *Aegilops tauschii* Coss. (Marais et al. 1998; Rouse et al. 2011), into bread wheat cultivars has previously been successful to provide resistance to stem rust *Puccinia graminis* f. sp. *tritici*. Therefore, it would be possible to bring novel salinity tolerance alleles from landraces or wild relatives into the elite cultivars to breed bread wheat with improved salinity tolerance.

Recently, a Portuguese bread wheat landrace Mocho de Espiga Branca was identified as having similar salinity tolerance to two Australian bread wheat cultivars, Gladius and Scout, despite accumulating more than 10× higher leaf Na^+ concentrations at 100 mM NaCl (Schilling et al, at the Australian Centre for Plant Functional Genomics (ACPFG)). Salinity tolerance in Mocho de Espiga Branca is more likely attributed to mechanisms other than Na^+ exclusion, such as tissue tolerance which has not been reported in bread wheat. Improving our understanding of the genetics allowing Mocho de Espiga Branca to maintain growth despite the high leaf Na^+ concentrations could provide opportunities to identify novel alleles with key roles in salinity tolerance of bread wheat. Introducing those novel alleles into elite cultivars would potentially accelerate the breeding of bread wheat with improved salinity tolerance.

Research aims

In order to understand salinity tolerance mechanisms contributed to salinity tolerance in Mocho de Espiga Branca, this PhD research project is aiming to address the following three major questions:

1. How does Mocho de Espiga Branca accumulate a high leaf Na^+ concentration?
2. What are the potential genomic regions responsible for the salinity tolerant traits in Mocho de Espiga Branca?
3. Can the tissue tolerance trait in Mocho de Espiga Branca be physiologically dissected?

References

Adolf, VI, Jacobsen, SE, Shabala, S (2013) Salt tolerance mechanisms in quinoa (*Chenopodium* quinoa Willd.). *Environmental and Experimental Botany* **92**, 43-54.

Al-Tamimi, N, Brien, C, Oakey, H, Berger, B, Saade, S, Ho, YS, Schmöckel, SM, Tester, M, Negrão, S (2016) Salinity tolerance loci revealed in rice using high-throughput non-invasive phenotyping. *Nature Communications* **7**, 13342.

Alqahtani, M, Roy, SJ, Tester, M (2019) Increasing salinity tolerance of crops. In 'Encyclopedia of sustainability science and technology.' (Ed. RA Meyers.) pp. 1-24. (Springer: New York, USA).

Apel, K, Hirt, H (2004) Reactive oxygen species: metabolism, oxidative stress, and signal transduction. *Annu. Rev. Plant Biol.* **55**, 373-399.

Ashraf, M, Khanum, A (1997) Relationship between ion accumulation and growth in two spring wheat lines differing in salt tolerance at different growth stages. *Journal of Agronomy and Crop Science* **178**, 39-51.

Ashraf, M, McNeilly, T (1988) Variability in salt tolerance of nine spring wheat cultivars. *Journal of Agronomy and Crop Science* **160**, 14-21.

Ashraf, M, O'leary, J (1996) Responses of some newly developed salt-tolerant genotypes of spring wheat to salt stress: 1. Yield components and ion distribution. *Journal of Agronomy and Crop Science* **176**, 91-101.

Asif, MA, Schilling, RK, Tilbrook, J, Brien, C, Dowling, K, Rabie, H, Short, L, Trittermann, C, Garcia, A, Barrett-Lennard, EG, Berger, B, Mather, DE, Gilliham, M, Fleury, D, Tester, M, Roy, SJ, Pearson, AS (2018) Mapping of novel salt tolerance QTL in an Excalibur x Kukri doubled haploid wheat population. *Theoretical and Applied Genetics* **131**, 2179-2196.

Byrt, CS, Platten, JD, Spielmeyer, W, James, RA, Lagudah, ES, Dennis, ES, Tester, M, Munns, R (2007) HKT1;5-like cation transporters linked to Na^+ exclusion loci in wheat, *Nax2* and *Kna1*. *Plant Physiology* **143**, 1918-1928.

Byrt, CS, Xu, B, Krishnan, M, Lightfoot, DJ, Athman, A, Jacobs, AK, Watson-Haigh, NS, Plett, D, Munns, R, Tester, M, Gilliham, M (2014) The Na^+ transporter, TaHKT1;5-D, limits shoot Na^+ accumulation in bread wheat. *The Plant Journal* **80**, 516-526.

Chhipa, B, Lal, P (1995) Na^+/K^+ ratios as the basis of salt tolerance in wheat. *Australian Journal of Agricultural Research* **46**, 533-539.

Colmer, TD, Munns, R, Flowers, TJ (2005) Improving salt tolerance of wheat and barley: future prospects. *Australian Journal of Experimental Agriculture* **45**, 1425-1443.

Davenport, R, James, RA, Zakrisson-Plogander, A, Tester, M, Munns, R (2005) Control of sodium transport in durum wheat. *Plant Physiology* **137**, 807-818.

Diedhiou, C, Golldack, D (2006) Salt-dependent regulation of chloride channel transcripts in rice. *Plant Science* **170**, 793-800.

Dodd, AN, Kudla, J, Sanders, D (2010) The language of calcium signaling. *Annual Review of Plant Biology* **61**, 593-620.

Dubcovsky, J, Maria, GS, Epstein, E, Luo, MC, Dvorak, J (1996) Mapping of the K^+/Na^+ discrimination locus *Kna1* in wheat. *Theoretical and Applied Genetics* **92**, 448-454.

El-Hendawy, SE, Hu, Y, Schmidhalter, U (2005) Growth, ion content, gas exchange, and water relations of wheat genotypes differing in salt tolerances. *Australian Journal of Agricultural Research* **56**, 123-134.

FAO, (2019a) FAO soils portal. http://www.fao.org/soils-portal/soil-management/management-of-some-problem-soils/salt-affected-soils/more-information-on-salt-affected-soils/en/. Accessed 26 May 2019.

FAO, (2019b). FAOSTAT http://www.fao.org/faostat/en/#data/QC. Accessed 26 May 2019.

Feuillet, C, Langridge, P, Waugh, R (2008) Cereal breeding takes a walk on the wild side. *Trends in Genetics* **24**, 24-32.

Flowers, T (2004) Improving crop salt tolerance. *Journal of Experimental Botany* **55**, 307-319.

Flowers, TJ, Colmer, TD (2008) Salinity tolerance in halophytes. *New Phytologist* **179**, 945-963.

Flowers, TJ, Colmer, TD (2015) Plant salt tolerance: adaptations in halophytes. *Annals of Botany* **115**, 327-331.

Flowers, TJ, Munns, R, Colmer, TD (2015) Sodium chloride toxicity and the cellular basis of salt tolerance in halophytes. *Annals of Botany* **115**, 419-431.

Forster, BP (2001) Mutation genetics of salt tolerance in barley: an assessment of Golden Promise and other semi-dwarf mutants. *Euphytica* **120**, 317-328.

Foyer, CH, Noctor, G (2005) Oxidant and antioxidant signalling in plants: a re-evaluation of the concept of oxidative stress in a physiological context. *Plant, Cell and Environment* **28**, 1056-1071.

Fricke, W, Peters, WS (2002) The biophysics of leaf growth in salt-stressed barley. A study at the cell level. *Plant Physiology* **129**, 374-388.

Furbank, RT, Tester, M (2011) Phenomics–technologies to relieve the phenotyping bottleneck. *Trends in Plant Science* **16**, 635-644.

Garthwaite, AJ, von Bothmer, R, Colmer, TD (2005) Salt tolerance in wild Hordeum species is associated with restricted entry of Na^+ and Cl^- into the shoots. *Journal of Experimental Botany* **56**, 2365-2378.

Genc, Y, McDonald, GK, Tester, M (2007) Reassessment of tissue Na^+ concentration as a criterion for salinity tolerance in bread wheat. *Plant Cell & Environment* **30**, 1486-1498.

Genc, Y, Oldach, K, Gogel, B, Wallwork, H, McDonald, GK, Smith, AB (2013) Quantitative trait loci for agronomic and physiological traits for a bread wheat population grown in environments with a range of salinity levels. *Molecular Breeding* **32**, 39-59.

Genc, Y, Oldach, K, Verbyla, AP, Lott, G, Hassan, M, Tester, M, Wallwork, H, McDonald, GK (2010) Sodium exclusion QTL associated with improved seedling growth in bread wheat under salinity stress. *Theoretical and Applied Genetics* **121**, 877-894.

Genc, Y, Taylor, J, Lyons, GH, Li, Y, Cheong, J, Appelbee, M, Oldach, K, Sutton, T (2019) Bread wheat with high salinity and sodicity tolerance. *Frontiers in Plant Science* **10**, 1280.

Golzarian, MR, Frick, RA, Rajendran, K, Berger, B, Roy, S, Tester, M, Lun, DS (2011) Accurate inference of shoot biomass from high-throughput images of cereal plants. *Plant Methods* **7**, 2.

Gorham, J, Bridges, J, Dubcovsky, J, Dvorak, J, Hollington, PA, Luo, MC, Khan, JA (1997) Genetic analysis and physiology of a trait for enhanced K^+/Na^+ discrimination in wheat. *New Phytologist* **137**, 109-116.

Greenway, H, Munns, R (1980) Mechanisms of salt tolerance in non-halophytes. *Annual Review of Plant Physiology and Plant Molecular Biology* **31**, 149-190.

Hanin, M, Ebel, C, Ngom, M, Laplaze, L, Masmoudi, K (2016) New insights on plant salt tolerance mechanisms and their potential use for breeding. *Frontiers in Plant Science* **7**, 1787.

Honsdorf, N, March, TJ, Berger, B, Tester, M, Pillen, K (2014) High-throughput phenotyping to detect drought tolerance QTL in wild barley introgression lines. *PLoS ONE* **9**, e97047.

Isayenkov, SV, Maathuis, FJM (2019) Plant salinity stress: Many unanswered questions remain. *Frontiers in Plant Science* **10**, 80.

Ismail, AM, Horie, T (2017) Genomics, physiology, and molecular breeding approaches for improving salt tolerance. *Annual Review of Plant Biology* **68**, 405-434.

James, RA, Blake, C, Byrt, CS, Munns, R (2011) Major genes for Na^+ exclusion, *Nax1* and *Nax2* (wheat *HKT1;4* and *HKT1;5*), decrease Na^+ accumulation in bread wheat leaves under saline and waterlogged conditions. *Journal of Experimental Botany* **62**, 2939-2947.

James, RA, Blake, C, Zwart, AB, Hare, RA, Rathjen, AJ, Munns, R (2012) Impact of ancestral wheat sodium exclusion genes *Nax1* and *Nax2* on grain yield of durum wheat on saline soils. *Functional Plant Biology* **39**, 609-618.

James, RA, Davenport, RJ, Munns, R (2006) Physiological characterization of two genes for Na^+ exclusion in durum wheat, *Nax1* and *Nax2*. *Plant Physiology* **142**, 1537-1547.

Kerber, ER, Dyck, PL (1973) Inheritance of stem rust resistance transferred from diploid wheat (*Triticum monococcum*) to tetraploid and hexaploid wheat and chromosome location of gene involved. *Canadian Journal of Genetics and Cytology* **15**, 397-409.

Kudla, J, Batistič, O, Hashimoto, K (2010) Calcium signals: the lead currency of plant information processing. *The Plant Cell* **22**, 541-563.

Lee, KS, Choi, WY, Ko, JC, Kim, TS, Gregorio, GB (2003) Salinity tolerance of japonica and indica rice (*Oryza sativa* L.) at the seedling stage. *Planta* **216**, 1043-1046.

Lindsay, MP, Lagudah, ES, Hare, RA, Munns, R (2004) A locus for sodium exclusion *(Nax1*), a trait for salt tolerance, mapped in durum wheat. *Functional Plant Biology* **31**, 1105-1114.

Logan, BA (2008) Reactive oxygen species and photosynthesis. In 'Antioxidants and Reactive Oxygen Species in Plants.' pp. 250-267.

Marais, G, Wessels, W, Horn, M, Du Toit, F (1998) Association of a stem rust resistance gene (*Sr45*) and two Russian wheat aphid resistance genes (*Dn5* and *Dn7*) with mapped structural loci in common wheat. *South African Journal of Plant and Soil* **15**, 67-71.

Mittler, R, Vanderauwera, S, Suzuki, N, Miller, G, Tognetti, VB, Vandepoele, K, Gollery, M, Shulaev, V, Van Breusegem, F (2011) ROS signaling: the new wave? *Trends in Plant Science* **16**, 300-309.

Munns, R (2002) Comparative physiology of salt and water stress. *Plant Cell & Environment* **25**, 239-250.

Munns, R, Day, DA, Fricke, W, Watt, M, Arsova, B, Barkla, BJ, Bose, J, Byrt, CS, Chen, Z-H, Foster, KJ, Gilliham, M, Henderson, SW, Jenkins, CLD, Kronzucker, HJ, Miklavcic, SJ, Plett, D, Roy, SJ, Shabala, S, Shelden, MC, Soole, KL, Taylor, NL, Tester, M, Wege, S, Wegner, LH, Tyerman, SD (2019a) Energy costs of salt tolerance in crop plants. *New Phytologist*. doi.org/10.1111/nph.15864.

Munns, R, Gilliham, M (2015) Salinity tolerance of crops - what is the cost? *New Phytologist* **208**, 668-673.

Munns, R, James, RA (2003) Screening methods for salinity tolerance: a case study with tetraploid wheat. *Plant and Soil* **253**, 201-218.

Munns, R, James, RA, Gilliham, M, Flowers, TJ, Colmer, TD (2016) Tissue tolerance: an essential but elusive trait for salt-tolerant crops. *Functional Plant Biology* **43**, 1103-1113.

Munns, R, James, RA, Lauchli, A (2006) Approaches to increasing the salt tolerance of wheat and other cereals. *Journal of Experimental Botany* **57**, 1025-1043.

Munns, R, James, RA, Xu, B, Athman, A, Conn, SJ, Jordans, C, Byrt, CS, Hare, RA, Tyerman, SD, Tester, M, Plett, D, Gilliham, M (2012) Wheat grain yield on saline soils is improved by an ancestral Na^+ transporter gene. *Nature Biotechnology* **30**, 360-U173.

Munns, R, Passioura, JB, Colmer, TD, Byrt, CS (2019b) Osmotic adjustment and energy limitations to plant growth in saline soil. *New Phytologist*. doi: 10.1111/nph.15862.

Munns, R, Rebetzke, GJ, Husain, S, James, RA, Hare, RA (2003) Genetic control of sodium exclusion in durum wheat. *Australian Journal of Agricultural Research* **54**, 627-635.

Munns, R, Tester, M (2008) Mechanisms of salinity tolerance. *Annual Review of Plant Biology* **59**, 651-681.

Negrão, S, Schmöckel, SM, Tester, M (2017) Evaluating physiological responses of plants to salinity stress. *Annals of Botany* **119**, 1-11.

Olson, EL, Brown-Guedira, G, Marshall, D, Stack, E, Bowden, RL, Jin, Y, Rouse, M, Pumphrey, MO (2010) Development of wheat lines having a small introgressed segment carrying stem rust resistance gene *Sr22*. *Crop Science* **50**, 1823-1830.

Olson, EL, Rouse, MN, Pumphrey, MO, Bowden, RL, Gill, BS, Poland, JA (2013) Introgression of stem rust resistance genes *SrTA10187* and *SrTA10171* from *Aegilops tauschii* to wheat. *Theoretical and Applied Genetics* **126**, 2477-2484.

Plett, DC, Møller, IS (2010) Na^+ transport in glycophytic plants: what we know and would like to know. *Plant Cell & Environment* **33**, 612-626.

Rengasamy, P (2002) Transient salinity and subsoil constraints to dryland farming in Australian sodic soils: an overview. *Australian Journal of Experimental Agriculture* **42**, 351-361.

Rouse, MN, Olson, EL, Gill, BS, Pumphrey, MO, Jin, Y (2011) Stem rust resistance in *Aegilops tauschii* germplasm. *Crop Science* **51**, 2074-2078.

Roy, SJ, Negrão, S, Tester, M (2014) Salt resistant crop plants. *Current Opinion in Biotechnology* **26**, 115-124.

Roy, SJ, Tucker, EJ, Tester, M (2011) Genetic analysis of abiotic stress tolerance in crops. *Current Opinion in Plant Biology* **14**, 232-239.

Rubio, F, Nieves-Cordones, M, Horie, T, Shabala, S (2019) Doing 'business as usual'comes with a cost: evaluating energy cost of maintaining plant intracellular K^+ homeostasis under saline conditions. *New Phytologist*. doi: 10.1111/nph.15852.

Shabala, S (2013) Learning from halophytes: physiological basis and strategies to improve abiotic stress tolerance in crops. *Annals of Botany* **112**, 1209-1221.

Shabala, S, Cuin, TA (2008) Potassium transport and plant salt tolerance. *Physiologia Plantarum* **133**, 651-669.

Shabala, S, Mackay, A (2011) Ion transport in halophytes. In 'Plant Responses to Drought and Salinity Stress: Developments in a Post-Genomic Era.' (Ed. I Turkan.) Vol. 57 pp. 151-199. (Academic Press Ltd-Elsevier Science Ltd: London).

Shabala, S, Wu, HH, Bose, J (2015) Salt stress sensing and early signalling events in plant roots: Current knowledge and hypothesis. *Plant Science* **241**, 109-119.

Shewry, PR (2009) Wheat. *Journal of Experimental Botany* **60**, 1537-1553.

Sirault, XR, James, RA, Furbank, RT (2009) A new screening method for osmotic component of salinity tolerance in cereals using infrared thermography. *Functional Plant Biology* **36**, 970-977.

Steinhorst, L, Kudla, J, 2019. How plants perceive salt. *Nature* **572**, 318-320.

Suzuki, N, Koussevitzky, S, Mittler, R, Miller, G (2012) ROS and redox signalling in the response of plants to abiotic stress. *Plant, Cell and Environment* **35**, 259-270.

Tester, M, Davenport, R (2003) Na^+ tolerance and Na^+ transport in higher plants. *Annals of Botany* **91**, 503-527.

Tilbrook, J, Schilling, RK, Berger, B, Garcia, AF, Trittermann, C, Coventry, S, Rabie, H, Brien, C, Nguyen, M, Tester, M (2017) Variation in shoot tolerance mechanisms not related to ion toxicity in barley. *Functional Plant Biology* **44**, 1194-1206.

Tyerman, SD, Munns, R, Fricke, W, Arsova, B, Barkla, BJ, Bose, J, Bramley, H, Byrt, C, Chen, ZH, Colmer, TD, Cuin, T, Day, DA, Foster, KJ, Gilliham, M, Henderson, SW, Horie, T, Jenkins, CLD, Kaiser, BN, Katsuhara, M, Plett, D, Miklavcic, SJ, Roy, SJ, Rubio, F, Shabala, S, Shelden, M, Soole, K, Taylor, NL, Tester, M, Watt, M, Wege, S, Wegner, LH, Wen, ZY (2019) Energy costs of salinity tolerance in crop plants. *New Phytologist* **221**, 25-29.

United States Salinity Laboratory Staff (1954) Diagnosis and improvement of saline and alkali soils. In 'Agricultural Handbook No. 60.' (US Government Printer: Washington)

Wicke, B, Smeets, E, Dornburg, V, Vashev, B, Gaiser, T, Turkenburg, W, Faaij, A (2011) The global technical and economic potential of bioenergy from salt-affected soils. *Energy & Environmental Science* **4**, 2669-2681.

Wrigley, C (2009) Wheat: a unique grain for the world. In 'Wheat: Chemistry and technology.' (Eds K Khan, PR Shewry.) Vol. 7 pp. 1-17. (AACC International, Inc.: U.S.A.).

Wu, HH (2018) Plant salt tolerance and Na^+ sensing and transport. *Crop Journal* **6**, 215-225.

Chapter 2 - *TaHKT1;5-D*: Switching a T to C makes bread wheat salty

Statement of Authorship

Title of Paper	*TaHKT1;5-D*: Switching a T to C makes bread wheat salty
Publication Status	☐ Published ☐ Accepted for Publication ☑ Submitted for Publication ☐ Unpublished and Unsubmitted work written in manuscript style
Publication Details	This manuscript has been written and formatted for publication in Nature Plants.

Principal Author

Name of Principal Author (Candidate)	Chana (Chana Borjigin)
Contribution to the Paper	Contributed to the experimental design, conducted the hydroponics experiment, ion analysis, RNA extraction, cDNA synthesis and gene sequencing, designed the CAPS marker and conducted the genotyping, grew and sampled plants for xylem sap collection and root ion fluxes measurement, analysed and interpreted the data and wrote manuscript.
Overall percentage (%)	65%
Certification:	This paper reports on original research I conducted during the period of my Higher Degree by Research candidature and is not subject to any obligations or contractual agreements with a third party that would constrain its inclusion in this thesis. I am the primary author of this paper.
Signature	Date 04/11/2019

Co-Author Contributions

By signing the Statement of Authorship, each author certifies that:

i. the candidate's stated contribution to the publication is accurate (as detailed above);
ii. permission is granted for the candidate in include the publication in the thesis; and
iii. the sum of all co-author contributions is equal to 100% less the candidate's stated contribution.

Name of Co-Author	Rhiannon K. Schilling
Contribution to the Paper	Conceived the work, contributed to the experimental design, conducted the pot experiment screening the wheat diversity lines for salinity tolerance and identified the high sodium phenotype of Mocho de Espiga Branca, interpreted the work and contributed to supervision, reviewed and commented on the manuscript.
Signature	Date 04/11/2019

Name of Co-Author	Jayakumar Bose
Contribution to the Paper	Measured root ion fluxes using MIFE technique and analysed the data, collected xylem sap for ion analysis, reviewed and commented on the manuscript.
Signature	Date 05/11/2019

Name of Co-Author	Maria Hrmova
Contribution to the Paper	Conducted 3D protein modelling and analysed sequence conservation patterns, and interpreted the results, reviewed and commented on the manuscript.
Signature	Date 04/11/2019

Name of Co-Author	Jiaen Qiu
Contribution to the Paper	Cloned the genes into the appropriated vectors and performed the electrophysiological work in *X. laevis* oocytes and analysed the data, reviewed and commented on the manuscript.
Signature	Date 04/11/2019

Name of Co-Author	Stefanie Wege
Contribution to the Paper	Conducted the confocal subcellular localisation work, reviewed and commented on the manuscript.
Signature	Date 04.11.2019

Name of Co-Author	Apriadi Situmorang
Contribution to the Paper	Cloned the genes into the appropriated vectors for confocal subcellular localisation work.
Signature	Date 04.11.2019

Name of Co-Author	Chris Brien
Contribution to the Paper	Generated the experimental layout for phenotyping the bread wheat diversity lines in the Smarthouse, reviewed and commented on the manuscript.
Signature	Date 5.11.2019

Name of Co-Author	Bettina Berger
Contribution to the Paper	Provided advice for and supervised the Smarthouse phenotyping experiment
Signature	Date 04.11.2019

Name of Co-Author	Matthew Gilliham		
Contribution to the Paper	Assisted conceiving the work and interpretation of electrophysiological work.		
Signature		Date	4-11-2019

Name of Co-Author	Allison S Pearson		
Contribution to the Paper	Conceived the work, contributed to the experimental design, interpreted the work and contributed to supervision, reviewed and commented on the manuscript.		
Signature		Date	4-11-2019

Name of Co-Author	Stuart J Roy		
Contribution to the Paper	Conceived the work, contributed to the experimental design, interpreted the work and contributed to supervision, reviewed and commented on the manuscript.		
Signature		Date	13/11/2019

TaHKT1;5-D: Switching a T to C makes bread wheat salty

Running title: *TaHKT1;5-D*: Switching a T to C makes bread wheat salty

Chana Borjigin[1,2], Rhiannon K Schilling[1,2,*], Jayakumar Bose[2,3], Maria Hrmova[1,2,4], Jiaen Qiu[2,3], Stefanie Wege[2,3], Apriadi Situmorang[2], Chris Brien[2,5], Bettina Berger[2,5] Matthew Gilliham[2,3], Allison S Pearson[1,2,3], Stuart J Roy[1,2,6]

[1]Australian Centre for Plant Functional Genomics, The University of Adelaide, PMB 1, Glen Osmond, South Australia 5064, Australia

[2]School of Agriculture, Food and Wine, The University of Adelaide, PMB 1, Glen Osmond, South Australia 5064, Australia

[3]ARC Centre of Excellence in Plant Energy Biology, The University of Adelaide, PMB 1, Glen Osmond, South Australia 5064, Australia

[4]School of Life Sciences, Huaiyin Normal University, Huai'an 223300, China

[5]Australian Plant Phenomics Facility, The Plant Accelerator, The University of Adelaide, PMB 1, Glen Osmond, South Australia 5064, Australia

[6]ARC Industrial Transformation Research Hub for Wheat in a Hot Dry Climate, The University of Adelaide, PMB 1, Glen Osmond, South Australia 5064, Australia

*Corresponding author

Rhiannon K Schilling E-mail: rhiannon.schilling@adelaide.edu.au

ORCID

Chana Borjigin	https://orcid.org/0000-0003-1043-8295
Rhiannon K Schilling	https://orcid.org/0000-0001-8853-6878
Jayakumar Bose	https://orcid.org/0000-0002-0565-2951
Maria Hrmova	https://orcid.org/0000-0002-3545-0605
Jiaen Qiu	https://orcid.org/0000-0001-9220-4219
Stefanie Wege	https://orcid.org/0000-0002-7232-5889
Apriadi Situmorang	https://orcid.org/0000-0003-1879-3355
Chris Brien	https://orcid.org/0000-0003-0581-1817
Bettina Berger	https://orcid.org/0000-0003-1195-4478
Matthew Gilliham	https://orcid.org/0000-0003-0666-3078
Allison S Pearson	https://orcid.org/0000-0001-8231-0149
Stuart J Roy	https://orcid.org/0000-0003-0411-9431

Abstract

Improving salinity tolerance in the most widely cultivated cereal, bread wheat (*Triticum aestivum* L.), is essential to increase grain yields on saline agricultural lands. A Portuguese landrace, Mocho de Espiga Branca accumulates up to 7-fold greater leaf and sheath sodium (Na^+) than two Australian cultivars, Gladius and Scout, under salt stress. Despite high leaf and sheath Na^+ concentrations, Mocho de Espiga Branca maintained similar salinity tolerance compared to Gladius and Scout. A naturally occurring single nucleotide substitution was identified in the gene encoding a major Na^+ transporter TaHKT1;5-D in Mocho de Espiga Branca, which resulted in a L190P amino acid residue variation. This variant prevents Mocho de Espiga Branca from retrieving Na^+ from the root xylem leading to a high shoot Na^+ concentration. The identification of the tissue tolerant Mocho de Espiga Branca will accelerate the development of more elite salt tolerant bread wheat cultivars.

Introduction

Globally, 45 million ha of irrigated and 32 million ha of dryland agricultural land is affected by salinity[1]. It is estimated that up to 1.2 million ha of land is lost to salinization each year[1]. To feed the rapidly growing human population, global food production must increase more than 70% by 2050, equating to an average increase of 44 million metric tons per year[2]. Bread wheat (*Triticum aestivum*) is the most widely cultivated cereal crop, in terms of area and provides one fifth of the total calories consumed worldwide[3]. Improving the salinity tolerance of bread wheat to maximise yields on saline agricultural land is required.

Salinity affects plants in two distinct stages. Shoot ion-independent stress (osmotic stress) arises immediately after plants are exposed to salt, inducing rapid physiological responses, such as stomatal closure and slower cell expansion, resulting in reduced plant growth[4]. Shoot ion-dependent stress (ionic stress) has a slower onset and occurs when salt, particularly Na^+ and Cl^-, accumulate to high concentrations in the shoot[4]. In this phase, reduced plant growth becomes more evident and premature leaf senescence occurs due to the toxicity of salt on cell metabolism[4].

Plants have three main mechanisms for tolerating salinity: osmotic stress tolerance via rapid, long distance signalling to maintain plant growth; ionic tissue tolerance by compartmentalising excessive Na^+ or Cl^- in vacuoles to avoid accumulation to toxic concentrations in the cytoplasm, and the exclusion of Na^+ from the shoot by retrieving Na^+ from the xylem into the root or through efflux of Na^+ into the soil to maintain a low shoot Na^+ concentration[4].

The High-Affinity Potassium Transporter 1;5 (HKT1;5) is known to be responsible for retrieving Na^+ from the transpiration stream in the root and preventing Na^+ from accumulating to high concentrations in the shoot[5]. Plant HKT proteins belong to the high-affinity K^+/Na^+ transporers Ktr/TrK/HKT superfamily and are divided into two groups based on a

serine/glycine substitution in the first loop of the proteins[6]. Members of the HKT1 group with a serine residue, typically transport Na^+, while the HKT2 group with a glycine side chain generally transport both Na^+ and K^+ [6]. In Arabidopsis (*Arabidopsis thaliana*) overexpression of *AtHKT1;1* in root stellar cells reduced shoot Na^+ accumulation by up to 64% compared to null segregants[7]. In bread wheat, the *AtHKT1;1* ortholog, *TaHKT1;5-D* reduces shoot Na^+ accumulation under salinity[8]. Durum wheat (*Triticum turgidum* L.), which lacks the D-genome accumulates high concentrations of Na^+ in the leaf[9]. However, when *TmHKT1;5-A* (*Nax2* locus) from a wheat relative *Triticum monococcum* L. was introduced into a commercial durum wheat, a reduction in leaf Na^+ concentration[10] and a 25% improvement in grain yield in the field were observed[11].

Breeding of salt tolerant bread wheat cultivars has focused on selecting genotypes with improved shoot Na^+ exclusion[12,13]. However, selection based on shoot Na^+ exclusion is not always correlated with increased salinity tolerance in bread wheat[14,15]. Barley (*Hordeum vulgare* L.) is one of the most salt tolerant cereal crops and has much higher leaf Na^+ concentrations than bread wheat yet is able to maintain shoot growth in saline soils[4,16]. The identification of a bread wheat line that accumulates high shoot Na^+ concentrations whilst maintaining salinity tolerance, similar to barley, will allow the chracterisation of sodium tissue toleraence mechanisms of wheat and therefore will accelerate the development of more salt tolerant bread wheat cultivars.

Here, we identified a Portuguese bread wheat landrace Mocho de Espiga Branca, which accumulated significantly higher leaf Na^+ concentrations while maintaining similar salinity tolerance as current commercial elite bread wheat cultivars. A naturally occurring single nucleotide polymorphism (SNP) in *TaHKT1;5-D* prevents Mocho de Espiga Branca from retrieving Na^+ from the root xylem, which results in a greater flux of Na^+ to the shoot and higher accumulation of Na^+ in leaf tissues.

Results

Mocho de Espiga Branca has high leaf and sheath Na^+ concentrations

Screening of 75 bread wheat accessions for salinity tolerance under 100 mM NaCl, identified a Portuguese landrace, Mocho de Espiga Branca, which had a similar salinity tolerance but accumulated 7-fold higher Na^+ concentration in the 4th leaf compared to all other lines, including Gladius and Scout (Fig. 1 and Supplementary Table 1). The 4th leaf K^+ and Cl^- concentrations of the 75 wheat lines were comparable under 100 mM NaCl (Supplementary Table 1).

In hydroponics, Mocho de Espiga Branca maintained a similar shoot and root biomass to Gladius and Scout at 0, 150 and 200 mM NaCl (Fig. 2a and Supplementary Fig. 1a,b), and all three cultivars had comparable salinity tolerance at 150 mM (0.69, 0.64 and 0.60, respectively) and 200 mM NaCl (0.39, 0.49 and 0.39, respectively) (Supplementary Fig. 1c,d). The 4th leaf blade and sheath Na^+ concentrations were up to 6-fold higher in Mocho de Espiga Branca than Gladius and Scout at 150 mM NaCl (Fig. 2b,c). At 200 mM NaCl, 4th leaf blade and sheath Na^+ concentrations in Mocho de Espiga Branca were 5-fold greater compared to Gladius and Scout (Fig. 2b,c). There was no difference in root Na^+ concentration at all NaCl treatments (Fig. 2d).

All three cultivars had similar K^+ concentrations in the 4th leaf blade and sheath under 0 mM NaCl (Supplementary Fig. 2a). At 150 and 200 mM NaCl, Mocho de Espiga Branca accumulated 70-79% less K^+ in the blade and 61-67% less K^+ in the sheath compared to Gladius and Scout (Supplementary Fig. 2a, b). The root K^+ concentration in Mocho de Espiga Branca was similar to Scout but significantly lower than Gladius under 0 mM NaCl, while no differences were observed between the three cultivars under 150 and 200 mM NaCl (Supplementary Fig. 2c).

The 4th leaf blade and sheath Cl^- concentrations in Mocho de Espiga Branca, Gladius and Scout were similar under 0 mM NaCl (Supplementary Fig. 2d,e). Mocho de Espiga Branca accumulated significantly higher Cl^- than Gladius and Scout in both tissues under 150 and 200 mM NaCl (Supplementary Fig. 2d,e). There were no significant differences in root Cl^- concentrations at 0 mM NaCl (Supplementary Fig. 2f). Mocho de Espiga Branca had significantly higher Cl^- than Gladius and Scout at 150 mM NaCl but only significantly higher than Scout at 200 mM NaCl (Supplementary Fig. 2f).

A natural single nucleotide substitution in the *TaHKT1;5-D* gene of Mocho de Espiga Branca alters Na^+ transport properties of the protein

A natural single SNP (T/C) in the coding sequence of *TaHKT1;5-D* was identified at the 569th base pair in Mocho de Espiga Branca, while the sequence of Gladius and Scout was identical to Chinese Spring (Fig. 3a). The SNP in Mocho de Espiga Branca resulted in an amino acid residue change from Leucine (L) to Proline (P) at the 190th residue in the Na^+ transporter protein TaHKT1;5-D (Fig. 3a). This L190P variant residue is predicted to be located on the 4th transmembrane α-helix in the area of the second glycine residue of the S78-G233-G353-G457 selectivity filter motif (Fig. 3b). Expression analysis of the *TaHKT1;5-D* in Mocho de Espiga Branca, Gladius and Scout showed no significant difference in expression (Supplementary Fig. 3b). A cleaved amplified polymorphic sequence (CAPS) marker tsl2SALTY-4D designed to this SNP in *TaHKT1;5-D* was used to genotype 71 diversity lines (Supplementary Fig. 3c and Supplementary Table 2). Mocho de Espiga Branca carried the C:C allele responsible for the TaHKT1;5-D L190P variation, while all other lines had the T:T allele as Gladius and Scout (Supplementary Fig. 3c and Supplementary Table 2).

3D molecular modelling revealed that overall folds of TaHKT1;5-D and TaHKT1;5-D L190P were similar (Fig. 3c,d). Detailed analysis of the microenvironments around α-helix 4 and α-helix 5 (two black arrows pointing to each other in Fig. 3d), revealed that L190 in α-helix 4 of

TaHKT1;5-D (Fig. 3d left) established four polar contacts at separations between 2.6 Å to 3.2 Å with V186, V187, Y193 and S194 neighbouring residues. These extensive polar contacts were not formed in the TaHKT1;5-D L190P variant (Fig. 3d right), which only established one polar contact at the separation at 2.7 Å. In TaHKT1;5-D, the packing angle between α-helix 4 (carrying L190P) and the neighbouring α-helix 5 was 16° sharper than that in TaHKT1;5D L190P (Fig. 3d). Sequence conservation patterns, based on 3D models of TaHKT1;5-D revealed that the P190 position in TaHKT1;5-D could not be found in databases, meaning that L190 could only be replaced by F, G, L, V, I, M, A, K and T, but not by P. Evaluation of differences of Gibbs free energies of TaHKT1;5-D revealed that the L190P mutation was energetically highly unfavourable (highly destabilising), and that the reverse mutation (P190 into L190) restored 70% of this energy loss.

To examine the effect of the L190P variant in the Na^+ transport properties of the TaHKT1;5-D transporter, *TaHKT1;5-D* cRNA from Mocho de Espiga Branca or Gladius was introduced in *X. laevis* oocytes. When exposed to different concentrations of Na^+ glutamate (1 and 30 mM Na^+), the oocytes with *TaHKT1;5-D* from Gladius had a significantly higher Na^+ elicited inward current, whereas those with *TaHKT1;5-D* from Mocho de Espiga Branca had limited current, similar to the H_2O-injected oocytes (Fig. 4a). The TaHKT1;5-D from Gladius showed a positive reversal potential shift when exposed to 30 mM Na^+ which was not observed with TaHKT1;5-D L190P from Mocho de Espiga Branca (Fig. 4a).

Transient expression of N-terminally GFP-tagged TaHKT1;5-D variants in *Nicotiana benthamiana* leaves revealed differences in GFP-signal pattern (Fig. 4b). The majority of GFP-TaHKT1;5-D signal co-localised with the plasma membrane (PM) marker CBL1n-RFP, and a minor fraction to mobile subcellular organelles (Fig. 4b). GFP-signal in leaves infiltrated with GFP-TaHKT1;5-D L190P, however, localised to internal cell structures, including a faint cytosolic signal and brighter non-mobile structures (Fig. 4b). Suggesting the TaHKT1;5-D

L190P might get degraded; possibly due to instability of the protein as revealed by homology modelling.

The Na^+ transport properties of the TaHKT1;5-D L190P variant was further investigated by comparing the xylem sap Na^+ concentrations of Mocho de Espiga Branca and Gladius grown hydroponically under 0 and 150 mM NaCl. Mocho de Espiga Branca accumulated a 3.5-fold greater xylem sap Na^+ than Gladius at 150 mM NaCl, while no significant differences were observed at 0 mM NaCl (Fig. 4c). There was no significant difference for xylem sap K^+ and Cl^- concentrations for either cultivar (Supplementary Fig. 4a,b).

The ability of Mocho de Espiga Branca to influx or efflux Na^+ at the root elongation zone was assessed in five day old seedlings using a basal salt medium (BSM) with ion fluxes monitored for 25 min. In the first minute after being exposed to 0.6 mM NaCl, Mocho de Espiga Branca and Gladius had an increase in net Na^+ efflux up to 10000 and 35000 nmol m^{-2} s^{-1} respectively compared to the BSM with 100 mM NaCl (Fig. 5a). However, Mocho de Espiga Branca changed within the first minute to Na^+ influx, while Gladius maintained Na^+ efflux for the duration of measurement (Fig. 5a). The transient net K^+ efflux was greater in Mocho de Espiga Branca than Gladius and the efflux rates gradually dropped to below 1000 nmol m^{-2} s^{-1} in both cultivars (Fig. 5b). Mocho de Espiga Branca had a net H^+ influx for 25 min, while Gladius initially became a net influxer for 8 min and then reverted to being a net effluxer for the remainder of the experiment after exposure to 0.6 mM Na^+ (Fig. 5c). Overall, Mocho de Espiga Branca had greater total Na^+ influx, K^+ efflux and H^+ influx compared to Gladius at the root elongation zone (Fig. 5 d,e,f).

In contrast, both cultivars had net Na^+ influx for the first few minutes followed by a gradual net efflux at the maturation zone of the primary root (Supplementary Fig. 5a). As expected salt stress induced K^+ efflux in both cultivars (Supplementary Fig. 5b). However, there was no

significant difference in net or total Na^+ and K^+ fluxes observed between the two cultivars, while Mocho de Espiga Branca had 2-fold greater net H^+ efflux than Gladius (Supplementary Fig. 5 a-f).

Discussion

A bread wheat landrace, Mocho de Espiga Branca, was identified with significantly higher leaf Na^+ concentrations and the ability to maintain growth under high salinity. DNA sequencing revealed a naturally occurring SNP in the coding region of the Na^+ transporter TaHKT1;5-D, resulting in a L190P amino acid residue change. This variation disrupted the capability of TaHKT1;5-D to retrieve Na^+ from the xylem, due to the protein being unable to transport Na^+ and/or degradation of the TaHKT1;5-D L190P variant.

3D structural modelling of TaHKT1;5-D and TaHKT1;5-D L190P revealed the important role of the L190P substitution in determining the functional properties of Na^+ transport in TaHKT1;5-D. The lack of the cooperative binding networks around α-helix 4 of TaHKT1;5-D L190P within the P190 environment (Fig. 3d) imposes a severe structural rigidity on the 3D folding of this transporter. The more obtuse packing angle between α-helix 4 and α-helix 5 of TaHKT1;5-D L190P compared to that in TaHKT1;5-D, indicated that the proline position affects packing of α-helices in this specific environment (Fig. 3d). Therefore, this α-helix is unlikely to function properly in the structural context preventing Na^+ ion conductance. In TaHKT1;5-D, a positive correlation was identified between structural characteristics of α-helix 4 and α-helix 5 (trends in angles based on α-helical planes), differences in Gibbs free energies of forward (L190P) and reverse (P190L) mutations and the ability to conduct Na^+. The inability of the Mocho de Espiga Branca L190P variant to transport Na^+ was confirmed by expressing the gene in *X. laevis* oocytes (Fig. 4a).

Studies also identified differences between the location of the Mocho de Espiga Branca L190P variant and common TaHKT1;5-D. Unlike common TaHKT1;5-Ds, which are localised on the plasma membrane of stelar cells, the L190P variant exhibited greater localisation of GFP signal in internal structures (Fig. 4b), suggesting the protein is being retained internally and/or is being targeted for degradation. Whether the TaHKT1;5-D L190P is functional and/or not on the

correct membrane, Mocho de Espiga Branca will not be able retrieve Na^+ from the xylem (Fig. 4c), explaining why this accession has high leaf blade and leaf sheath Na^+ (Fig. 1 and 2).

This work is, to our knowledge, the first that shows a naturally occurring mutation in *TaHKT1;5* directly effects both the Na^+ transport properties of the protein and the plant phenotype. Even with a samll amount of salt in the soil mixture of the 0 mM NaCl pot experiment, which is not present in hydroponics, allowed the accumulation of high levels of shoot Na^+ in Mocho de Espiga Branca compared to Gladius and Scout in this study (Supplimentary Table 1). Previously, differences in the amino acid sequences between Nipponbare and Pokkali *OsHKT1;5* were hypothesised to be responsible for differences in shoot Na^+ accumulation, however, the transport properties of these proteins were not directly tested[17], a similar observation was recently made in barley[18]. Similarly artificially induced mutations in TmHKT1;5-A, which occurred during cloning of the gene, were shown to disrupt Na^+ transport properties in *X. laevis* but this was not linked to a plant phenotype[19]. A similar natural HKT1;5 variant (L189P) has recently been identified in barley accessions accumulating high grain Na^+ concentration, which also lacked the ability to transport Na^+ in *X. laevis* oocytes and was similarly shown to be on internal subcellular structures (Houston et al. unpublished).

Both Mocho de Espiga Branca and Gladius had similar concentrations of K^+ in the xylem sap (Supplementary Fig. 4a), however Mocho de Espiga Branca accumulated less K^+ in the leaf blade and sheath (Supplementary Fig. 2a,b). The greater K^+ efflux at the root elongation zone in Mocho de Espiga Branca (Fig.5 b,e) suggests the significant reduction in K^+ in the leaf blade and sheath is associated with increased K^+ leakage from the roots. Root Na^+ and K^+ concentrations were similar between the two cultivars (Fig. 2d and Supplementary Fig. 2c), even though there was a greater root Na^+ influx (Fig. 5a,d), increased shoot Na^+ (Fig. 2b,c), a higher root K^+ efflux (Fig. 5b,e) and reduced shoot K^+ (Supplementary Fig. 2a,b) in Mocho de Espiga Branca. Bread wheat may have a mechanism, which enables the maintenance of optimal

root Na^+ and K^+ concentrations contributing to the tolerance of the whole plant to salinity stress. In both cultivars, a high concentration of Cl^- was transported in the xylem sap (Supplementary Fig. 4b), which accumulated in the leaf sheath to a greater extent than the leaf blade (Supplementary Fig. 2d,e). This is in agreement with previous findings of Cl^- partitioning into the leaf sheath in response to salinity and suggests that the leaf sheath may have an important role in Cl^- exclusion preventing it from accumulating to toxic concentrations in the leaf blade[20,21].

Based on the observed functional defects in Na^+ transport resulting from the TaHKT1;5-D L190P variant and the ion analysis findings in this study, we propose a model to compare root-to-shoot ion transport between Mocho de Espiga Branca and Gladius (Fig. 6). Due to the naturally occurring SNP in *TaHKT1;5-D*, we suggest that Mocho de Espiga Branca has impaired retrieval of Na^+ from the root xylem which results in a greater influx of Na^+ in the xylem sap and a higher accumulation in the leaf blade and sheath compared to Gladius (Fig. 6).

The results of this study confirm the importance of *TaHKT1;5-D* in the Na^+ exclusion mechanism of bread wheat to limit the levels of Na^+ that accumulate. It is evident, however, that *TaHKT1;5-D* does not represent the only mechanism responsible for the salinity tolerance of a whole plant, as Mocho de Espiga Branca maintained similar tolerance to Gladius and Scout despite carrying the non-functional *TaHKT1;5-D*. It appears that although *TaHKT1;5-D* has a key role in Na^+ exclusion, salinity tolerance in bread wheat may not necessarily be entirely related to the plants ability to maintain a low shoot Na^+ concentration. The lack of a relationship between shoot Na^+ concentration and salinity tolerance in bread wheat has been observed in other studies[15,22]. This raises the question of how Mocho de Espiga Branca and these other bread wheat accessions maintain growth despite accumulating a high concentration of shoot Na^+? There must be other tolerance mechanisms, such as tissue tolerance, that are responsible for the plant's ability to tolerate high shoot Na^+ concentrations under salinity. Tissue tolerance

mechanisms, such as vacuolar Na^+ compartmentation, the synthesis of compatible solutes and production of enzymes responsible for reactive oxygen species (ROS) metabolism are reported to be essential in plant growth maintenance[4,23]. Specific signalling pathway mechanisms, such as those for ROS, which have been shown to play a role in regulating vasculature Na^+ concentrations[24,25], or Ca^{2+} pathways, which regulate gene expression and protein activities[26,27], could also be important for the plant and/or cell's ability to tolerate high concentrations of shoot Na^+. Therefore, future studies towards improving salinity tolerance of bread wheat should focus on identifying genetics and physiological mechanisms involved in the plant's tolerance to high shoot Na^+ (tissue tolerance) rather than preferentially focusing on Na^+ exclusion. This will now be easier, knowing it is possible for wheat to survive high shoot Na^+ concentrations.

In summary, this study identified a bread wheat landrace, Mocho de Espiga Branca that maintains shoot growth while accumulating very high leaf Na^+ concentrations under salinity – a novel bread wheat line with tissue tolerance. A naturally occurring SNP variation in the coding region of *TaHKT1;5-D* of Mocho de Espiga Branca results in the amino acid residue substitution L190P in the Na^+ transporter TaHKT1;5-D, and this single substitution appeared to negatively affect the Na^+ transport function of the protein, which results in high leaf Na^+ concentrations. Access to both Mocho de Espiga Branca and the CAPS marker tsl2SALTY-4D for tracking the SNP variation in TaHKT1;5-D will allow identification of other bread wheat with high leaf Na^+ allele, thereby providing more plant materials to understand salinity tissue tolerence mechnisms better. This will enable plant breeders to develop salinity tolerant bread wheat varieties in the future.

Online Methods

Plant materials and growth condition

Two Australian commercial bread wheat cultivars Gladius and Scout and a set of 73 bread wheat diversity lines consisting of advanced cultivars, landraces and synthetic hexaploids were initially screened for salinity tolerance in this study[28]. In the subsequent physiological characterizations, one of the 73 bread wheat diversity lines, a Portuguese landrace Mocho de Espiga Branca, and the commercial cultivars Gladius and Scout were used. Plants in all the glasshouse experiments were grown under natural light with a daytime temperature at 22 °C and 15 °C at night.

Screening of bread wheat diversity set in a pot trial

A total of 75 lines (Gladius and Scout together with the 73 diversity lines) were screened for salinity tolerance in a fully automated conveyor system within a temperature controlled Smarthouse at the Australian Plant Phenomics Facility (The Plant Accelerator®, University of Adelaide, Australia; Latitude: -34.971366°, Longitude: 138.639758°) between August and September of 2014. Uniform sized seeds of each line were placed into 50 mL polypropylene tubes and imbibed in reverse osmosis (RO) water at room temperature for 4 h, tubes were drained and placed in the dark at 4 ºC for three days before sowing. Three seeds from each line were sown in a free-draining plastic pot (145 mm diameter × 190 mm height) filled with 2.5 kg of a soil mixture (50% (v/v) University of California mix, 35% (v/v) peat mix and 15% (v/v) clay loam). The pots were arranged according to a split-plot experimental design with two consecutive pots forming a main plot. The lines were allocated to the main plots and were unequally replicated with Gladius and Scout replicated 12 times, 21 randomly-selected lines of the 73 diversity lines were replicated 4 times and the remaining 52 lines were replicated three times. The subplot design randomized the two treatment levels (0 and 100 mM NaCl) in each main plot. The main plot design was a blocked row-and-column design generated using DiGGer[29] and the subplot randomization was generated using dae[30], packages for the R

statistical computing environment[31]. At the emergence of the 2nd leaf, plants were thinned to one uniformly sized plant per pot. At emergence of the 3rd leaf, pots were loaded onto an individual cart in the Smarthouse, where they were weighed daily and automatically watered to maintain the soil water content in each pot at 17% (w/w). At the emergence of the 4th leaf, 213 mL of either 0 or 170 mM NaCl solution was applied to a saucer below each pot. Plants were not watered again until the soil water content reduced below 17% (w/w), and then each pot was watered again daily to maintain a final treatment concentration of 0 or 100 mM NaCl in the respective pot.

The shoot area of each plant was non-destructively imaged using a LemnaTec 3D Scanalyzer system (LemnaTec GmbH) for a total of 15 days (4 days before and 11 days after the NaCl treatment). Three red-green-blue (RGB) images (one top view and two side view images with a 90° angle) were recorded daily for each plant to calculate the projected shoot area (PSA) in pixels. 11 days after the NaCl treatment, the 4th leaf blade of each plant was collected, weighed and dried in an oven at 60 °C for two days before the dry weight was recorded. The dried 4th leaf blade was subsequently used for measuring Na^+, K^+ and Cl^- concentrations.

Determining leaf blade, leaf sheath and root Na^+ concentration in hydroponics

To measure the Na^+, K^+ and Cl^- concentrations in the 4th leaf blade and sheath and roots, Mocho de Espiga Branca, Gladius and Scout were grown using a fully supported hydroponics system under three concentrations of NaCl (0, 150 and 200 mM) in a controlled glasshouse at The Plant Accelerator® between June and August 2017. The hydroponic system was equipped with a trolley fitted with two growth trays each containing 42 tubes filled with polycarbonate pellets and a tank containing 80 L of a modified Hoagland solution (mM): NH_4NO_3 (0.2); KNO_3 (5.0); $Ca(NO_3)_2 \cdot 4H_2O$ (2.0); $MgSO_4 \cdot 7H_2O$ (2.0); KH_2PO_4 (0.1); $Na_2Si_3O_7$ (0.5); NaFe(III)EDTA (0.05); $MnCl_2 \cdot 4H_2O$ (0.005); $ZnSO_4 \cdot 7H_2O$ (0.01); $CuSO_4 \cdot 5H_2O$ (0.0005) and $Na_2MoO_3 \cdot 2H_2O$ (0.0001). Uniform sized seeds from each genotype were surface sterilized using ultraviolet (UV)

light for two min and germinated in petri dishes on moist filter paper for 4 days at room temperature before transplanting. 14 replicates from each cultivar were grown in each treatment trolley. The NaCl treatment was applied at the emergence of the 4th leaf by adding 116.88 g of NaCl twice daily for a 25 mM NaCl increment until a final concentration of either 150 mM or 200 mM was reached, and no NaCl was added to the 0 mM NaCl treatment. 3.8 g of supplemental $CaCl_2 \cdot 2H_2O$ was added into the 150 and 200 mM NaCl treatment tanks at each 25 mM NaCl increment in order to maintain constant Ca^{2+} activity in all three treatments. The plants were irrigated by the nutrient solution in a 20 min flood and rain cycle and the complete nutrient solution was replaced every seven days. The pH of the solution was maintained between 6.5 and 7.0 throughout the experiment using a 3.2% (v/v) HCl solution and a portable waterproof specific Ion–pH–mV–Temperature meter (Modal WP-90, TPS Pty Ltd, Australia). After 21 days of NaCl treatment, the 4th leaf blade and sheath and the remaining shoots were sampled separately and weighed. Plant roots were weighed after sampling and approximately 5 cm of the root tip was used for RNA extraction. The roots from the 150 mM and 200 mM treatments were rinsed in 10 mM $CaSO_4$ solution and blotted on paper towel to remove traces of NaCl before sampling. The weighed 4th leaf blade, 4th leaf sheath, shoots and roots were dried in an oven at 60 °C for two days to record the dry weight. The dried 4th leaf blade and sheath and root tissue were used for the subsequent Na^+, K^+ and Cl^- concentration analysis.

Na^+, K^+ and Cl^- concentration analysis

The harvested dried 4th leaf blade and root samples were digested in 10 mL of 1% (v/v) HNO_3 (v/v), and the 4th leaf sheath was digested in 5 mL of 1% (v/v) HNO_3 (v/v) at 85 °C for 4 h in a SC154 HotBlock® (Environmental Express Inc., South Carolina, US). Na^+ and K^+ concentrations were measured using a flame photometer (Model 420; Sherwood Scientific Ltd., Cambridge, UK), and Cl^- concentration was measured using a chloride analyzer (Model 926; Sherwood Scientific Ltd., Cambridge, UK).

RNA extraction and cDNA synthesis

The harvested 5 cm root tips from the hydroponics experiment was snapped frozen in liquid nitrogen and stored at -80 °C until RNA extraction. The root tissue was ground to a fine powder using a 2010 Geno/Grinder® (SPEX SamplePrep) at 1000 ×g for 30 s, and total RNA was extracted from the tissue powder using a Direct-Zol RNA MiniPrep kit with DNase I treatment (Zymo Research) according to the manufacturer's instruction. Final elution was performed with 40 µL DNA/RNAase-Free water supplied and the eluted RNA was subsequently quantified using a ND-1000 Spectrophotometer (NanoDrop Technologies) and quantified on a 1% (w/v) agarose gel (Bioline) by electrophoresis. cDNA synthesis was performed on 500 ng of RNA using High Capacity cDNA Reverse Transcription Kit (Thermo Fisher Scientific) according to the manufacturer's instruction in a 20 µL reaction and stored at -20 °C until use.

***TaHKT1;5-D* coding sequence amplification and sequencing**

The entire coding sequence of the TaHKT1;5-D gene from Mocho de Espiga Branca, Gladius and Scout were amplified using Phusion® High-Fidelity DNA polymerase (New England Biolabs) following the manufacturer's instruction. The primers used for PCR amplification were: forward primer *cTaHKT1;5-D_FP_1* (5'-ATGGGTTCTTTGCATGTCTCCT-3') and reverse primer *cTaHKT1;5-D_RP_1551* (5'-TTATACTATCCTCCATGCCTCGC-3') (Supplementary Table 2). PCR was conducted on a T100™ Thermal Cycler (Bio-Rad) using the following conditions: initial denaturation at 98 °C for 30 s, 35 cycles of 98 °C for 30 s, 64 °C for 30 s, 72 °C for 1 min, final extension at 72 °C for 10 min and held at 4 °C. The PCR product was visualized on a 1% (w/v) agarose gel (Bioline) by electrophoresis at 90 V for 1 h and the 1.5 kb target band was collected for purification using NucleoSpin® Gel and PCR Clean-up kit (Macherey-Nagel) according to the manufacturer's instruction prior to sequencing. Three replicates from each of Mocho de Espiga Branca, Gladius and Scout TaHKT1;5-D coding sequence were tested with primers listed in Supplementary Table 2 for Sanger sequencing carried out at the Australian Genome Research Facility (AGRF, South Australia).

TaHKT1;5-D gene expression in roots

To determine *TaHKT1;5-D* expression in Mocho de Espiga Branca, Gladius and Scout, a PCR was conducted on the synthesised cDNA in a 25 µL reaction consisting of 1 µL cDNA, 0.5 µL each of 10 µM forward primer 5'-CGACCAGAAAAGGATAACAAGCAT-3' and reverse primer 5'-AGCCAGCTTCCCTTGCCAA-3', 5 µL *Taq* 5× Master Mix (New England Biolabs) and 18 µL Milli-Q water (18.2 MΩ cm). The final PCR products were visualized on a 1% (w/v) agarose gel (Bioline) by electrophoresis at 90 V for 1 h. The targeted *TaHKT1;5-D* product was 283 bp. The *TaGAP* gene (230 bp) was used as a positive control and a Milli-Q water sample was included as a negative control.

To quantify *TaHKT1;5-D* expression in the root tissue of Mocho de Espiga Branca, Gladius and Scout, Real-time PCR was performed on five replicates from each of the cultivars using an Applied Biosystems™ QuantStudio™ 6 Flex (Life Technologies), and reference genes *TaActin* and *TaCyclophilin* were used. The reaction was performed in a 10 µL reaction consisting of two µL 1:20 diluted synthesised cDNA, 0.5 µL each of 10 µM forward and reverse primers stated above, 5 µL KAPA SYBR FAST 2× Master Mix (Sigma-Aldrich) and 2 µL Milli-Q water. The 283 bp final product from each cultivar was confirmed by Sanger sequencing carried out at AGRF (South Australia), and the reference genes stability was assessed with the geNorm function of qBASE+ software using default settings[32].

DNA extraction and quantification

Genomic DNA (gDNA) extraction of Mocho de Espiga Branca, Gladius, Scout and 70 bread wheat diversity lines was performed using a phenol/chloroform/iso-amyl alcohol extraction method as described elsewhere with modifications[33]. Briefly, the leaf tissue was frozen in a 10 mL tube at -80 °C and ground to a fine powder using a 2600 Cryo-Station (SPEX® SamplePrep) and a 2010 Geno/Grinder (SPEX® SamplePrep) at 1000 ×g for 30 s. 2 mL of gDNA extraction buffer [1% (w/v) sarkosyl, 100 mM Tris-HCl, 100 mM NaCl, 10 mM EDTA, 2% (w/v)

insoluble Polyvinyl-polypyrrolidone] was added to the ground tissue, vortexed, followed by the addition of 2 mL phenol/chloroform/iso-amyl alcohol (25:24:1). The sample was placed on ice for 20 min and vortexed thoroughly in every 5 min before centrifuging at 3630 ×g for 15 min. The supernatant was transferred into a labelled BD Vacutainer™ SST™ II Advance tube (Becton, Dickinson and Company, New Jersey, US) and 2 mL of phenol/chloroform/iso-amyl alcohol (25:24:1) was added. The sample was vortexed and centrifuged as above, and the supernatant was collected into a new 10 mL tube. The gDNA was precipitated using 2 mL of 100% (v/v) iso-propanol and 200 µL of 3 M sodium acetate (pH 4.8) and washed using 1 mL of 70% (v/v) ethanol before re-suspending overnight in 80 µL of R40 at 4°C. The re-suspended gDNA was quantified using a ND-1000 Spectrophotometer (NanoDrop Technologies).

Cleaved Amplified Polymorphic Sequence (CAPS) assay and genotyping

A CAPS marker tsl2SALTY-4D was designed to confirm the allele effect of the SNP (T/C) identified in Mocho de Espiga Branca *TaHKT1;5-D* for high leaf Na^+ concentration in comparison to Gladius and Scout. The extracted DNA from Mocho de Espiga Branca, Gladius, Scout and 68 bread wheat diversity lines were used for a PCR to amplify a 945 bp DNA fragment containing SNP. The PCR analysis was conducted in a 10 µL reaction consisting of 1 µg of DNA, 0.24 µL each of 10 µM forward primer 5'-ATGGGTTCTTTGCATGTCTCCT-3' and reverse primer 5'-CGCTAGCACGAACGCCG-3', 2 µL of *Taq* 5× Master Mix (New England Biolabs) and Milli-Q water. The reaction was performed on a T100™ Thermal Cycler (Bio-Rad) using the following conditions: initial denaturation at 95 °C for 4 min, 35 cycles of 95 °C for 30 s, 56 °C for 30 s, 68 °C for 1 min, final extension at 68 °C for 5 min and held at 12 °C. The PCR amplification was followed by digestion using the restriction enzyme *FauI*. It was conducted in a 10 µL reaction consisting of 1 µg of the PCR products, 0.4 µL of *FauI* enzyme (New England Biolabs), one µL of 10× CutSmart® Buffer (New England Biolabs) and Milli-Q water. The digestion was performed on a T100™ Thermal Cycler (Bio-Rad) for 1 h at 55 °C followed by 20 min of inactivation at 65 °C and held at 12 °C. The digested product was

visualized on a 2% (w/v) agarose gel (Bioline) by electrophoresis at 90 V for 90 min and the genotype of each line at the SNP position was confirmed according to the product bands on the gel. Lines which had the C:C genotype had two fragments present at 573 and 372 bp, whilst lines carrying the T:T genotype had a single fragment present.

Construction of 3D molecular models of TaHKT1;5-D and TaHKT1;5-D L190P

The most suitable template for wheat HKT1;5 transporter proteins was the *B. subtilis* KtrB K^+ transporter (Protein Data Bank accession 4J7C, chain I)[34] as previously identified[19]. The K^+ ion in KtrB was substituted by Na^+ during modelling of TaHKT1;5 proteins. 3D models of TaHKT1;5-D and TaHKT1;5-D L190P in complex with Na^+ were generated with Modeller 9v19[35] as described previously[17,36] incorporating Na^+ ionic radii[19] taken from the CHARMM force field[37], on the Linux station running the Ubuntu 12.04 operating system. Best scoring models (from an ensemble of 50) were selected based on the combination of Modeller Objective[38] and Discrete Optimised Protein Energy[39] functions, PROCHECK[40], ProSa 2003[41] and FoldX[42]. Structural images were generated in the PyMOL Molecular Graphics System V1.8.2.0 (Schrődinger LLC, Portland, OR, USA). Calculations of angles between selected α-helices in HKT1;5 models were executed in Chimera[43] and evaluations of differences ($\Delta\Delta G = \Delta G_{mut} - \Delta G_{wt}$) of Gibbs free energies was performed with FoldX[41]. Sequence conservation patterns were analysed with ConSurf[44,45] based on 3D models of TaHKT1;5-D using 370 sequences at the sequence identities of 30% and higher (specifications: HMMMER homolog search algorithm, UNIREF-90 Protein database with the E-value cut-off of 1×10^{-4}, Bayesian Model of substitution for proteins.

Characterization of TaHKT1;5-D from Mocho de Espiga Branca and Gladius in *X. laevis* oocytes

Na^+ transport properties of TaHKT1;5-D from Mocho de Espiga Branca and Gladius were characterized in *X. laevis* oocytes using two-electrode voltage clamping (TEVC) as previously

described[8,11]. pGEMHE-DEST containing *TaHKT1;5-D* was linearized using sbfI-HF (New England Biolabs) before synthesising cRNA using the mMESSAGE mMACHINE T7 Kit (Ambion) following manufacturer's instructions. 46 nL/23 ng of the cRNA from Mocho de Espiga Branca or Gladius, or equal volumes of RNA-free water (H_2O control) were injected into oocytes. Injected oocytes were incubated for 48 h and TEVC was carried out as described[11]. Membrane currents were recorded in the HMg solution (6 mM $MgCl_2$, 1.8 mM $CaCl_2$, 10 mM MES, and pH 6.5 adjusted with a Tris base) ± Na^+ glutamate. The osmolality of the solution was adjusted to 240 - 260 mOsmol/kg using mannitol and a micro-osmometer (Model 210, Fiske Associates Inc, USA).

Subcellular localisation of TaHKT1;5-D

Transient expression of fluorescent fusion proteins was performed as previously described[46]. In brief, *TaHKT1;5-D* coding sequences of Mocho de Espiga Branca and Gladius were recombined into pMDC43[47] to generate N-terminally green fluorescent protein (GFP) tagged proteins. The red fluorescent protein (RFP) tagged plasma membrane marker nCBL1-RFP that was used for co-localisation[48]. All constructs were transformed into *Agrobacterium tumefaciens* strain Agl-1 and agro-infiltration was performed on fully expanded leaves of 4- to 6-week-old tobacco (*Nicotiana benthamiana*) plants[46]. After two to three days, leaf sections were imaged using a Nikon A1R Confocal Laser-Scanning Microscope equipped with a 63× water objective lens and NIS-Elements C software (Nikon Corporation). Excitation/emission conditions were GFP (488 nm/500–550 nm) and RFP (561 nm/570–620 nm).

Xylem sap Na^+ and K^+ concentration analysis

Xylem sap was collected from hydroponically grown plants of Mocho de Espiga Branca and Gladius at 0 and 150 mM NaCl after 21 days from the start of the NaCl treatment. The shoot was cut off at the base of the plant and inserted into a Scholander-type pressure chamber (Model 1005, PMS Instrument Company, USA) to extrude the xylem sap by slowly filling the chamber

with compressed air. The sap was immediately collected into a clean, pre-weighed 1.5 mL tube. From the 0 mM NaCl treatment, xylem sap of seven plants from each cultivars was collected, and xylem sap of eight Mocho de Espiga Branca and seven Gladius plants was collected from the 150 mM NaCl treatment. Tubes containing the xylem sap was weighed for each plant and the samples were stored at 4°C until Na^+ and K^+ concentrations were measured using a flame photometer (Model 420, Sherwood Scientific Ltd., Cambridge, UK).

Net and total Na^+, K^+ and H^+ flux analyses using Microelectrode Ion Flux Estimation (MIFE)

To investigate whether there were differences in Na^+, K^+ and H^+ transport in the plant roots between Mocho de Espiga Branca and Gladius, net fluxes of Na^+, K^+ and H^+ were measured at root maturation and elongation zones using the non-invasive MIFE technique (University of Tasmania, Hobart, Australia)[49,50].

Root Na^+ retrieval measurements were performed at the elongation zone (approximately 600 µm from the root cap). Uniform sized sterilized seeds from Mocho de Espiga Branca and Gladius were germinated on moist filter paper in Petri dishes covered with aluminium foil, at 4 °C overnight and then placed at room temperature in the dark for three days before transplanting. 12 seedlings from each cultivar were transplanted into a hydroponic tank containing 10 L modified Hoagland solution as previously described. NaCl was added into the solution at an increment of 25 mM (14.16 g) twice daily for two days to achieve a final concentration of 100 mM NaCl. The pH of the solution was maintained between 6.5 and 7.0 throughout the experiment using 3.2% (v/v) of the HCl solution and a portable waterproof specific Ion–pH–mV–Temperature meter (Modal WP-90, TPS Pty Ltd, Australia). Two days after being exposed to 100 mM NaCl, the entire roots of Mocho de Espiga Branca (n = 9) and Gladius (n = 8) were first preconditioned in BSM solution containing 100 mM NaCl (0.2 mM KCl + 0.1 mM $CaCl_2 \cdot 2H_2O$ + 100 mM NaCl) in a Petri dish for 30 min and then the primary

root was immobilized on a 10 mL perspex measuring chamber containing 7 mL of the same BSM. The steady-state fluxes were measured for 5 min in the initial BSM solution before changing the bathing solution to 7 mL of the new BSM solution containing 0.6 mM NaCl (0.2 mM KCl + 0.1 mM $CaCl_2 \cdot 2H_2O$ + 0.6 mM NaCl). The resulting fluxes were measured for 25 min and the integral of each replication was added to derive the cumulative total fluxes. The osmolality of the two BSM solutions and the Hoagland solution were maintained between 208 and 222 mOsmol/kg using mannitol and a vapour pressure osmometer (Model 5500, Wescor, Inc., USA).

Root Na^+ uptake measurements were performed at the maturation zone (beyond 2.5 cm from root tip), uniform sized sterilized seeds were germinated as described above, placed at 4 °C overnight and placed at room temperature in the dark for three days before measurement. The primary root of Mocho de Espiga Branca (n = 12) and Gladius (n = 11) seedlings was immobilized on a 10 mL perspex measuring chamber containing 6 mL of the BSM solution (0.2 mM KCl + 0.1 mM $CaCl_2 \cdot 2H_2O$ + 0.6 mM NaCl) and pre-conditioned for 20 min before recording steady-state Na^+, K^+ and H^+ fluxes for 5 min then 100 mM NaCl was added and the resulting fluxes were recorded for 25 min.

Statistical analysis

Prism 7 for Windows (version 7.02; GraphPad Software, Inc.) was used to generate graphs. GenStat® 15th edition for Microsoft Windows (version 15.3.09425; VSN International Ltd, UK) was used to perform an Analysis of Variance (ANOVA) and Tukey's multiple comparison test was used to determine which means were significantly different at a probability level of $p \leq 0.05$.

Data availability statement

Imaging data obtained from the APPF The Plant Accelerator is published online after publication and available from https://www.plantphenomics.org.au/data/#zegami. The remaining datasets generated during and/or analysed during the current study are available from the corresponding author on reasonable request.

Acknowledgments

This project was funded by the Grains Research and Development Corporation (GRDC): Project UA00145, UA00151, and the GRDC and the International Wheat Yield Partnership (IWYP): Projects IWYP39/ACP0009; IWYP60/ANU00027. The Australian Centre for Plant Functional Genomics (ACPFG) was jointly funded by the Australian Research Council (ARC) and the GRDC, SW was supported by the ARC DE160100804. The Plant Accelerator®, Australian Plant Phenomics Facility, is funded under the National Collaborative Research Infrastructure Strategy (NCRIS). The authors thank Assoc. Prof. Kenneth Chalmers and Dr. Melissa Garcia for providing seeds, The Plant Accelerator® for assisting with the glasshouse experiments and Adelaide microscopy for assistance with imaging. We also thank Prof. Rana Munns (CSIRO, Black Mountain, Canberra and University of Western Australia, Perth, Australia) for valuable comments and discussion on the manuscript. CB thanks the China Scholarship Council and the University of Adelaide Joint Postgraduate Scholarships Program for her PhD stipend, and acknowledges the Research Travel Scholarship and the Global Learning Travel Grant at the University of Adelaide and The Plant Nutrition Trust for financial support to attend conferences.

Author Contributions

CBo conducted the hydroponics experiment, gene sequencing, genotyping, data analysis and wrote manuscript; RKS conceived the work, screened the wheat diversity lines for salinity tolerance and identified Mocho de Espiga Branca, interpreted the work and contributed to supervision; JB conducted the MIFE experiment, xylem sap collection and performed data analysis; MH conducted 3D protein modelling and analysed sequence conservation patterns, and interpreted the results; JQ and AS cloned the genes into the appropriated vectors, JQ performed the electrophysiological work in *X. laevis* oocytes and data analysis; SW conducted the confocal subcellular localisation work; CBr generated the experimental design of the Smarthouse experiment; BB provided advice for and supervised the Smarthouse phenotyping experiment; MG assisted conceiving the work; ASP conceived the work, interpreted the work and contributed to supervision; SJR conceived the work, interpreted the work and contributed to supervision. All authors reviewed and commented on the manuscript.

Competing Interest

The authors declare that they have no conflict of interest.

References

1. FAO. FAO soils portal. (2019). http://www.fao.org/soils-portal/soil-management/management-of-some-problem-soils/salt-affected-soils/more-information-on-salt-affected-soils/en/. Accessed 26 May 2019.
2. Tester, M. & Langridge, P. Breeding technologies to increase crop production in a changing world. *Science* **327**, 818-822 (2010).
3. FAO. FAOSTAT. (2019). http://www.fao.org/faostat/en/#data/QC. Accessed 26 May 2019.
4. Munns, R. & Tester, M. Mechanisms of salinity tolerance. *Annual Review of Plant Biology* **59**, 651-681 (2008).
5. Hamamoto, S. *et al.* HKT transporters mediate salt stress resistance in plants: from structure and function to the field. *Current Opinion in Biotechnology* **32**, 113-120 (2015).
6. Platten, J.D. *et al.* Nomenclature for *HKT* transporters, key determinants of plant salinity tolerance. *Trends in Plant Science* **11**, 372-374 (2006).
7. Møller, I.S. *et al.* Shoot Na^+ exclusion and increased salinity tolerance engineered by cell type-specific alteration of Na^+ transport in *Arabidopsis*. *The Plant Cell* **21**, 2163-2178 (2009).
8. Byrt, C.S. *et al.* The Na^+ transporter, TaHKT1;5-D, limits shoot Na^+ accumulation in bread wheat. *The Plant Journal* **80**, 516-526 (2014).
9. Munns, R., Rebetzke, G.J., Husain, S., James, R.A. & Hare, R.A. Genetic control of sodium exclusion in durum wheat. *Australian Journal of Agricultural Research* **54**, 627-635 (2003).
10. James, R.A., Davenport, R.J. & Munns, R. Physiological characterization of two genes for Na^+ exclusion in durum wheat, *Nax1* and *Nax2*. *Plant Physiology* **142**, 1537-1547 (2006).

11. Munns, R. *et al.* Wheat grain yield on saline soils is improved by an ancestral Na^+ transporter gene. *Nature Biotechnology* **30**, 360-364 (2012).

12. Ashraf, M. & O'leary, J. Responses of some newly developed salt-tolerant genotypes of spring wheat to salt stress: 1. Yield components and ion distribution. *Journal of Agronomy and Crop Science* **176**, 91-101 (1996).

13. Poustini, K. & Siosemardeh, A. Ion distribution in wheat cultivars in response to salinity stress. *Field Crops Research* **85**, 125-133 (2004).

14. Genc, Y. *et al.* Quantitative trait loci for agronomic and physiological traits for a bread wheat population grown in environments with a range of salinity levels. *Molecular Breeding* **32**, 39-59 (2013).

15. Genc, Y. *et al.* Bread wheat with high salinity and sodicity tolerance. *Frontiers in Plant Science* **10**, 1280 (2019).

16. Tilbrook, J. *et al.* Variation in shoot tolerance mechanisms not related to ion toxicity in barley. *Functional Plant Biology* **44**, 1194-1206 (2017).

17. Cotsaftis, O., Plett, D., Shirley, N., Tester, M. & Hrmova, M. A two-staged model of Na^+ exclusion in rice explained by 3D modeling of HKT transporters and alternative splicing. *PLoS ONE* **7**, e39865 (2012).

18. van Bezouw, R.F. *et al.* Shoot sodium exclusion in salt stressed barley (*Hordeum vulgare* L.) is determined by allele specific increased expression of *HKT1; 5*. *Journal of Plant Physiology* **241**, 153029 (2019).

19. Xu, B. *et al.* Structural variations in wheat HKT1;5 underpin differences in Na^+ transport capacity. *Cellular and Molecular Life Sciences* **75**, 1133-1144 (2018).

20. Boursier, P., Lynch, J., Lauchli, A. & Epstein, E. Chloride partitioning in leaves of salt-stressed sorghum, maize, wheat and barley. *Functional Plant Biology* **14**, 463-473 (1987).

21. Boursier, P. & Läuchli, A. Mechanisms of chloride partitioning in the leaves of salt-stressed *Sorghum bicolor* L. *Physiologia Plantarum* **77**, 537-544 (1989).

22. Genc, Y., McDonald, G.K. & Tester, M. Reassessment of tissue Na^+ concentration as a criterion for salinity tolerance in bread wheat. *Plant Cell & Environment* **30**, 1486-1498 (2007).

23. Flowers, T.J. & Colmer, T.D. Salinity tolerance in halophytes. *New Phytologist* **179**, 945-963 (2008).

24. Mittler, R. *et al.* ROS signaling: the new wave? *Trends in Plant Science* **16**, 300-309 (2011).

25. Suzuki, N., Koussevitzky, S., Mittler, R. & Miller, G. ROS and redox signalling in the response of plants to abiotic stress. *Plant, Cell and Environment* **35**, 259-270 (2012).

26. Kudla, J., Batistič, O. & Hashimoto, K. Calcium signals: the lead currency of plant information processing. *The Plant Cell* **22**, 541-563 (2010).

27. Thoday-Kennedy, E.L., Jacobs, A.K. & Roy, S.J. The role of the CBL–CIPK calcium signalling network in regulating ion transport in response to abiotic stress. *Plant Growth Regulation* **76**, 3-12 (2015).

28. Garcia, M. *et al.* Genome-wide association mapping of grain yield in a diverse collection of spring wheat (*Triticum aestivum* L.) evaluated in southern Australia. *PLoS ONE* **14**, e0211730. (2019).

29. Coombes, N. DiGGer design search tool in R. in *New South Wales Department of Primary Industry) Available at http://nswdpibiom.org/austatgen/software/ [Verified 29 August 2017]* (2009).

30. Brien, C. Dae: Functions useful in the design and ANOVA of experiments. R package version 2.3-1. (2014).

31. R Core Team. R: a language and environment for statistical computing. (R Foundation for statistical computing, Vienna, 2014).

32. Hellemans, Jan, et al. qBase relative quantification framework and software for management and automated analysis of real-time quantitative PCR data. *Genome Biology* **8**, R19 (2007).

33. Rogowsky, P.M., Guidet, F.L.Y., Langridge, P., Shepherd, K.W. & Koebner, R.M.D. Isolation and characterization of wheat-rye recombinants involving chromosome arm 1ds of wheat. *Theoretical and Applied Genetics* **82**, 537-544 (1991).

34. Vieira-Pires, R.S., Szollosi, A. & Morais-Cabral, J.H. The structure of the KtrAB potassium transporter. *Nature* **496**, 323-328 (2013).

35. Sali, A. & Blundell, T.L. Comparative protein modeling by satisfaction of spatial restraints. *Journal of Molecular Biology* **234**, 779-815 (1993).

36. Waters, S., Gilliham, M. & Hrmova, M. Plant high-affinity potassium (HKT) transporters involved in salinity tolerance: structural insights to probe differences in ion selectivity. *International Journal of Molecular Sciences* **14**, 7660-7680 (2013).

37. Brooks, B.R. *et al.* CHARMM: The biomolecular simulation program. *Journal of Computational Chemistry* **30**, 1545-1614 (2009).

38. Shen, M.Y. & Sali, A. Statistical potential for assessment and prediction of protein structures. *Protein Science* **15**, 2507-2524 (2006).

39. Eswar, N., Eramian, D., Webb, B., Shen, M.-Y. & Sali, A. Protein structure modeling with MODELLER. in *Structural Proteomics: High-Throughput Methods*, Vol. 426 (eds. Kobe, B., Guss, M. & Huber, T.) 145-159 (2008).

40. Laskowski, R.A., Macarthur, M.W., Moss, D.S. & Thornton, J.M. PROCHECK: a program to check the stereochemical quality of protein structures. in *Journal of Applied Crystallography* Vol. 26 283-291 (1993).

41. Sippl, M.J. Recognition of errors in three-dimensional structures of proteins. *Proteins-Structure Function and Genetics* **17**, 355-362 (1993).

42. Schymkowitz, J.W.H. *et al.* Prediction of water and metal binding sites and their affinities by using the Fold-X force field. *Proceedings of the National Academy of Sciences of the United States of America* **102**, 10147-10152 (2005).

43. Pettersen, E.F. *et al.* UCSF Chimera - a visualization system for exploratory research and analysis. *Journal of Computational Chemistry* **25**, 1605-1612 (2004).

44. Landau, M. *et al.* ConSurf 2005: the projection of evolutionary conservation scores of residues on protein structures. *Nucleic Acids Research* **33**, W299-W302 (2005).

45. Celniker, G. *et al.* ConSurf: Using evolutionary data to raise testable hypotheses about protein function. *Israel Journal of Chemistry* **53**, 199-206 (2013).

46. Henderson, S.W. *et al.* Grapevine and arabidopsis cation-chloride cotransporters localize to the golgi and trans-golgi network and indirectly influence long-distance ion transport and plant salt tolerance. *Plant Physiology* **169**, 2215-2229 (2015).

47. Curtis, M.D. & Grossniklaus, U. A gateway cloning vector set for high-throughput functional analysis of genes in planta. *Plant Physiology* **133**, 462-469 (2003).

48. Batistic, O., Sorek, N., Schultke, S., Yalovsky, S. & Kudla, J. Dual fatty acyl modification determines the localization and plasma membrane targeting of CBL/CIPK Ca^{2+} signaling complexes in *Arabidopsis*. *The Plant Cell* **20**, 1346-1362 (2008).

49. Bose, J. *et al.* Rapid regulation of the plasma membrane H^+-ATPase activity is essential to salinity tolerance in two halophyte species, *Atriplex lentiformis* and *Chenopodium quinoa*. *Annals of Botany* **115**, 481-494 (2015).

50. Newman, I.A. Ion transport in roots: measurement of fluxes using ion-selective microelectrodes to characterize transporter function. *Plant Cell & Environment* **24**, 1-14 (2001).

Figures

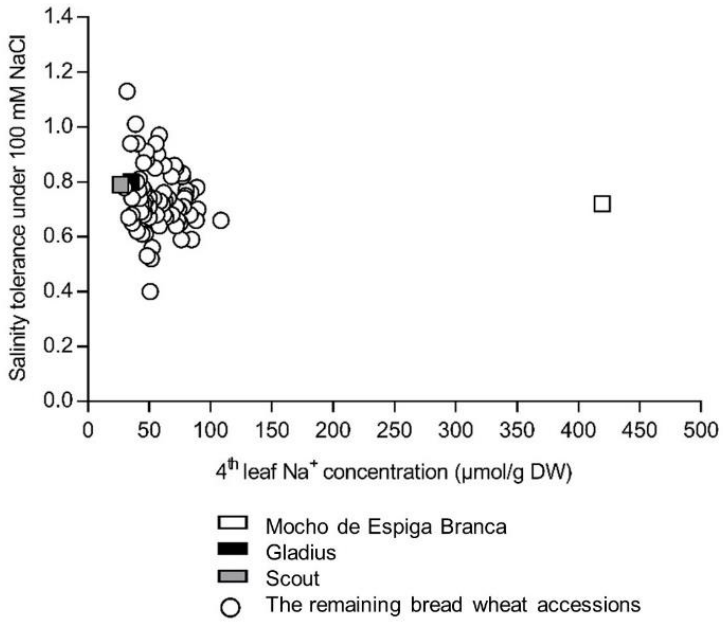

Fig. 1: Salinity tolerance and 4th leaf Na^+ concentration of Mocho de Espiga Branca relative to 72 bread wheat diversity lines and two Australian cultivars Gladius and Scout in soil with 100 mM NaCl. The 4th leaf Na^+ concentration is determined 11 days after treatment with 100 mM NaCl. Salinity tolerance is defined as projected shoot area (PSA) under 100 mM NaCl relative to 0 mM NaCl determined from the final day of imaging. Data presented as means (n = 3-4 except for Gladius and Scout, where n = 12). The standard error of the mean (SEM) for the 4th leaf Na^+ concentration is presented in Supplementary Table 1.

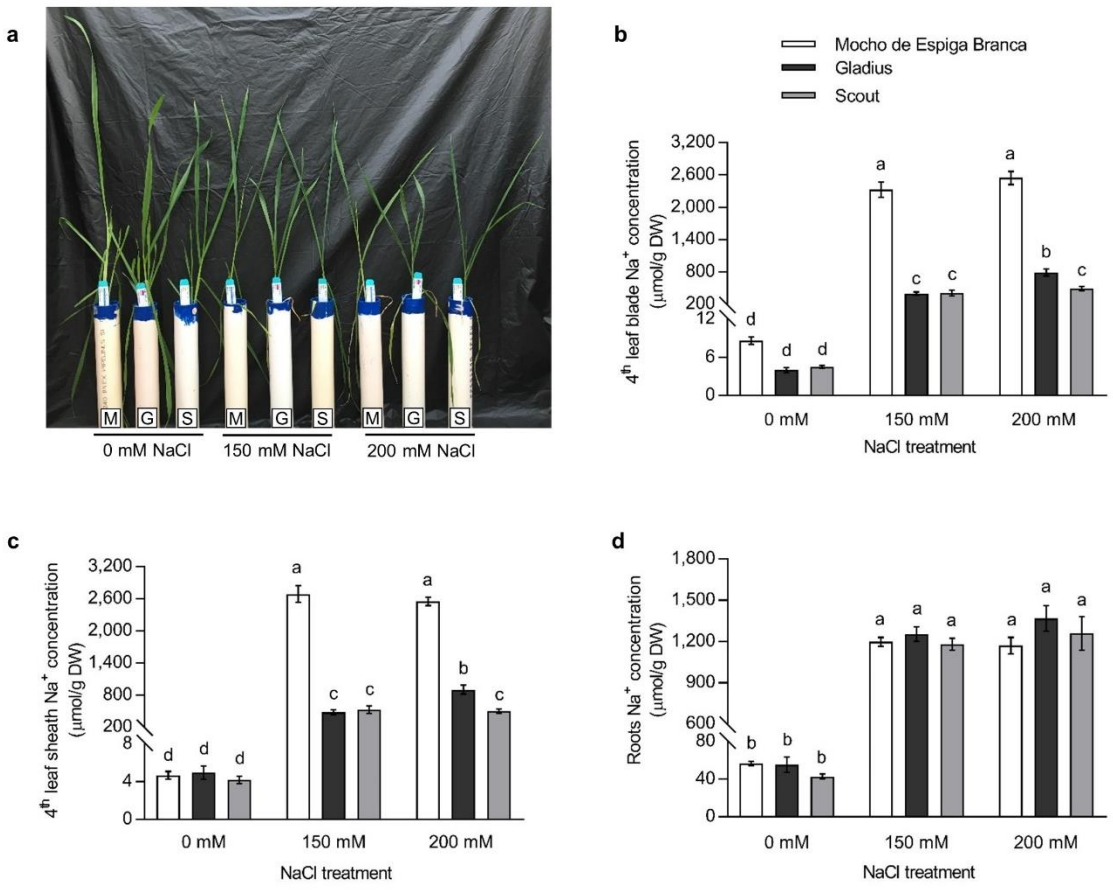

Fig. 2: Na^+ concentration in the 4th leaf blade, sheath, and roots of Mocho de Espiga Branca, Gladius and Scout in hydroponics. **a**, Representative image of 6-week-old plants from the hydroponic experiment with 0, 150 and 200 mM NaCl treatments applied at the emergence of the 4th leaf. M = Mocho de Espiga Branca, G = Gladius and S = Scout. Na^+ concentration in **b,** 4th leaf blade; **c,** 4th leaf sheath and **d,** roots determined 21 days after treatments with 0, 150 and 200 mM NaCl. Data presented as means ± SEM (n = 14). Bars with different letters indicate significant differences determined by two-way ANOVA with Tukey's multiple comparison test at $p \leq 0.05$.

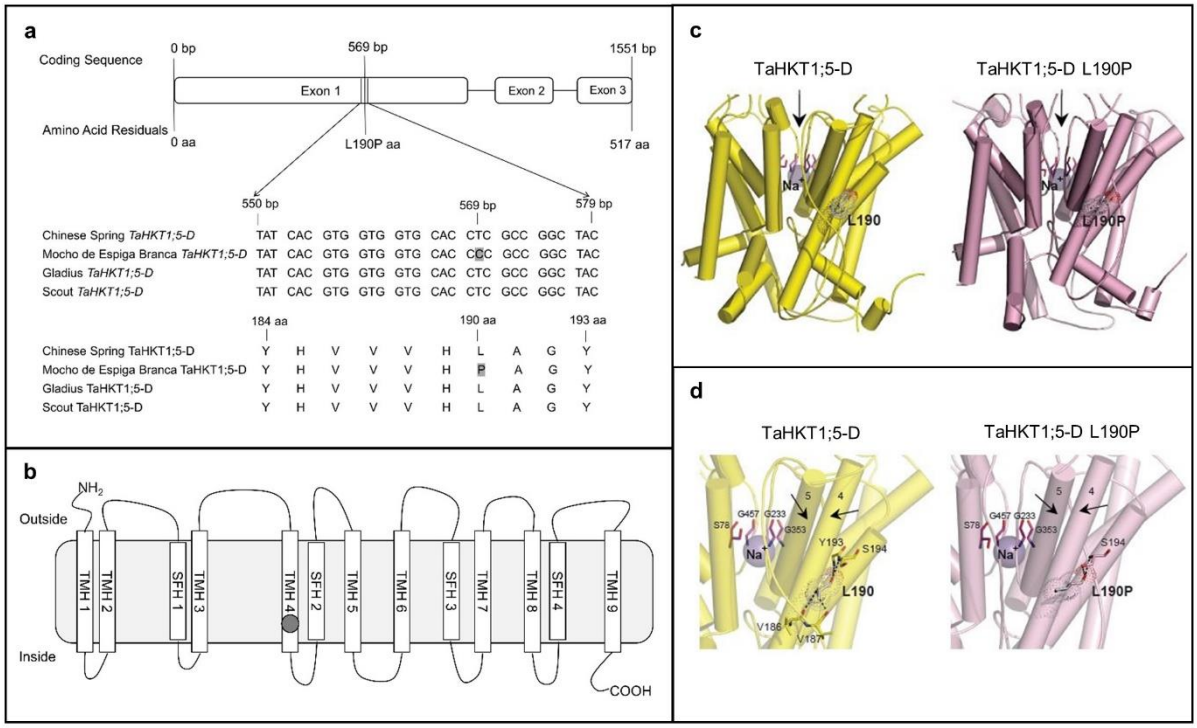

Fig. 3: A SNP in Mocho de Espiga Branca *TaHKT1;5-D* results in a L190P amino acid residue variation in the Na^+ transporter TaHKT1;5-D. **a,** Partial alignment of *TaHKT1;5-D* coding and amino acid sequences in Mocho de Espiga Branca, Gladius and Scout compared to Chinese Spring. **b,** Schematic of the TaHKT1;5-D protein showing the transmembrane α-helices (TMH 1-9) and selectivity filter α-helices (SFH 1-4) adapted from Xu et al. (2018); the Na^+ selectivity filter motif S78-G233-G353-G457 indicated in blank circles and location of the L190P variant indicated in a grey circle. **c,** Molecular models of TaHKT1;5-D (left, yellow) and TaHKT1;5-D L190P (right, salmon) transport proteins in cartoon representations with cylindrical α-helices illustrating 3D folds. Constrictions in selectivity filters are bound by four residues (cpk magenta sticks) that contain Na^+ ions (violet spheres). Black arrows illustrate directional flows of Na^+ that are likely to enter the permeation trajectory by-passing selectivity filter constrictions. Variant residues L190 and L190P (cpk sticks and dots, bold types) between wild-type TaHKT1;5-D and the L190P mutant are indicated; the dots illustrate volumes of van der Waals radii. **d,** Detailed views of α-helices, which neighbour selectivity filter constriction, containing Na^+ (violet spheres), located near selectivity filter residues S78, G233, G353, G457 (cpk magenta) for TaHKT1;5-D (left) and the L190P mutant (right), which are crucial for permeation

function. In each protein, polar contacts (cpk sticks and dots) of L190 (TaHKT1;5-D) and L190P (TaHKT1;5-D L190P) positioned on α-helices 4, are indicated by dashed lines (separations between 2.6 Å and 3.2 Å).

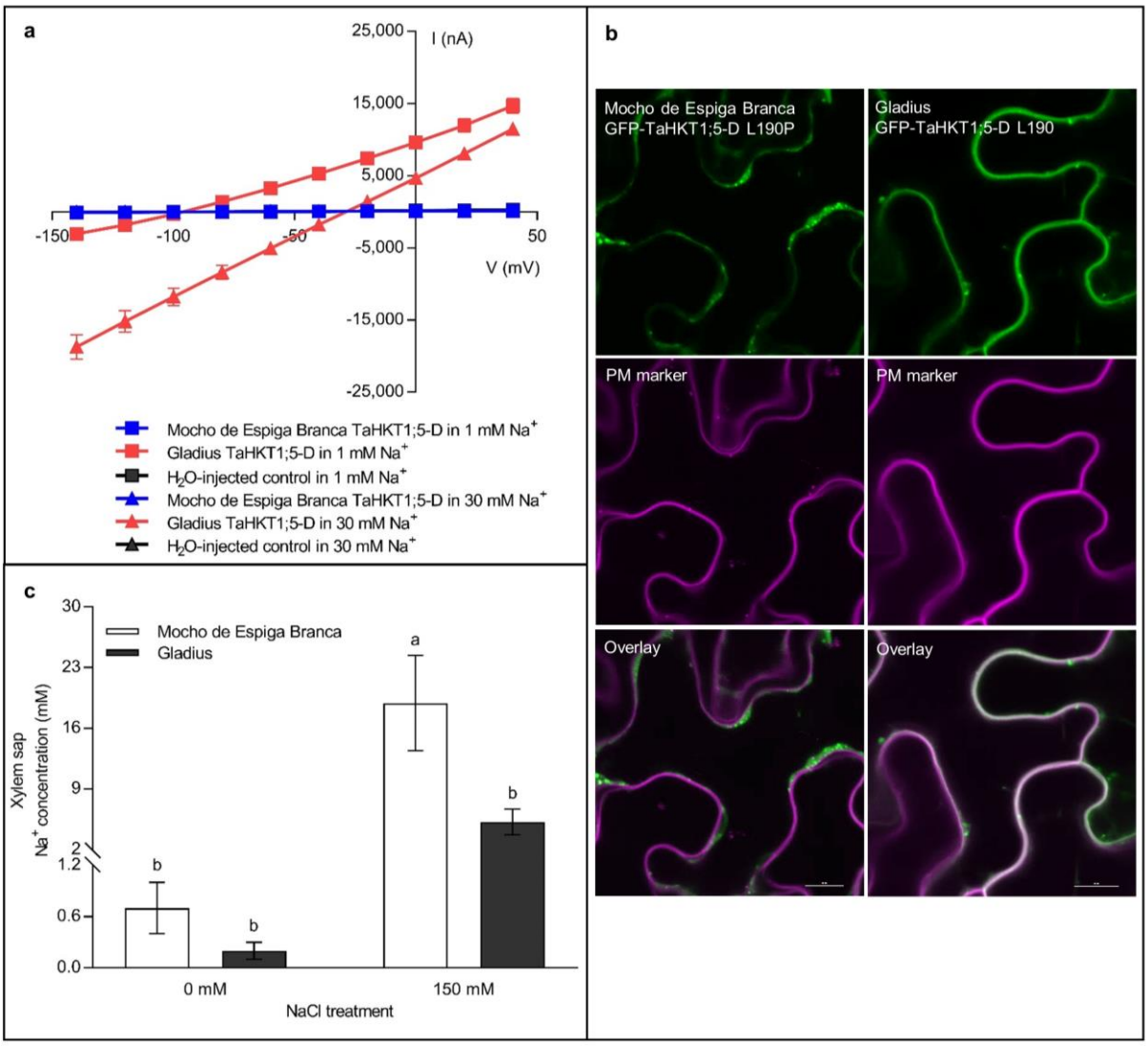

Fig. 4: The physiological characterisation of L190P variation in TaHKT1;5-D and the evaluation of the xylem sap Na^+ concentration in Mocho de Espiga Branca. **a,** Current-voltage (I-V) curve observed from Mocho de Espiga Branca (blue) or Gladius (red) *TaHKT1;5-D* cRNA-injected or H_2O-injected (black) *X. laevis* oocytes exposed to 1 mM Na^+ and 30 mM Na^+ glutamate at a voltage range from -120 to +40 mV. Data represents means ± SEM (*n* = 3-5). **b,** Transient co-expression of GFP-TaHKT1;5-D variants with a plasma membrane marker in *N. benthamiana* epidermal cells. Leaves were co-infiltrated with *Agrobacterium tumefaciens* strains harbouring either GFP-TaHKT1;5-D L190 (Gladius) or L190P (Mocho de Espiga Branca) and a plasma membrane marker CBL1n-RFP. GFP signal is shown in green in the left panel while RFP-signal is shown in magenta in the middle panel. Representative images are shown. Scale bars = 10 μm. **c,** The xylem sap Na^+ concentration of Mocho de Espiga Branca and Gladius under 0 and 150 mM NaCl concentrations. Xylem sap was collected from

hydroponically grown plants 21 days after 0 and 150 mM NaCl was applied at the emergence of 4th leaf. Bars with different letters indicate significant differences determined by two-way ANOVA with Tukey's multiple comparison test at $p \leq 0.05$.

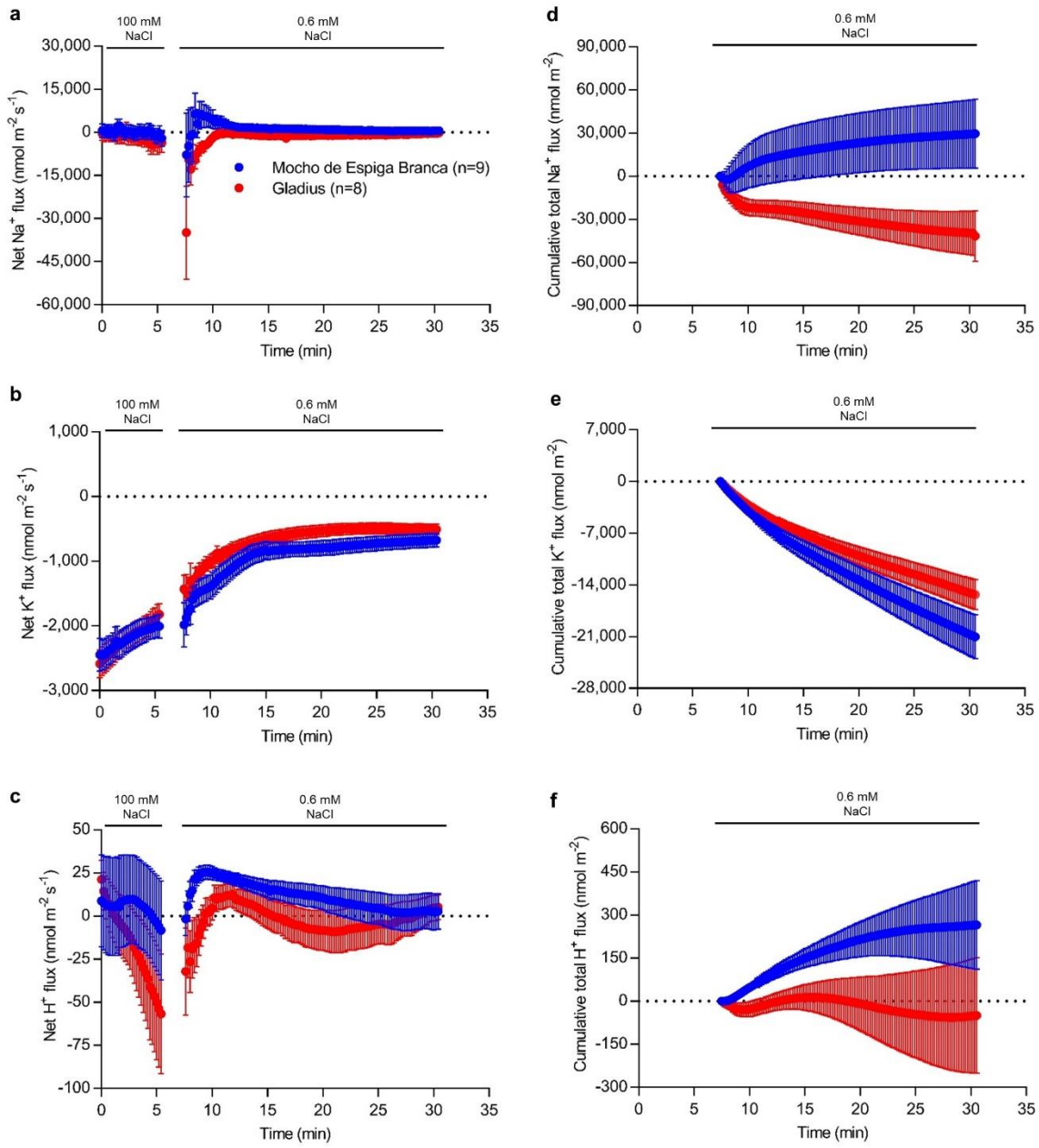

Fig. 5: Ion fluxes measured at the root elongation zone after removal from 100 mM NaCl. Six-seven-day old Mocho de Espiga Branca or Gladius seedlings were treated with 100 mM NaCl for two days before removal from the solution, the resultant ion fluxes were measured at the elongation zone (between 200 to 600 µm from the root cap) of the primary root of the plants for 25 min. Net **a,** Na^+; **b,** K^+ and **c,** H^+ fluxes. Cumulative total **d,** Na^+; **e,** K^+ and **f,** H^+ fluxes over 25 min. Data presented as means ± SEM (n = 8-9).

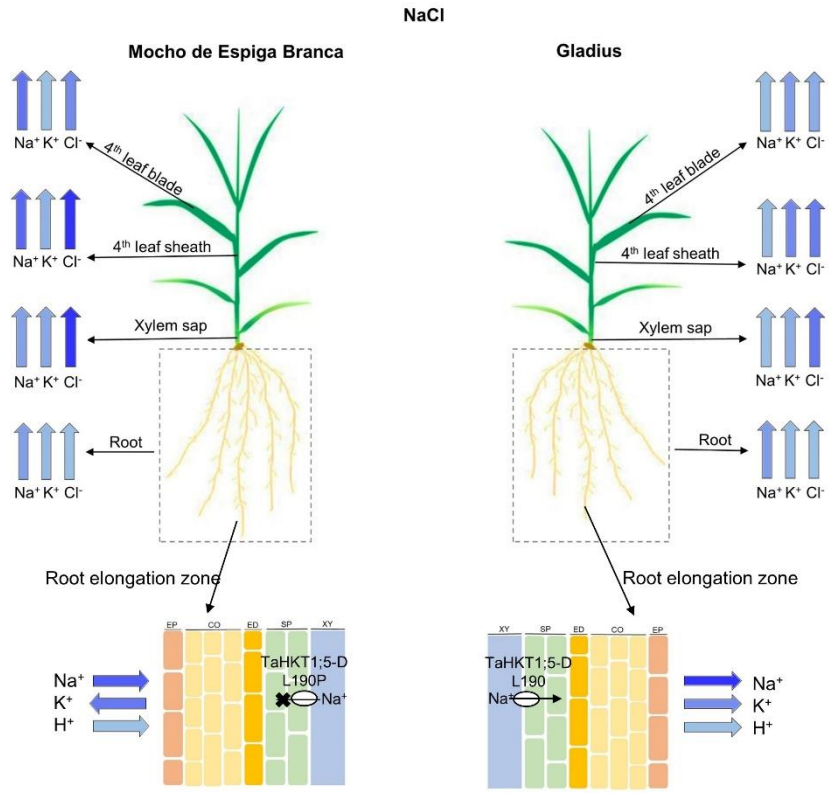

Fig. 6: Ion transport model for Mocho de Espiga Branca and Gladius plants under NaCl stress. Colour intensity of the arrows is proportional to the measured ion concentrations, with a greater intensity representing a higher concentration. At the root elongation zone, the direction of the arrow indicates the direction of the ion flux, EP = epidermis, CO = cortex, ED = endodermis, SP = stellar parenchyma and XY = xylem apoplast. TaHKT1;5-D L190P in Mocho de Espiga Branca and TaHKT1;5-D L190 in Gladius are indicated as a white circle. The TaHKT1;5-D L190P variant in Mocho de Espiga Branca leads to reduced retrieval of Na^+ from the xylem into the roots resulting in a greater influx of Na^+ in the xylem sap and a higher accumulation of Na^+ in the leaf blade and sheath compared to Gladius. Mocho de Espiga Branca also has greater Na^+ influx at the root elongation zone compared to Gladius. There was no difference in root Na^+ concentration between the two cultivars. The K^+ concentration was also similar between Mocho de Espiga Branca and Gladius both in the roots and xylem sap, however, Mocho de Espiga Branca had less K^+ in the leaf blade and sheath compared to Gladius. In both cultivars, a high concentration of Cl^- was transported in the xylem sap and accumulated to a high concentration in the leaf sheath compared to leaf blade.

Supplementary Figures

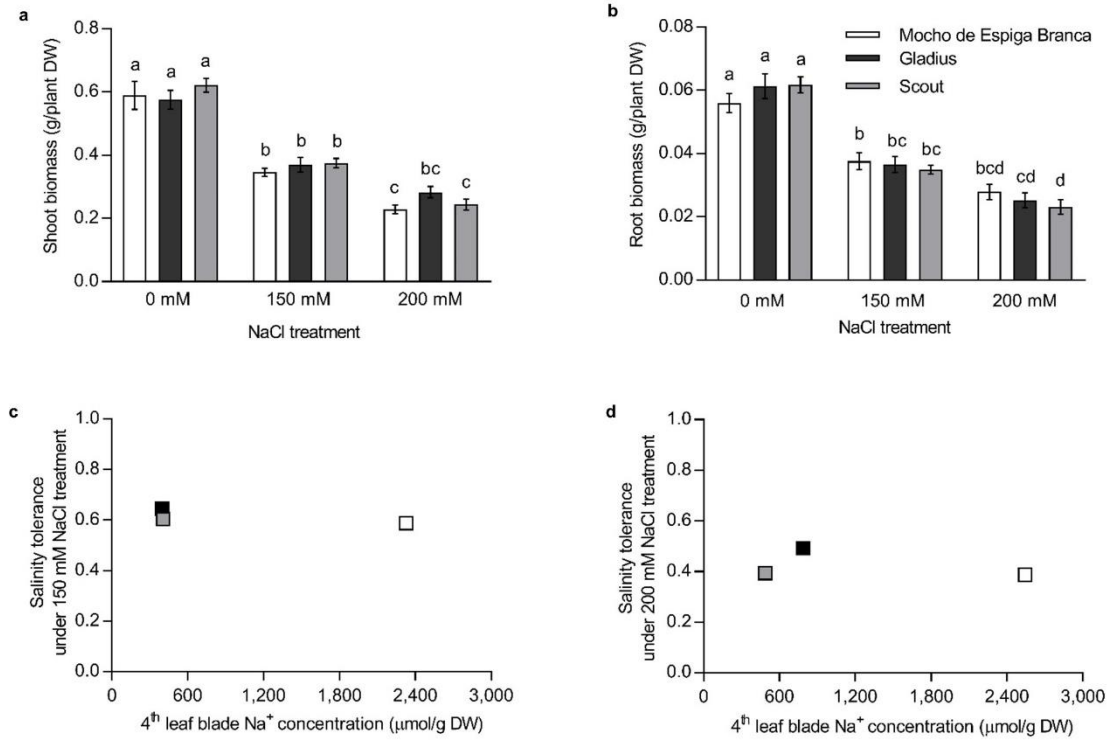

Supplementary Fig. 1: Plant biomass and salinity tolerance of plants in relation to their 4th leaf Na^+ concentration in Mocho de Espiga Branca and two Australian cultivars Gladius and Scout in a hydroponic system with 0, 150 and 200 mM NaCl concentrations. Plant biomass, salinity tolerance and the 4th leaf Na^+ concentration were determined 21 days after 0, 150 and 200 mM NaCl treatments were applied at the emergence of the 4th leaf. Salinity tolerance is defined as the shoot dry weight under 150 or 200 mM NaCl divided by the shoot dry weight under 0 mM NaCl. **a,** Shoot dry weight (g DW/plant); **b,** Root dry weight (g DW/plant). **c,** Salinity tolerance of Mocho de Espiga Branca, Gladius and Scout in relation to their 4th leaf Na^+ concentration under 150 and **d,** 200 mM NaCl. Data are presented as means ± SEM (n = 14). Bars with different letters indicate significant differences determined by two-way ANOVA with Tukey's multiple comparison test at $p \leq 0.05$.

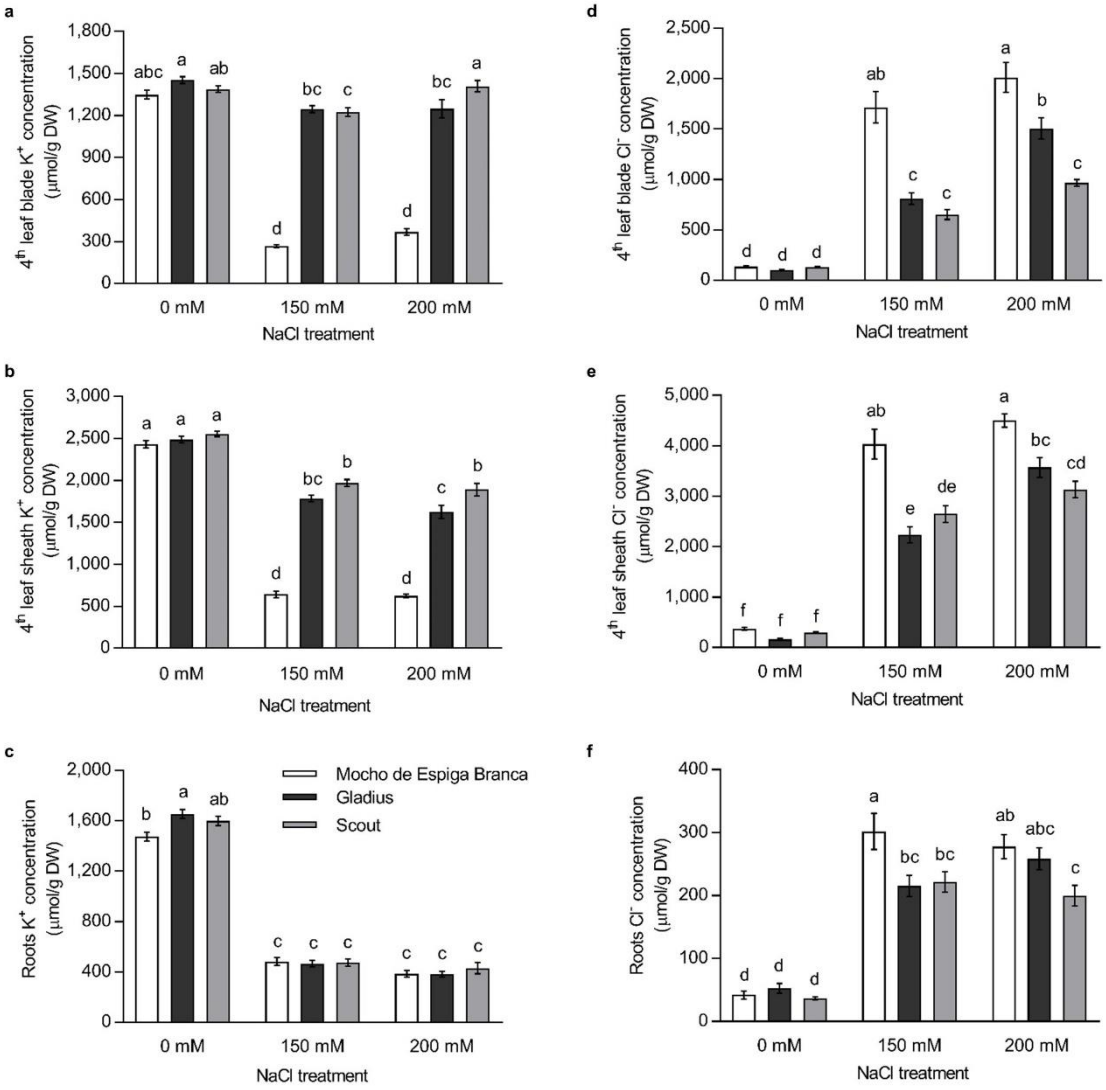

Supplementary Fig. 2: K^+ and Cl^- concentrations in the 4th leaf blade, sheath, and roots of Mocho de Espiga Branca, Gladius and Scout in a hydroponic system. K^+ concentrations in **a,** 4th leaf blade; **b,** 4th leaf sheath; **c,** roots; and Cl^- concentration in **d,** 4th leaf blade; **e,** 4th leaf sheath and **f,** roots determined 21 days after 0, 150 and 200 mM NaCl treatments were applied at the emergence of the 4th leaf. Data are presented as means ± SEM ($n = 14$). Bars with different letters indicate significant differences determined by two-way ANOVA with Tukey's multiple comparison test at $p \leq 0.05$.

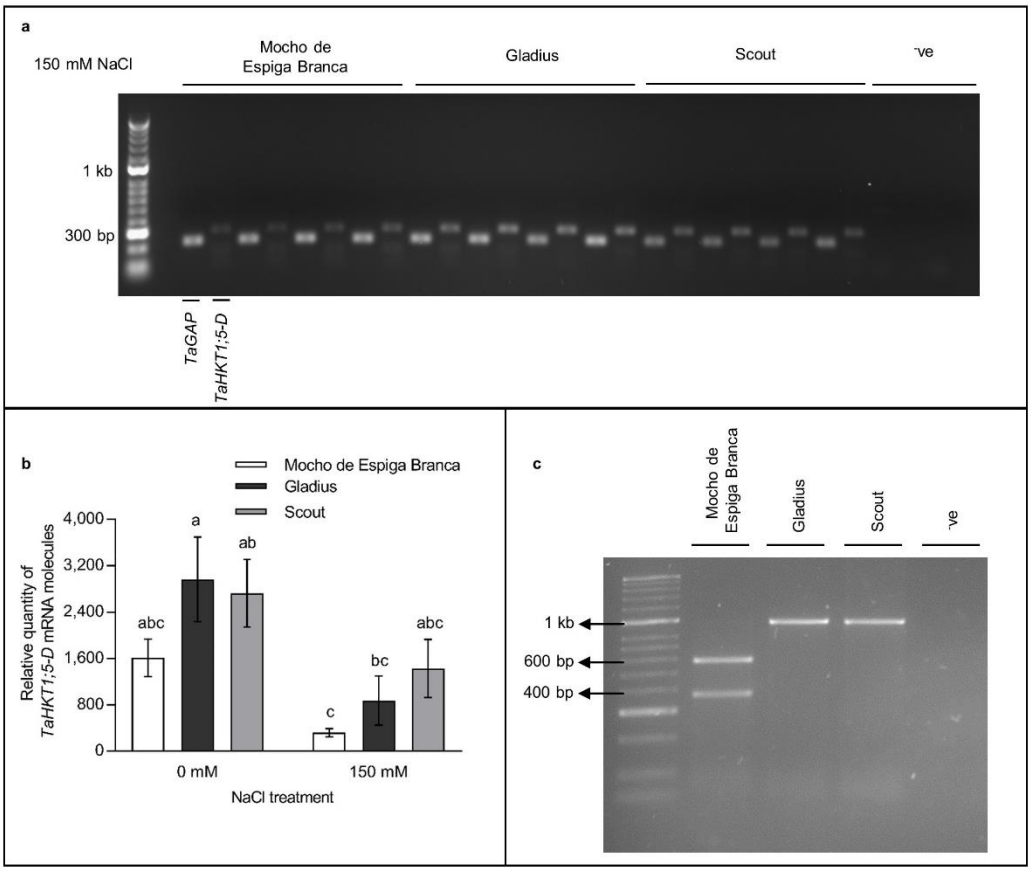

Supplementary Fig. 3: Expression of *TaHKT1;5-D* in the root tissue and CAPS marker tsl2SALTY-4D genotyping of Mocho de Espiga Branca, Gladius and Scout. Roots from Mocho de Espiga Branca, Gladius and Scout were hydroponically grown for 21 days under 0 and 150 mM NaCl concentrations which were applied at the emergence of the 4th leaf. **a,** Expression of *TaHKT1;5-D* in Mocho de Espiga Branca, Gladius and Scout in comparison to positive control (*TaGAP*) and a negative control (-ve, Milli-Q water) visualized on 1% (w/v) agarose gel. **b,** Real-time PCR analysis of *TaHKT1;5-D* mRNA transcript levels relative to *TaActin* and *TaCyclophilin* in root tissue of Mocho de Espiga Branca, Gladius and Scout. Data represents means ± SEM (n = 15). Bars with different letters indicate significant differences determined by two-way ANOVA with Tukey's multiple comparison test at $p \leq 0.05$. **c,** Agarose gel visualization of the CAPS marker tsl2SALTY-4D genotyping of Mocho de Espiga Branca (T:T), Gladius (C:C) and Scout (C:C). Mocho de Espiga Branca has two fragments at 573 and 372 bp, and Gladius and Scout have a single fragment at 945 bp; H_2O sample is a negative control.

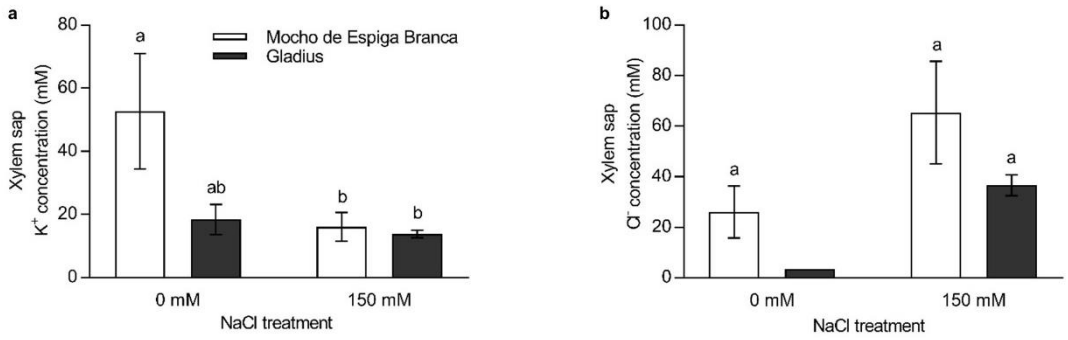

Supplementary Fig. 4: Xylem sap K^+ and Cl^- concentration of Mocho de Espiga Branca and Gladius under 0 and 150 mM NaCl concentrations. **a,** Xylem sap K^+ concentration (mM). **b,** Xylem sap Cl^- concentration (mM). ,Xylem sap was collected from hydroponically grown plants 21 days after 0 and 150 mM NaCl were applied at the emergence of 4th leaf. Data presented as mean ± SEM (n = 6-8 except for Cl^- concentration in Gladius under 0 mM NaCl where n = 2). Bars with different letters indicate significant differences determined by two-way ANOVA with Tukey's multiple comparison test at $p \leq 0.05$.

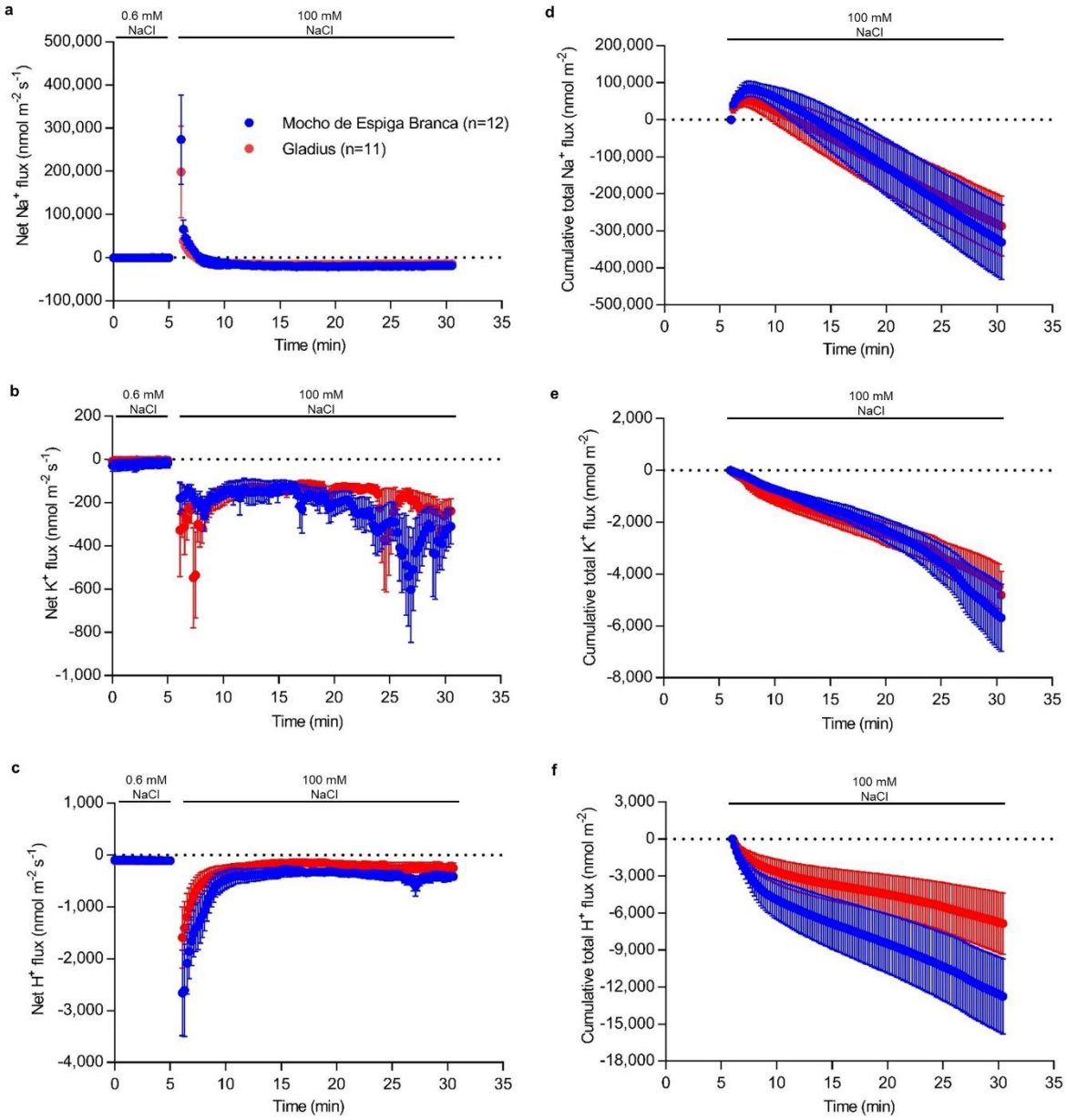

Supplementary Fig. 5: Ion fluxes measured at root mature zone after a sudden exposure to 100 mM NaCl concentration. Five-day-old Mocho de Espiga Branca or Gladius seedlings were treated with 100 mM NaCl, and the resultant ion fluxes were measured at the root maturation zone (approximately two cm above the root apex) of the primary root for 25 min. Net **a,** Na^+; **b,** K^+ and **c,** H^+ fluxes. Cumulative total **d,** Na^+; **e,** K^+ and **f,** H^+ fluxes over 25 min. Data are presented as means ± SEM (n = 11-12).

Supplementary Tables

Supplementary Table 1: Screening of 75 bread wheat lines for salinity tolerance. The 4th leaf Na^+, K^+ and Cl^- concentrations, final point projected shoot area (PSA), and salinity tolerance (PSA under 100 mM NaCl relative to 0 mM NaCl treatment) of the plants are determined 11 days after 100 mM NaCl treatment applied at the emergence of 4th leaf (n = 3-4 except for Gladius and scout, where n = 12).

Bread wheat lines ID	4th leaf Na^+ concentration (µmol/g DW)				4th leaf K^+ concentration (µmol/g DW)				4th leaf Cl^- concentration (µmol/g DW)				PSA (pixels)				Salinity Tolerance
	0 mM NaCl		100 mM NaCl		0 mM NaCl		100 mM NaCl		0 mM NaCl		100 mM NaCl		0 mM NaCl		100 mM NaCl		
	Mean	SEM	Mean	SEM	Mean	SEM	Mean	SEM	Mean	SEM	Mean	SEM	Mean	SEM	Mean	SEM	
Mocho de Espiga Branca	344.1	21.2	419.3	44.4	1533.2	545.5	1172.1	138.2	284.9	16.0	375.4	45.2	44412	3608	31583	1567	0.71
Odessa EXP STA 17413	55.2	4.8	108.3	13.0	1547.3	55.3	1506.7	66.3	197.6	9.3	373.0	35.6	55874	9492	36694	4718	0.66
Pitic 62	42.4	2.5	89.7	11.7	1157.0	137.8	1246.3	49.4	268.4	13.2	457.4	26.7	62190	5687	43762	6694	0.70
W 98	78.2	8.8	88.9	13.3	1195.7	33.9	1297.5	42.9	258.5	7.9	408.4	20.1	40359	2702	31767	4244	0.79
Buck Atlantico	58.6	3.4	88.3	6.7	1255.0	30.6	1328.8	18.0	196.0	10.5	374.6	34.2	37660	7989	23932	1520	0.64
LW 337	45.9	7.4	84.5	13.9	1542.3	163.2	1521.9	88.8	191.7	39.7	278.9	37.5	60895	15773	33604	3917	0.55
G 72300	56.0	14.7	83.9	6.5	1382.2	81.6	1453.8	39.7	211.4	26.4	337.2	19.7	56603	9453	42977	10955	0.76
LW 333	55.1	2.3	83.3	11.5	1269.6	79.6	1477.3	44.7	182.0	20.7	327.1	42.8	64642	5622	43970	6942	0.68
Siete Cerros	73.0	8.6	80.0	6.8	1303.9	136.8	1236.3	95.7	251.6	7.8	387.7	29.1	38272	6491	29151	4469	0.76
N 46	65.5	11.0	79.5	3.9	1473.4	75.7	1448.4	47.9	180.3	14.5	364.2	23.4	45152	8875	32147	4486	0.71
Ciano 79	45.8	2.2	78.7	5.3	1240.7	82.5	1094.7	17.9	202.3	13.7	472.4	39.7	40783	2261	29916	1692	0.73
Meira	74.0	5.6	77.7	16.6	1485.4	76.6	1431.6	38.8	269.5	30.5	329.6	32.3	40727	13542	27257	4731	0.67
Menflo	64.5	11.3	77.2	8.6	1441.7	91.1	1527.7	176.9	200.9	34.3	305.6	22.2	24767	5521	17588	6990	0.71
Sokool	56.5	3.6	76.8	8.6	1415.3	48.3	1495.0	14.6	210.1	9.9	363.4	26.8	43137	7854	35617	7594	0.83
Persia 21	46.6	3.7	76.1	5.6	1116.1	260.8	1126.2	133.1	217.6	21.2	384.1	57.9	26361	1605	15464	1489	0.59
LW 335	33.3	6.6	75.1	14.6	1288.6	87.6	1254.8	20.8	177.3	16.1	361.6	45.3	51511	8844	33763	7250	0.66
H 1534	56.3	6.5	74.0	13.7	1482.5	170.0	1443.2	81.6	233.0	26.9	353.8	38.9	55459	3845	38617	3063	0.70
M708/G25/N163	42.5	4.4	73.1	17.6	1186.5	38.5	1213.9	19.2	101.6	11.0	279.4	5.0	52768	4081	34776	3842	0.66
Odessa EXP STA 19565	67.4	22.4	71.8	6.4	1494.6	88.4	1498.1	34.3	239.8	46.3	371.3	17.9	46250	4804	32633	2602	0.71
LW 336	58.7	10.2	71.8	9.5	1411.5	32.3	1275.8	68.0	159.1	7.9	319.2	15.4	54627	8314	33259	2841	0.61
Coppadra	69.8	11.6	71.7	16.8	1370.7	26.1	1069.7	122.8	147.7	11.0	331.2	60.5	35456	7072	27780	1437	0.78
S975-A4-A1	42.5	16.8	70.5	31.4	1086.5	42.6	1092.5	34.5	191.4	8.9	403.5	27.4	35552	9372	28230	3661	0.79
U-Man-Syao-Mai	42.7	1.3	68.4	8.1	1566.9	11.0	1545.4	28.8	296.5	12.8	439.4	43.8	74314	692	50733	6244	0.68
Frontana 3671	57.0	4.4	68.2	11.7	1169.1	60.0	1165.4	41.6	182.9	9.5	451.5	45.0	46276	4451	37705	4898	0.81
Palestinskaya	63.7	2.1	65.6	11.3	1328.5	183.6	1597.0	55.2	186.0	6.8	346.8	10.9	56726	8251	42585	9109	0.75
Taferstat	35.6	8.1	63.5	7.2	1391.5	57.2	1402.4	59.0	163.2	15.0	348.0	20.8	56758	18604	34659	6344	0.61
H 1703	51.3	3.3	62.8	10.2	997.3	38.5	1081.8	89.8	247.9	4.8	430.9	46.5	56744	11703	39641	6404	0.70
BuckBuck 'S'	27.9	2.0	62.0	2.7	1385.7	49.7	1203.3	124.8	149.8	10.1	403.8	45.4	23268	930	20036	2603	0.86
India 231	40.4	4.3	61.7	2.0	1372.2	115.0	1452.8	91.8	219.0	3.0	370.4	7.0	56586	3192	38619	4556	0.68
Persia 7	38.2	1.8	61.7	6.8	1507.2	95.2	1417.9	20.3	169.0	5.9	344.7	11.8	46281	8299	34724	4521	0.75
Africa Mayo	75.3	15.2	60.7	13.4	1069.8	161.5	1104.9	67.9	136.0	8.3	247.6	9.4	40222	5454	29209	5826	0.73

Suzuki 24	48.6	5.6	58.7	6.1	1593.4	56.8	1665.2	32.2	195.7	9.3	321.2	18.2	31078	1503	22988	3952	0.74
Granarolo	33.1	6.0	58.0	15.0	1460.7	113.0	1509.9	27.6	189.2	9.8	387.9	26.5	32622	5428	30414	3236	0.93
India 227	41.9	4.8	58.0	13.3	1487.3	25.9	1544.6	55.6	177.1	4.6	354.7	22.4	60450	2364	38476	4715	0.64
India 322	40.6	9.4	56.7	2.8	1366.4	37.5	1425.5	7.2	223.0	16.6	380.4	13.9	33737	3630	29897	708	0.89
Suzuki 17	46.3	2.8	56.1	4.0	1286.7	44.3	1416.7	71.3	225.1	8.2	395.6	13.7	61693	7686	42194	8052	0.68
Persia 4	42.1	4.9	55.4	4.4	1192.8	84.1	1350.8	29.6	232.1	6.9	391.3	4.8	42046	6482	37948	2930	0.90
Zilve	50.5	5.5	54.7	13.2	1167.9	72.3	1250.6	91.1	164.4	13.4	279.4	40.4	40630	7978	32427	5205	0.80
Vorobey	39.7	3.5	53.6	7.1	1410.8	56.6	1431.7	55.6	223.8	11.0	334.1	24.7	46390	5274	34900	6974	0.75
6/01/2003	33.5	0.3	52.2	4.0	1506.8	60.6	1377.8	41.3	165.3	10.6	242.5	53.9	39909	10500	21405	3273	0.54
Academie de Pekin	54.5	3.4	51.6	4.5	1501.0	132.5	1675.9	73.4	214.0	11.8	313.5	20.1	56077	14450	29591	9868	0.53
H 1685	42.7	2.7	50.7	4.8	1164.3	94.6	1327.4	79.3	205.9	15.7	334.2	20.9	46326	8359	18769	4166	0.41
Bahatane 87	43.4	7.7	50.0	6.6	1284.9	103.4	1524.5	55.4	208.7	8.2	404.2	26.8	47959	7085	33608	5239	0.70
Optata 85	52.1	6.8	49.9	1.1	1187.6	45.7	1421.7	94.9	252.9	32.0	389.8	30.9	55237	15738	35165	6692	0.64
Jupateco 73	50.7	5.0	49.9	6.7	1116.2	65.2	1239.1	97.4	202.1	10.8	342.0	6.6	49038	3785	34487	2805	0.70
H 1440	40.9	9.2	48.2	25.9	1105.9	193.3	1232.8	57.8	257.8	33.2	406.0	20.1	48773	10795	23738	1967	0.49
N67M2	54.5	2.8	47.9	1.5	1395.3	59.4	1547.6	44.4	159.0	9.9	346.4	13.9	47050	2161	41140	3314	0.87
Yecora 70	53.2	15.1	47.8	3.9	985.5	41.9	1071.1	68.1	149.9	10.3	343.3	18.6	42059	4769	37583	3187	0.89
Thori 212-var 8/1	53.2	11.5	46.7	16.7	1361.7	237.9	1583.1	93.0	209.0	5.1	350.5	46.5	53654	18310	30324	6803	0.57
Estanzuela Dorado	40.4	3.1	46.7	11.4	1525.0	16.8	1429.0	45.5	236.9	19.3	391.1	28.4	46303	7140	32351	2042	0.70
LW 349	31.0	6.1	45.8	2.5	1333.4	115.0	1380.6	91.6	244.5	30.1	437.6	24.6	47171	3720	32684	3029	0.69
Cul 10	38.6	4.6	45.6	10.3	1370.0	11.5	1426.5	52.6	249.7	11.9	350.2	24.2	43008	3963	33340	5076	0.78
Asia Minor 71	43.0	2.3	45.4	5.5	1431.9	113.6	1407.1	90.7	220.3	17.9	333.8	27.1	47986	4658	33728	3544	0.70
Inia 66	31.1	5.1	45.3	2.6	1077.8	37.9	1099.2	47.6	140.2	10.1	341.4	19.6	45643	3648	39638	4615	0.87
Suzuki 23	46.7	3.2	45.3	8.7	1302.9	50.0	1364.8	72.7	217.6	14.2	345.5	28.9	55852	13176	36789	6721	0.66
Suzuki 12	38.6	4.9	44.3	2.2	1367.6	21.6	1406.2	47.2	226.7	5.2	341.6	31.7	34649	4371	26075	2099	0.75
LW 334	37.3	3.0	44.1	11.1	1470.9	91.8	1510.0	49.1	215.8	20.1	343.1	7.5	42538	8041	24862	627	0.58
Suzuki 3	40.5	7.0	43.4	5.6	1323.1	95.0	1321.4	149.4	211.0	16.3	399.8	11.6	46577	7073	33342	4926	0.72
LW 369	49.5	4.5	43.2	6.0	1490.0	102.3	1478.7	78.7	219.0	13.2	291.2	33.3	40132	13614	24864	2502	0.62
EMU'S'	33.8	9.0	42.5	3.8	1302.0	58.4	1403.1	48.1	178.9	5.0	318.4	24.3	52824	3900	39115	2930	0.74
PBW 343	37.7	4.3	41.9	4.8	1327.8	63.9	1344.5	61.2	202.0	4.7	372.3	5.5	52671	8935	41154	2564	0.78
Genaro F81	33.5	2.5	41.5	3.4	1421.1	35.8	1453.0	57.3	215.7	5.6	342.3	18.3	42576	3623	33261	4212	0.78
Pamukale	36.7	6.9	40.0	4.6	1253.8	84.8	1261.3	144.3	142.7	15.9	283.4	23.9	32395	8781	29610	7900	0.91
Daeraad	43.0	6.4	40.0	3.9	1413.6	229.4	1593.7	122.1	185.0	37.5	315.1	21.5	37283	8166	21845	788	0.59
BT 2281	36.6	8.1	39.5	9.0	1175.6	15.5	1175.9	77.8	184.4	20.7	343.4	39.6	30783	6128	24017	3961	0.78
Cul 9	43.0	3.6	38.7	9.9	1256.1	196.3	1314.2	124.9	149.7	17.9	242.8	40.9	26316	2186	26505	2567	1.01
BT 2277	31.8	3.6	36.2	3.6	1092.1	121.5	1092.2	248.6	233.0	16.9	392.6	14.2	46627	9505	30502	6148	0.65
117-var 12/564	52.3	12.0	35.9	5.4	1275.1	53.0	1411.3	59.9	189.7	25.4	322.5	24.2	40584	3485	27356	1888	0.67
Andes 56	29.1	7.5	35.8	2.0	1406.9	180.3	1402.2	110.6	198.4	12.8	356.1	10.4	41104	14982	27522	4944	0.67
Gladius	27.8	1.7	35.3	4.2	1286.7	21.2	1341.3	27.3	165.1	4.2	291.1	9.9	26528	1411	20865	1101	0.79
Suzuki 9	40.4	4.2	34.9	2.9	1479.1	46.1	1490.7	38.2	239.3	9.9	377.7	12.6	44448	9287	39482	4712	0.89
Tacupeto 2001	39.9	1.0	33.3	4.0	1330.1	8.8	1392.9	115.6	253.5	15.4	379.2	21.9	59746	7059	39630	2554	0.66
Roelfs F2007	37.3	6.1	32.0	3.6	1338.9	52.8	1422.2	35.3	262.2	23.5	361.9	23.3	31099	9664	29905	2283	0.96
Synthetic W7985	30.5	2.1	29.6	1.9	1554.0	38.9	1474.8	25.0	189.6	12.5	217.8	19.5	30690	3944	23569	2845	0.77
Scout	24.9	2.2	26.5	2.5	1306.7	35.6	1305.9	30.9	152.5	5.7	236.3	8.8	28479	1831	22338	1979	0.78

Supplementary Table 2: Genotyping of Mocho de Espiga Branca, Gladius, Scout and 68 bread wheat diversity lines for the SNP (T/C) resulting in TaHKT1;5-D L190P variation using the CAPS marker tsl2SALTY-4D designed for the SNP.

***TaHKT1;5-D* SNP allele**	**Bread wheat accessions**
C:C	Mocho de Espiga Branca
T:T	Gladius, Scout, Odessa EXP STA 17413, Pitic 62, W 98, Buck Atlantico, LW 337, G 72300, LW 333, Siete Cerros, N 46, Ciano 79, Meira, Menflo, Sokool, Persia 21, LW 335, H 1534, M708/G25/N163, Odessa EXP STA 19565, LW 336, Coppadra, S975-A4-A1, Frontana 3671, Palestinskaya, Taferstat, BuckBuck 'S', India 231, Persia 7, Suzuki 24, Granarolo, India 227, India 322, Suzuki 17, Persia 4, Zilve, Vorobey, 6/01/2003, Academie de Pekin, H 1685, Bahatane 87, Optata 85, Jupateco 73, H 1440, N67M2, Yecora 70, Thori 212-var 8/1, Estanzuela Dorado, LW 349, Cul 10, Asia Minor 71, Inia 66, Suzuki 23, Suzuki 12, LW 334, Suzuki 3, LW 369, EMU'S', PBW 343, Genaro F81, Pamukale, Daeraad, BT 2281, Cul 9, BT 2277, 117-var 12/564, Andes 56, Suzuki 9, Tacupeto 2001, Roelfs F2007

Supplementary Table 3: Primers used for *TaHKT1;5-D* coding sequence amplification and sequencing. FP = Forward Primer; RP = Reverse Primer; Primers marked '*' are from Byrt, et al (2014).

Primers	**Start (bp)**	**Length (bp)**	**Sequences (5'- 3')**
cTaHKT1,5-D_FP_1	1	22	ATGGGTTCTTTGCATGTCTCCT
cTaHKT1,5-D_RP_328	328	20	GCATGCTCGTGAACACCTCG
cTaHKT1;5-D_FP_429	429	20	CCTAGAGCTCGCTGTTACCA
*cTaHKT1; 5-D_FP_693**	693	17	CTGCGGCTTCGTCCCGA
*cTaHKT1; 5-D_FP_1194**	1194	24	CGACCAGAAAAGGATAACAAGCAT
cTaHKT1; 5-D_RP_1551	1551	23	TTATACTATCCTCCATGCCTCGC

Chapter 3 - Identifying the genetic control of salinity tolerance in a bread wheat landrace Mocho de Espiga Branca

Statement of Authorship

Title of Paper	Identifying the genetic control of salinity tolerance in a bread wheat landrace Mocho de Espiga Branca
Publication Status	☐ Published ☐ Accepted for Publication ☐ Submitted for Publication ☑ Unpublished and Unsubmitted w ork w ritten in manuscript style
Publication Details	This manuscript has been written and formatted for publication in Frontiers in Plant Science.

Principal Author

Name of Principal Author (Candidate)	Chana (Chana Borjigin)
Contribution to the Paper	Contributed to the experimental design, conducted glasshouse experiment, performed ion concentration measurement and analysed the data, extracted DNA and constructed GBS library, conducted QTL analysis and wrote the manuscript.
Overall percentage (%)	75%
Certification:	This paper reports on original research I conducted during the period of my Higher Degree by Research candidature and is not subject to any obligations or contractual agreements with a third party that would constrain its inclusion in this thesis. I am the primary author of this paper.
Signature	Date 04/11/2019

Co-Author Contributions

By signing the Statement of Authorship, each author certifies that:

i. the candidate's stated contribution to the publication is accurate (as detailed above);
ii. permission is granted for the candidate in include the publication in the thesis; and
iii. the sum of all co-author contributions is equal to 100% less the candidate's stated contribution.

Name of Co-Author	Rhiannon K. Schilling
Contribution to the Paper	Conceived the work, contributed to the experimental design, generated the F_2 seed, interpreted the work and contributed to supervision, reviewed and commented on the manuscript.
Signature	Date 04/11/2019

Name of Co-Author	Nathaniel Jewell
Contribution to the Paper	Performed statistical analysis on the phenotypic data.
Signature	Date 5/11/19

Name of Co-Author	Chris Brien
Contribution to the Paper	Generated the experimental layout for high throughput phenotyping experiment in the Smarthouse, performed statistical analysis on the phenotypic data.
Signature	Date 5/11/2019

Name of Co-Author	Juan Carlos Sanchez-Ferrero
Contribution to the Paper	Analysed the GBS data.
Signature	Date 5-11-2019

Name of Co-Author	Paul J. Eckermann
Contribution to the Paper	Developed the genetic linkage map and assisted the QTL analysis.
Signature	Date 5/11/19

Name of Co-Author	Nathan S. Watson-Haigh
Contribution to the Paper	Analysed the GBS data.
Signature	Date 5/11/19

Name of Co-Author	Bettina Berger
Contribution to the Paper	Provided advice for the Smarthouse phenotyping experiment and contributed to phenotypic data analysis.
Signature	Date 04.11.2019

Name of Co-Author	Allison S. Pearson
Contribution to the Paper	Conceived the work, contributed to the experimental design, interpreted the work and contributed to supervision, reviewed and commented on the manuscript.
Signature	Date 12/11/2019

Name of Co-Author	Stuart J. Roy
Contribution to the Paper	Conceived the work, contributed to the experimental design, interpreted the work and contributed to supervision, reviewed and commented on the manuscript.
Signature	Date 13/11/2013

Identifying the genetic control of salinity tolerance in a bread wheat landrace Mocho de Espiga Branca

Running title: Identifying the genetic control of salinity tolerance in Mocho de Espiga Branca

Chana Borjigin[1,2], Rhiannon K. Schilling[1,2], Nathaniel Jewell[2,3], Chris Brien[2,3], Juan Carlos Sanchez-Ferrero[1,2], Paul J. Eckermann[1,2], Nathan S. Watson-Haigh[1,2], Bettina Berger[2,3], Allison S. Pearson[1,2,4], Stuart J. Roy[1,2,5,*]

[1] Australian Centre for Plant Functional Genomics, PMB 1, Glen Osmond, South Australia 5064, Australia.

[2] School of Agriculture, Food and Wine, The University of Adelaide, PMB 1, Glen Osmond, South Australia 5064, Australia.

[3] The Plant Accelerator, Australian Plant Phenomics Facility, The University of Adelaide, PMB 1, Glen Osmond, South Australia 5064, Australia.

[4] ARC Centre of Excellence in Plant Energy Biology, The University of Adelaide, PMB 1, Glen Osmond, South Australia 5064, Australia.

[5] ARC Industrial Transformation Research Hub for Wheat in a Hot and Dry Climate, The University of Adelaide, PMB1, Glen Osmond, South Australia 5064 Australia.

*Corresponding author:

Stuart J. Roy E-mail: stuart.roy@adelaide.edu.au

Keywords: salt tolerance, QTL, sodium, chloride, plant growth, phenotyping

Abstract

Salinity tolerance in bread wheat is often reported to be associated with low leaf sodium (Na^+) concentrations. However, a Portuguese bread wheat landrace, Mocho de Espiga Branca, which accumulates significantly higher leaf Na^+ but has comparable salinity tolerance to commercial bread wheat cultivars at 150 mM NaCl has recently been identified. To determine the genetic loci behind the salinity tolerance of this Portuguese landrace, an F_2 mapping population was developed by crossing Mocho de Espiga Branca with an Australian cultivar Gladius. A total of 412 F_2 progeny were phenotyped using both non-destructive and destructive techniques for 19 salinity tolerance sub-traits. The population was genotyped using Genotyping-by-Sequencing (GBS) for genetic map construction and subsequent quantitative trait loci (QTL) analysis. Genomic regions significantly associated with salinity tolerance were detected on chromosomes 1A, 1D, 4B and 5A for the sub-traits of relative and absolute growth rate (RGR, AGR), and on chromosome 2A, 2B, 4D and 5D for Na^+, potassium (K^+) and chloride (Cl^-) accumulation. Using the wheat physical map, a number of candidate genes that encode proteins associated with plant salinity tolerance have been identified including Na^+/H^+ antiporters, K^+ channels, H^+-ATPase, calcineurin B-like proteins (CBLs), CBL-interacting protein kinases (CIPKs), calcium dependent protein kinases (CDPKs) and calcium-transporting ATPase. This study provides a new insight into the genetic control of salinity tolerance in Mocho de Espiga Branca to assist with the future development of salt tolerant bread wheat cultivars.

Introduction

Bread wheat is one of the main sources of calories in the human diet (Shewry, 2009; Wrigley, 2009). With sufficient water and nutrient supply, wheat can achieve high yields (10 t/ha) (Shewry, 2009). However, global average wheat yield is currently only 3.5 t/ha due to many factors including both biotic and abiotic stresses (Shewry, 2009; FAO, 2019). Salinity is one of the major abiotic stresses and soils with an electrical conductivity (EC_e) of 4 dS/m (or 40 mM of NaCl) are generally considered saline, reducing plant growth and yield of cereal crops including bread wheat (Flowers, 2004; Colmer et al., 2005; Munns and Tester, 2008). Improving the tolerance of bread wheat to salinity therefore would help to minimise the gap between wheat yield potential and actual yield.

The ability to exclude Na^+ and maintain a high cytosolic K^+:Na^+ in shoot tissue are considered key salinity tolerance mechanisms (Munns et al., 2006). In bread wheat, a locus *Kna1* associated with Na^+ exclusion and enhanced K^+:Na^+ in the shoot was detected on chromosome 4D, and *TaHKT1;5-D* was identified as a candidate underlying the locus (Dvorak et al., 1994; Byrt et al., 2007; Byrt et al., 2014). The importance of Na^+ exclusion in salinity tolerance has been reported in many crops including durum wheat (Munns et al., 2003; Munns et al., 2012), rice (Ren et al., 2005), tomato (Martinez-Rodriguez et al., 2008) and maize (Fortmeier and Schubert, 1995). Although studies have shown correlations between greater Na^+ exclusion and K^+:Na^+ discrimination to grain yield in wheat under salinity (Chhipa and Lal, 1995; Ashraf and O'leary, 1996; Ashraf and Khanum, 1997), this relationship does not always exist across all genotypes (Ashraf and McNeilly, 1988; El-Hendawy et al., 2005; Genc et al., 2013; Genc et al., 2019), indicating the importance of other sub traits linked to the salinity tolerance of bread wheat. These sub traits could include tolerance to high leaf Na^+ (and/or Cl^-) by compartmentalising toxic ions into vacuoles and, osmotic adjustment by synthesising organic solutes to prevent ion toxicity damaging cellular metabolism in the cytoplasm (Colmer et al., 2005; Munns and Tester, 2008; Munns et al., 2016). Retention of Na^+ and Cl^- into older leaves to maintain growth in the

new and younger leaves is also reported as key traits associated with salinity tolerance (Boursier et al., 1987; Boursier and Läuchli, 1989; Colmer et al., 1995; Colmer et al., 2005).

In order to survive under salinity stress, cereal crops use more than one tolerance mechanism to maintain growth (Rajendran et al., 2009; Tilbrook et al., 2017; Asif et al., 2018). Most of the salt tolerant barley lines, particularly landraces, are known to have both shoot ion-independent tolerance and Na^+ exclusion from the shoot (Tilbrook et al., 2017). A durum wheat landrace Line 149 was identified with major Na^+ exclusion loci *Nax1* and *Nax2* on the chromosome 2A and 5A originated from a wheat relative *Triticum monococcum* L. (Munns et al., 2003; Lindsay et al., 2004; James et al., 2006). Introducing the *Nax2* locus (*TmHKT1;5-A*) into a commercial durum wheat cultivar (*Triticum turgidum* ssp. durum var. Tamaroi) significantly reduced the leaf Na^+ accumulation and the lines with *Nax2* locus contributing to a 25% improvement in grain yield in the field compared to the near isogenic lines without this locus (James et al., 2011; James et al., 2012; Munns et al., 2012). Therefore, it is likely that landraces could provide a valuable source of genetic variation in salinity tolerance and that could be used to enhance the overall salinity tolerance of current elite cereal cultivars.

Previously, a Portuguese bread wheat landrace, Mocho de Espiga Branca was found to accumulate up to 6-fold greater leaf and sheath Na^+ concentrations whilst maintaining similar shoot growth as Gladius, an Australian commercial cultivar, under 150 mM NaCl. Borjigin et al (Chapter 2) identified that a naturally occurring SNP in *TaHKT1;5-D* which prevents Mocho de Espiga Branca from retrieving Na^+ from the root xylem, resulting in a greater flux of Na^+ to the shoot and higher accumulation of Na^+ in the leaves. However, the genetic control of the salinity tolerance (including Na^+ tissue tolerance) in Mocho de Espiga Branca has not yet been established. The aim of this study is to detect QTL associated with salinity tolerance sub-traits in an F_2 population of Mocho de Espiga Branca and Gladius to determine which genetic regions may be involved in Na^+ tolerance.

Materials and Methods

Plant materials and growth conditions

An F_2 mapping population was derived from a bi-parental cross between a Portuguese bread wheat landrace Mocho de Espiga Branca and an Australian commercial cultivar Gladius (doubled haploid (DH) – derived from Rac875/Karichauff//Excalibur/Kukri/3/Rec875/Krichauff/4/-Rac875//Excalibur/Kukri [3794]). 412 F_2 progeny from a single cross along with 20 Mocho de Espiga Branca and 7 Gladius were phenotyped at 150 mM NaCl in a fully automated conveyor system within a temperature controlled Smarthouse at the Australian Plant Phenomics Facility (The Plant Accelerator®, University of Adelaide, Australia; latitude: -34.971366°, longitude: 138.639758°) between June and August in 2016. The pot experiment was conducted under natural daylight with a day temperature of 22 ºC and 15 ºC at night. Seeds were imbibed at room temperature for 4 hours and placed in the dark at 4 ºC and after 3 days, 3 uniform seeds were sown in each 2.5 L pot (15cm × 20cm) containing 2.3 kg of soil (50% University of California mix, 35% peat mix and 15% clay loam) and at the emergence of the 2nd leaf seedlings were thinned to a single seedling per pot. At emergence of the 3rd leaf (16 days after planting (DAP)) plants were loaded onto an individual cart in the Smarthouse, where the pots were weighed daily and automatically watered to maintain a soil water content at 17% (g/g) gravimetric water content. At the emergence of the 4th leaf (23 DAP), 213 mL of 0.26 M NaCl stock solution was applied to the saucer to reach a final concentration of 150 mM NaCl in the soil solution. Plants were not watered again until the soil water content was below 17% (g/g). Each pot was then watered automatically to 17% (g/g) and maintained at a final concentration of 150 mM NaCl.

Image acquisition and plant growth analysis

Non-destructive plant imaging using three 5 megapixel red-green-blue (RGB) cameras was performed measuring plant shoot area by capturing one top view and two side view images with a 90° rotation of each plant daily using the LemnaTec Scanalyzer 3D (LemnaTec GmbH,

Aachen, Germany) (Rajendran et al., 2009; Golzarian et al., 2011; Takahashi et al., 2015). Imaging started 4 days before salt treatment and continued for 12 days after the application of NaCl. The imaging data was prepared using the package imageData (Brien, 2018b) for the R statistical computing environment (R Core Team, 2018). The total shoot pixel area derived from the 3 RGB images was used to derive the projected shoot area (PSA) in kilo pixels which has been previously been shown to be correlated with shoot biomass (Rajendran et al., 2009; Golzarian et al., 2011; Takahashi et al., 2015). The smoothed PSA values were calculated by fitting a cubic smoothing spline to the PSA for each plant using the R function smooth.splines with degrees of freedom (*df*) of 5. The smoothed absolute growth rate (AGR) and the smoothed relative growth rate (RGR) were calculated for each plant using smoothed PSA by subtracting the consecutive smoothed PSA and ln(smoothed PSA) values, respectively, and then dividing by the differences in time (Al-Tamimi et al., 2016). Based on the plots for smoothed PSA, AGR and RGR, the smoothed PSA on 19, 22, 24, 28, 31 and 35 days after planting (DAP), the smoothed AGR and RGR intervals of one to four days prior to salt treatment ($AGR_{19\text{-}22}$ and $RGR1_{19\text{-}22}$), and one to five days ($AGR_{24\text{-}28}$ and $RGR_{24\text{-}28}$), five to eight days ($AGR_{28\text{-}31}$ and $RGR_{28\text{-}31}$) and eight to twelve days ($AGR_{31\text{-}35}$ and $RGR_{31\text{-}35}$) after salt treatment were selected to represent the plant growth response in the experiment according to the growth patterns observed (Supplementary Figure 1). A predicted osmotic tolerance (OST) was determined by dividing the growth of the plant immediately after salt application by the growth immediately prior to the salt application ($RGR_{24\text{-}28}$ / $RGR_{19\text{-}22}$). To produce phenotypic means, a mixed-model analysis was performed for each trait using the R package ASReml-R (Butler et al., 2009) and asremlPlus (Brien, 2018a) packages for the R statistical computing environment (R CoreTeam, 2018).

Leaf Na^+, K^+ and Cl^- concentration analysis

The 4th leaf blade, which fully expanded during salt stress, was sampled 12 days after NaCl treatment. Fresh weight was measured and then oven dried at 65 ºC for 2 days. The dried leaf

was weighed and digested in 10 mL of 1% HNO_3 at 85 ºC for 4 hours on a SC154 HotBlock® (Environmental Express, Inc., South Carolina, US). Na^+ and K^+ concentrations were measured using a Flame Photometer (Model 420; Sherwood Scientific Ltd., Cambridge, UK), and Cl^- concentration was measured using a Chloride Analyzer (Model 926; Sherwood Scientific Ltd) with the titration solution consisting of combined acid buffer (0.006% nitric acid, 90% water and 10% acetic acid; v/v) and gelatine solution (1.2%; w/v) at 4:1 ratio.

DNA extraction and quantification

The 3rd leaf blade was sampled on ice for genomic DNA (gDNA) extraction using the phenol/chloroform/iso-amyl alcohol (25:24:1) extraction method (Rogowsky et al., 1991) and the extracted gDNA was quantified using the Quant-iT™ PicoGreen™ dsDNA Assay Kit (Invitrogen, USA) following the manufacturer's instructions.

SNP discovery and genetic linkage map construction

Genotyping-by-sequencing (GBS) was used for SNP discovery as described by Poland et al. (2012) with some minor modifications. 20 Mocho de Espiga Brnaca, 7 Gladius and 412 F_2 progeny were sequenced to achive good coverege of the genome. Briefly, 10 µL of DNA from each plant was normalized to 20 ng/µL and arranged into 96-well PCR plates. After the restriction digest and ligation, each sample was pooled into a single 2 mL tube and purified using the PureLink™ Quick PCR Purification Kit (Invitrogen, USA) following the manufacturer's instructions. The purified product was multiplexed in eight 25 µL PCR reactions consisting of 10 µL ligated sample, 5 µL *Taq*® 5× Master Mix (New Energy Biology, USA), 0.65 µL each of 10 µM Illumina forward and reverse primers and 8.7 µL Milli-Q water using the following conditions: an initial denaturation at 95 °C for 30 sec followed by 16 cycles of amplification at 95 °C for 30 sec, 62 °C for 20 sec, 68 °C for 1 min 20 sec a final extension at 72 °C for 5 min and held at 8 °C. The final PCR product was pooled together, purified as described previously and eluted into 30 µL Milli-Q water to form a final GBS library. The

library was quantified using a High Sensitivity D1000 ScreenTape® at the Australian Genome Research Facility (AGRF, SA, Australia). An Illumina High-Seq 2500 machine (Illumina Inc, USA) at the South Australian Health and Medical Research Institute (SAHMRI, SA, Australia) was used to perform the Next Generation Sequencing (NGS) of the GBS libraries to generate 150 base pair (bp) paired-end sequences.

From the NGS, 109 million reads were observed for Mocho de Espiga Branca, 23.4 million for Gladius and 5.9 million for total F_2 progeny. Approximately 45% of the reads were mapped to the IWGSC RefSeq v1.0 genome assembly. Of the mapped reads, 44325 SNPs were observed between Mocho de Espiga Branca and Gladius, and after discarding SNPs that had less than 7× coverage, 5455 SNPs were selected for genotyping the F_2 population. The markers with more than 90% missing values and/or with high segregation distortion ($p \leq 0.00001$) were removed and a total of 2343 SNP markers with an average marker ratio of 26.7% : 45.5% : 27.8% for homozygous Mocho de Espiga Branca genotype (AA), heterozygous (AB) and homozygous Gladius genotype (BB) were used for map construction using the R package ASMap (Taylor and Butler, 2017). The markers were distributed across all 21 chromosomes and assigned to 21 linkage groups which spanned a total of 4808.7 cM with an average spacing of 2.1 cM between markers (Table 1). Two additional markers tsl2SALTY-4D and wMAS000033 were added to the genetic map on chromosome 4D and 5A, respectively (Figure 1). The marker tsl2SALTY-4D on chromosome 4D is a cleaved amplified polymorphic sequence (CAPS) marker which was previously designed to distinguish between the Na^+ exclusion gene *TaHKT1;5-D* alleles contributing to high and low leaf Na^+ concentration (Supplementary Figure 2) (Chapter 2). There was no genetic linkage between the two markers on chromosome 4D, this chromosome was established based on the physical position of the two markers for the purpose of QTL analysis. The wMAS000033 marker on chromosome 5A is a known Kompetitive allele specific PCR (KASP™) assay marker for vernalisation gene *TaVrn-A1* (Grogan et al., 2016; Garcia et al., 2019).

Quantitative trait loci (QTL) analysis

QTL analysis was conducted for 19 subtraits including 15 growth traits and 4 ion concentration traits using WinQTL Cartographer 2.5 (Wang et al., 2012). Single marker analysis (SMA) was performed using a simple linear regression model to identify individual markers that are significantly ($p \leq 0.001$) associated to the traits. Composite interval mapping (CIM) was performed using the standard Model 6. The genome-wide significance threshold (or Logarithm of odd, LOD) was estimated using 1000 permutations at a significance level of $p \leq 0.05$ and a walk speed of 1 cM. The notation of QTL followed the format: *Qphenotype.lab-chrmosome* with the '*asl*' indicating 'Adelaide Salt Lab', and for the QTL detected for growth traits the subscript '*x-y*' after *phenotype* referred to the days after planting.

Identification of annotated genes underlying QTL using physical mapping

To determine the genes underlying the QTL detected using CIM and the genetic region containing the significant markers detected using SMA, the IWGSC (International Wheat Genome Sequencing Consortium) RefSeq v1.0 full pseudomolecule ID of all the markers within the detected region that were up to 2 LOD drops from the maximum likelihood of each QTL or all the significant markers detected in SMA, were obtained using the coordinate converter tool in DAWN (Diversity Among Wheat Genome) at http://crobiad.agwine.adelaide.edu.au/dawn/ (Watson-Haigh et al., 2018). The IWGSC RefSeq v1.0 scaffolds containing the markers and the scaffolds bridging the neighbouring markers within the selected region were retrieved from https://urgi.versailles.inra.fr/jbrowseiwgsc/gmod_jbrowse/?data=myData%2FIWGSC_RefSeq_v1 prior to retrieval of all the annotated IWGSC Chromosome Survey Sequence (CSS) genes on the scaffolds. The predicted functional properties of those IWGSC CSS genes along with their corresponding Munich Information Center for Protein Sequences (MIPS) annotation hit ID and rice annotation hit ID were detected using POTAGE (PopSeq Ordered *Triticum aestivum* Gene Expression) at http://crobiad.agwine.adelaide.edu.au/potage/ (Suchecki et al., 2017).

Results

Phenotyping of the Mocho de Espiga Branca × Gladius F_2 population for salinity tolerance sub-traits

After 12 days at 150 mM NaCl, Mocho de Espiga Branca accumulated 18-fold greater 4th leaf Na^+ concentration than Gladius (Table 2), and 298 of the 412 F_2 progeny were negatively skewed towards the Gladius phenotype (Figure 2A). The 4th leaf K^+ concentration in Mocho de Espiga Branca was approximately 35% less than Gladius (Table 2), and 290 of the F_2 lines were positively skewed towards the Gladius phenotype (Figure 2B). The 4th leaf K^+:Na^+ of Mocho de Espiga Branca was 97% less than Gladius, and 258 of the F_2 population were positively skewed towards the Gladius phenotype (Figure 2C). Mocho de Espiga Branca accumulated a 1.2-fold higher Cl^- concentration in the 4th leaf compared to Gladius, and the F_2 population was normally distributed for the trait (Figure 2D). The similar distribution patterns were observed in the F_2 population for the leaf ion concentration sub-traits calculated based on the dry weight of the leaf (Figure 2A, 2B, 2C) and the leaf sap (Supplementary Figure 3A, 3B, 3C).

Mocho de Espiga Branca had significantly higher PSA and AGR than Gladius throughout the experiment, while no significant differences were observed between the two cultivars for RGR and predicted OST (Table 2). For all growth traits including the predicted OST, the F_2 population was normally distributed (Figure 2E and Supplementary Figure 4A-N).

QTL for salinity tolerance sub-traits in the F_2 population

Seven QTL were detected at five unique loci for six salinity tolerance sub-traits with a range of phenotypic variation and additive effects using CIM (Table 3). A single QTL for plant growth under salinity was detected on chromosome 1A for the sub-trait $AGR_{31\text{-}35}$ (*$QAGR_{31\text{-}35}$.asl-1A*) with a LOD score of 4.1. It accounted for 4.4% of the phenotypic variation and the additive effect was -0.3. There was a single QTL detected for plant growth performance before salt

treatment for PSA_{19} (*$QPSA_{19}$.asl-4A*) on chromosome 4A, with a LOD score of 4.3 and 4.8% phenotypic variation, with an additive effect of -0.7.

A single QTL was detected on chromosome 4D for 4th leaf Na^+ concentration (*QNa.asl-4D*), with a LOD score of 204 and accounted for 87.2% of the phenotypic variation with an additive effect of 666 being inherited from Mocho de Espiga Branca (Table 3). The single QTL for 4th leaf K^+ concentration was detected on chromosome 4D (*QK.asl-4D*) with a LOD score of 77.1 and had a total phenotypic variation of 57.3% with an additive effect of -304 from Gladius (Table 3). A QTL was detected on chromosome 4D for 4th leaf K^+:Na^+ (*QK:Na.asl-4D*) with a LOD score of 24.7, phenotypic variation of 24.4% and a negative additive effect of -10.9 from Gladius (Table 3). The Cl^- concentration from the 4th leaf Cl^- had two QTL detected, one on chromosome 2B (*QCl.asl-2B*) and the other on chromosome 5D (*QCl.asl-5D*) with LOD scores of 5.3 and 6.4, respectively. These two QTL accounted for 6.4 and 10.8% of the phenotypic variation with an additive effect of -66.8 and 17.6, respectively (Table 3).

In addition to the QTL detected using CIM, significant markers ($p \leq 0.001$) were identified using SMA for five salinity tolerance sub-traits and have been summarised in Table 4. Five significant markers on chromosome 5A were detected for $AGR_{31\text{-}35}$ and were located within the interval of 233.3-238.8 cM. Five markers significantly associated with $RGR_{19\text{-}22}$ were located within the interval 265.5-270.4 cM on chromosome 1B. For the sub-trait $RGR_{28\text{-}31}$ 47 significant markers within the interval of 24.1-73.6 cM on chromosome 4B and for $RGR_{31\text{-}35}$, there was a number of significant markers with one marker located at 79.2 cM on chromosome 1D, 13 markers within 39.9-46.2 cM on chromosome 4B and three markers at 297.7 cM on chromosome 5A. A total of 29 markers significantly associated with 4th leaf K^+ were detected on the genetic map and were located in the interval 54.3-110.7 cM on chromosome 2A.

Predicted candidate genes associated to salinity tolerance sub-traits in QTL regions

A list of expressed genes were identified for the QTL (*$QAGR_{31\text{-}35}$.asl-1A, $QPSA_{19}$.asl-4A, QNa.asl-4D, QK.asl-4D, QK:Na.asl-4D, QCl.asl-2B, QCl.asl-5D*) detected using CIM (Appendix File 1) and the genomic region containing the significant markers detected using SMA (Appendix File 2).

A total of 17 scaffolds with 792 expressed genes were identified for the QTL detected for plant growth under salinity (*$QAGR_{31\text{-}35}$.asl-1A*) on chromosome 1A (Appendix File 1). Within this region, a number of genes were shortlisted as potential candidates including genes that encode K^+ channels (*AKT1* and *AKT2*), cation/H^+ antiporters (*CHX16* and *CHX 20*), H^+-ATPase 9, calcineurin B-like (CBL) protein (*CBL9*) and calcium dependent protein kinases (*CDPKs*) based on their role in ion homeostasis and Ca^+ signalling in plants under stress (Table 5) (Hirsch et al., 1998; Dennison et al., 2001; Luan et al., 2002; Luan, 2009; Chanroj et al., 2012; Boudsocq and Sheen, 2013).

The QTL detected for plant shoot growth prior to salt treatment were located on 73 scaffolds containing 1618 expressed genes (Appendix File 1) on chromosome 4A, with many potential candidates including potassium transporter 2, sodium hydrogen exchanger 2 (*NHX2*) and proline transporter 2 (*ProT2*) due to their possible function in plant growth regulation and abiotic stress tolerance (Table 5) (Ueda et al., 2001; Elumalai et al., 2002; Gierth and Mäser, 2007; Wei et al., 2011).

For the three co-located QTL (*QNa.asl-4D, QK.asl-4D* and *QK:Na.asl-4D*), a single scaffold44094 containing 64 expressed genes was retrieved (Appendix File 1). The gene *TaHKT1;5-D* encoding cation transporter was shortlisted as potential candidate based on its role in limiting root-to-shoot Na^+ transport to enable the plant to maintain low concentrations of Na^+ in shoot (Table 5) (Byrt et al., 2007; Byrt et al., 2014).

The 4th leaf Cl^- accumulation QTL (*QCl.asl-2B*) was located on 18 scaffolds with 288 expressed genes (Appendix File 1). Within this region, potassium transporter 2, *NHX2*, *CIPK3* and *CIPK29* were shortlisted as potential candidates based on their role in plant salinity tolerance (Table 5) (Gierth and Mäser, 2007; Luan, 2009; Wei et al., 2011). For the 4th leaf Cl^- accumulation QTL (*QCl.asl-5D*), 61 scaffolds containing 1491 expressed genes were retrieved (Appendix File 1) with candidates including Na^+/H^+ antiporter 2 (*NHD2*), *NHX5*, *CHXs* and *CDPKs* based on their potential roles in maintaining ion homeostasis and stress tolerance (Table 5) (Luan et al., 2002; Bassil et al., 2011; Shi et al., 2018).

Within the significant marker interval for the AGR_{31-35} on chromosome 5A, two scaffolds (scaffold21633 and scaffold31523) with 164 expressed genes were observed (Appendix File 2). Of the expressed genes retrieved, the most obvious potential candidate was the gene encoding a two pore potassium channel a (*TPK*) based on its reported role in plant K^+ homoeostasis (Table 6) (Gobert et al., 2007; Isayenkov et al., 2011).

Within the significant marker interval for RGR_{28-31} on chromosome 4B, 131 scaffolds with 2877 expressed genes were found (Appendix File 2). Within this region, candidates including *CBL3*, *CIPK 3* and *CIPK9* genes were shortlisted based on their role in regulating ion homeostasis and Ca^+ signalling pathways under stress (Table 6) (Luan, 2009; Liu et al., 2012).

A single scaffold115569 with 98 expressed genes on chromosome 1D (Appendix File 2) was retrieved within the significant marker interval for RGR_{31-35} with the most obvious candidate being *CIPK18* (Table 6). For the significant marker interval RGR_{31-35} on chromosome 4B, a total of 73 scaffolds containing 1331 expressed genes were identified (Appendix File 2). Within this region, a number of candidates were shortlisted including genes *CBL18*, *CDPKs*, *CHXs*, potassium transporter 2 and aquaporin-like superfamily protein due to their potential role in regulating ion homeostasis and water transport in plants (Table 6) (Quigley et al., 2001;

Kaldenhoff and Fischer, 2006b; Kaldenhoff and Fischer, 2006a; Luan, 2009; Weinl and Kudla, 2009; Shi et al., 2018). For the significant marker interval $RGR_{31\text{-}35}$ on chromosome 5A, a single scaffold34444-3 containing 89 expressed genes was retrieved (Appendix File 2), with an obvious candidate being voltage-dependent anion-selective channel (VDAC) due to its physiological functions associated with plant developmental processes and abiotic stress responses (Table 6) (Desai et al., 2006; Takahashi and Tateda, 2013).

A total of 65 scaffolds with 2021 expressed genes were present within the significant marker interval for the 4^{th} leaf K^+ concentration on chromosome 2A (Appendix File 2). Within this region, genes shortlisted as potential candidates include the potassium channels (*AKT1* and *SKOR*), *CIPK23* and chloride channel C (*CLC-c*) (Table 6) based on their role in maintaining cation homeostasis and plant salinity tolerance (Table 6) (Gaxiola et al., 1998; Hirsch et al., 1998; Cheong et al., 2007; Shabala and Cuin, 2008; Ragel et al., 2015; Wang et al., 2016).

Discussion

In this study, a total of 412 Mocho de Espiga × Gladius F_2 progeny were phenotyped using both non-destructive and destructive tools for 19 salinity tolerance sub-traits. The F_2 population was genotyped using GBS to construct a high density genetic linkage map and to perform QTL analysis (Elshire et al., 2011; Poland et al., 2012). Genomic regions significantly associated with salinity tolerance were detected on chromosomes 1A, 1D, 4B and 5A for the sub-traits of plant growth (PSA, AGR and RGR), and on chromosome 2A, 2B, 4D and 5D for leaf ion (Na^+, K^+ and Cl^-) accumulation.

A QTL for the sub-trait $AGR_{31\text{-}35}$ (*$QAGR_{31\text{-}35}$.asl-1A*) for plant growth under salinity was detected on chromosome 1A. This QTL was associated with shoot ion-dependent tolerance, as these plants were at the later growth stage (31-35 DAP). At this growth stage, the plants had been exposed to salinity for 8-12 days and 114 F_2 lines had accumulated more than 400 µmol/g DW Na^+ in the leaf at 35 DAP. Similar to *$QAGR_{31\text{-}35}$.asl-1A*, there has been a QTL for shoot biomass previously detected on chromosome 1A in bread wheat when using a recombinant inbred lines (RILs) mapping population (Masoudi et al., 2015). This suggests the gene(s) residing on this chromosome may be important to maintaining plant growth under salinity (Masoudi et al., 2015). Among 792 expressed genes within the region of *$QAGR_{31\text{-}35}$.asl-1A*, there are two predicted *AKT* genes (*AKT1* and *AKT2*) that encode K^+ channels. *AKT1* is known to regulate root K^+ uptake under low K^+ conditions in *Arabidopsis*, whilst *AKT2* mediates K^+ transport in phloem (Hirsch et al., 1998; Lacombe et al., 2000; Gajdanowicz et al., 2011). K^+ is one of the most important inorganic cations in plants and involved in many metabolic processes such as protein synthesis and signalling mechanisms (Shabala and Cuin, 2008; Shabala, 2017). Collectively, these findings support the concept that regulation of K^+ homeostasis is essential for maintaining plant growth at later stage of salt exposure.

This study also detected QTLs on chromosome 5A for AGR_{31-35} and RGR_{31-35} and chromosomes 1D and 4B for RGR_{31-35} (Table 4). QTL associated with plant growth under salinity have previously been reported on chromosome 1D, 4B and 5A for seedling vigour (Oyiga et al., 2018), leaf growth rate (Amin and Diab, 2013) and shoot biomass (Ma et al., 2007; Genc et al., 2010; Amin and Diab, 2013; Ghaedrahmati et al., 2014; Masoudi et al., 2015; Oyiga et al., 2018). Within the physical interval on 4B in this study, many Ca^+ signalling genes (*CBLs*, *CDPKs* and *CIPKs*) were identified. This supports the notion that Ca^+ signalling has an important role in plants tolerance to salinity (Batistič and Kudla, 2009; Luan, 2009; Boudsocq and Sheen, 2013). Advanced mapping population, such as RILs derived from Mocho de Espiga Branca and Gladius, would be required to fine mapping and detect the genes that are tightly associated with maintaining growth while having a high leaf Na^+ concentration.

Salinity tolerance is a complex trait and plants may use multiple tolerance mechanisms to maintain growth across different developmental stages. The genomic region detected on chromosome 1B (for RGR_{19-22}) and 4A (for PSA_{19}) for the plant growth prior to the salt stress was not detected for the plant growth after salinity stress was applied. Although the same region on chromosome 4B was identified to be associated to RGR at both 28-31 and 31-35 DAP, it appears that genes on chromosome 1D and 5A associated with plant growth have significant contribution to the studied trait at 31-35 DAP. In rice, QTL were identified for transpiration use efficiency (TUE) during the early response phase following salinity treatment were no longer significant after 6 days of salinity treatment (Al-Tamimi et al., 2016). This, in addition to the findings of the current study, suggests that the genetic response of plants to salinity treatments varies across different stages of salinity stress.

Two QTL for leaf Cl^- concentration were detected on chromosome 2B (*QCl.asl-2B*) and 5D (*QCl.asl-5D*). To date, very few studies have reported QTL for plant Cl^- accumulation in bread wheat under salinity (Asif et al., 2019). A major QTL was previously detected for leaf Cl^-

accumulation on chromosome 5A, while 13 other minor QTL were detected on chromosomes 1D, 2A, 2B, 3A, 3B, 6D, 7A and 7D using a double haploid (DH) mapping population in hydroponics or field trials under salinity stress (Genc et al., 2014). The QTL detected previously for leaf Cl^- accumulation and the *QCl.asl-2B* detected in this study were both located on the long arm of chromosome 2B, which may indicate the importance of the genes within this region of the genome to the regulation of plants Cl^- transport in saline conditions. Within the physical interval underlying *QCl.asl-5D* and *QCl.asl-2B* in this study, genes encoding proteins potentially involved in ion transport and homeostasis in plants were detected including *NHX5* and *CHX*s (Table 5). *CHX*s have been demonstrated to have potential roles in maintaining organelle pH and K^+ homeostasis and cellular stress responses in salinity (Yokoi et al., 2002; Bassil et al., 2011; Chanroj et al., 2012). There were also genes such as *CBLs* and *CIPKs* that encode proteins involved in signalling and regulation of cell response to stress (Table 5). Previous reviews have reported a number of *CBLs* and *CIPKs* with their potential roles in tolerance to low-K^+, positive regulation of ABA signalling and plant abiotic stress tolerance (Batistič and Kudla, 2009; Dodd et al., 2010; Kudla et al., 2010; Thoday-Kennedy et al., 2015; Steinhorst and Kudla, 2019).

A SNP in an important Na^+ exclusion gene *TaHKT1;5-D* was found to be responsible for high leaf Na^+ concentration in Mocho de Espiga Branca as it resulted in an impired Na^+ transporter TaHKT1;5-D which prevented Na^+ tranport (Chapter 2). Therefore, it is expected that *TaHKT1;5-D* is the most obvious candidate for controlling leaf Na^+ concentration in the Mocho de Espiga Branca × Gladius F_2 population in this stduy. A marker tsl2SALTY-4D distinguishing between *TaHKT1;5-D* alleles responsible for high and low leaf Na^+ concentration was reported (Chapter 2) and it explained up to 87.2% of the phenotypic variation in leaf Na^+ concentartion and K^+:Na^+ in the Mocho de Espiga Branca × Gladius F_2 population. Previously, *TaHKT1;5-D* has been identified as the most obvious candidate for a locus *Knal* on chromosome 4DL for reduced shoot Na^+ accumulation and enhanced leaf K^+:Na^+

discrimination in bread wheat (Dubcovsky et al., 1996; Byrt et al., 2007; Byrt et al., 2014). *TmHKT1;5-A*, a homologues of *TaHKT1;5-D* originated from the wheat ancestral relative *Triticum monococcum* L., was also reported to be the candidate gene for a Na^+ exclusion loci (*Nax2*) in durum wheat on chromosome 5A (Munns et al., 2003; Huang et al., 2006; James et al., 2011). In barley, the *HvHK1;5* was recently detected on chromosome 4H for leaf Na^+ accumulation using Genome Wide Association study (GWAS) (Hazzouri et al., 2018). Our finding agrees with these previous studies and strongly supports that *TaHKT1;5-D* is a key gene determining leaf Na^+ in bread wheat.

A genomic region significantly associated with leaf K^+ concentration was detected on chromosome 2A. A total of 2024 expressed genes are present in this interval including those that encode K^+ channel AKT1 and stellar K^+ outwardly rectifying channel (SKOR), chloride channel C (CLC-c) and CIPK 23. CIPK23 is reported to be involved in the activation of AKT1 by interacting with CBL1 and CBL9 at the plasma membrane to regulate K^+ uptake in root cells in response to low K^+ stress in plant (Nieves-Cordones et al., 2014; Wang et al., 2016). The *SKOR* and *CLC-c* have also been reported to play important role in K^+ transport and cation homeostasis in plants (Gaxiola et al., 1998; Shabala and Cuin, 2008). Therefore, it could be this region on chromosome 2A that is associated with plant K^+ maintenance and contributing to the salinity tolerance of the bread wheat.

In conclusion, a number of QTL for salinity tolerance sub-traits were detected using an F_2 mapping population of Mocho de Esgiga Branca × Gladius under salt stress in a controlled glasshouse. Using the bread wheat genome, candidate genes that encode proteins associated with plant salinity tolerance sub-traits were identified. These include genes encoding K^+ channels, Na^+/H^+ antiporters, H^+-ATPase, CBLs, CIPKs and CDPKs. This study provides a new insight into the genetic control of salinity tolerance in Mocho de Espiga Branca to assist with the future improvement of salinity tolerance in bread wheat cultivars. Future work should

focus on developing advanced mapping population derived from Mocho de Espiga Branca and Gladius to reduce the interval of the detected QTL regions in order to identify tightly linked candidate genes responsible for Na^+ tissue tolerance in Mocho de Espiga Branca.

Conflict of Interest

The authors declare that they have no conflict of interest.

Author Contributions

CBo conceived the work, conducted glasshouse experiment, ion concentration measurement, performed data analysis, interpreted the work and wrote manuscript; RKS conceived the work, generated the F_2 seed, interpreted the work and contributed to supervision; ASP conceived the work, interpreted the work and contributed to supervision; CBr, NJ and BB provided statistical design and analysis; JCS and NSW analysed the GBS data; PJE developed the genetic linkage map and assisted the QTL analysis; SJR conceived the work, interpreted the work and contributed to supervision. All authors reviewed and commented on the manuscript.

Acknowledgments

This project was funded by the Grains Research and Development Corporation (GRDC): Project UA00145, UA00151, and the Australian Centre for Plant Functional Genomics (ACPFG) was jointly funded by the Australian Research Council (ARC), and the International Wheat Yield Partnership (IWYP): Project IWYP60/ANU00027, The Australian Plant Phenomics Facility, The Plant Accelerator® provided infrastructure and technical support and is funded under the National Collaborative Research Infrastructure Strategy (NCRIS). CB thanks the China Scholarship Council and the University of Adelaide Joint Postgraduate Scholarships Program for her PhD stipend, and acknowledges the financial support from the Research Travel Scholarship and the Global Learning Travel Grant at the University of Adelaide, and the Plant Nutrition Trust to attend conferences. The authors thank Assoc. Prof. Kenneth Chalmers and Dr. Melissa Garcia for providing F1 seed of Mocho de Espiga Branca × Gladius, and Ms. Christine Trittermann and Ms. Laura Short for technical assistance.

References

Al-Tamimi, N., Brien, C., Oakey, H., Berger, B., Saade, S., Ho, Y.S., Schmöckel, S.M., Tester, M., and Negrão, S. (2016). Salinity tolerance loci revealed in rice using high-throughput non-invasive phenotyping. *Nature Communications* 7, 13342.

Amin, A.Y., and Diab, A.A. (2013). QTL mapping of wheat (*Triticum aestivum* L.) in response to salt stress. *International Journal of Biotechnology Research* 3**,** 47-60.

Ashraf, M., and Khanum, A. (1997). Relationship between ion accumulation and growth in two spring wheat lines differing in salt tolerance at different growth stages. *Journal of Agronomy and Crop Science* 178**,** 39-51.

Ashraf, M., and Mcneilly, T. (1988). Variability in salt tolerance of nine spring wheat cultivars. *Journal of Agronomy and Crop Science* 160**,** 14-21.

Ashraf, M., and O'leary, J. (1996). Responses of some newly developed salt-tolerant genotypes of spring wheat to salt stress: 1. Yield components and ion distribution. *Journal of Agronomy and Crop Science* 176**,** 91-101.

Asif, M.A., Pearson, A.S., Schilling, R.K., and Roy, S.J. (2019). Opportunities for developing salt-tolerant wheat and barley varieties. *Annual Plant Reviews* 2**,** 1-61.

Asif, M.A., Schilling, R.K., Tilbrook, J., Brien, C., Dowling, K., Rabie, H., Short, L., Trittermann, C., Garcia, A., Barrett-Lennard, E.G., Berger, B., Mather, D.E., Gilliham, M., Fleury, D., Tester, M., Roy, S.J., and Pearson, A.S. (2018). Mapping of novel salt tolerance QTL in an Excalibur × Kukri doubled haploid wheat population. *Theoretical and Applied Genetics* 131**,** 2179-2196.

Bassil, E., Ohto, M.-A., Esumi, T., Tajima, H., Zhu, Z., Cagnac, O., Belmonte, M., Peleg, Z., Yamaguchi, T., and Blumwald, E. (2011). The *Arabidopsis* intracellular Na^+/H^+ antiporters NHX5 and NHX6 are endosome associated and necessary for plant growth and development. *The Plant Cell* 23**,** 224-239.

Batistič, O., and Kudla, J. (2009). Plant calcineurin B-like proteins and their interacting protein kinases. *Biochimica et Biophysica Acta (BBA)-Molecular Cell Research* 1793**,** 985-992.

Boudsocq, M., and Sheen, J. (2013). CDPKs in immune and stress signaling. *Trends in Plant Science* 18**,** 30-40.

Boursier, P., and Läuchli, A. (1989). Mechanisms of chloride partitioning in the leaves of salt-stressed *Sorghum bicolor* L. *Physiologia Plantarum* 77**,** 537-544.

Boursier, P., Lynch, J., Lauchli, A., and Epstein, E. (1987). Chloride partitioning in leaves of salt-stressed sorghum, maize, wheat and barley. *Functional Plant Biology* 14**,** 463-473.

Brien, C. (2018a). asremlPlus: Augments the use of 'ASReml-R'in fitting mixed models. *R package version***,** 4.1-02.

Brien, C.J. (2018b). "imageData: Aids in processing and plotting data from a Lemna-Tec Scananalyzer". Version 0.1-50. http://cran.at.r-project.org/package=imageData.

Butler, D., Cullis, B., Gilmour, A., and Gogel, B. (2009). "Analysis of Mixed Models for S language environments: ASReml-R reference manual. Brisbane". DPI Publications).

Byrt, C.S., Platten, J.D., Spielmeyer, W., James, R.A., Lagudah, E.S., Dennis, E.S., Tester, M., and Munns, R. (2007). HKT1;5-like cation transporters linked to Na^+ exclusion loci in wheat, *Nax2* and *Kna1*. *Plant Physiology* 143**,** 1918-1928.

Byrt, C.S., Xu, B., Krishnan, M., Lightfoot, D.J., Athman, A., Jacobs, A.K., Watson-Haigh, N.S., Plett, D., Munns, R., Tester, M., and Gilliham, M. (2014). The Na^+ transporter, TaHKT1;5-D, limits shoot Na^+ accumulation in bread wheat. *The Plant Journal* 80**,** 516-526.

Chanroj, S., Wang, G., Venema, K., Zhang, M.W., Delwiche, C.F., and Sze, H. (2012). Conserved and diversified gene families of monovalent cation/H^+ antiporters from algae to flowering plants. *Frontiers in Plant Science* 3**,** 25.

Cheong, Y.H., Pandey, G.K., Grant, J.J., Batistic, O., Li, L., Kim, B.G., Lee, S.C., Kudla, J., and Luan, S. (2007). Two calcineurin B-like calcium sensors, interacting with protein kinase CIPK23, regulate leaf transpiration and root potassium uptake in Arabidopsis. *The Plant Journal* 52**,** 223-239.

Chhipa, B., and Lal, P. (1995). Na^+/K^+ ratios as the basis of salt tolerance in wheat. *Australian Journal of Agricultural Research* 46**,** 533-539.

Colmer, T.D., Epstein, E., and Dvorak, J. (1995). Differential solute regulation in leaf blades of various ages in salt-sensitive wheat and a salt-tolerant wheat × *lophopyrum-elongatum* (host) A. Löve amphiploid. *Plant Physiology* 108**,** 1715-1724.

Colmer, T.D., Munns, R., and Flowers, T.J. (2005). Improving salt tolerance of wheat and barley: future prospects. *Australian Journal of Experimental Agriculture* 45**,** 1425-1443.

Dennison, K.L., Robertson, W.R., Lewis, B.D., Hirsch, R.E., Sussman, M.R., and Spalding, E.P. (2001). Functions of AKT1 and AKT2 potassium channels determined by studies of single and double mutants of Arabidopsis. *Plant Physiology* 127**,** 1012-1019.

Desai, M., Mishra, R., Verma, D., Nair, S., Sopory, S., and Reddy, M. (2006). Structural and functional analysis of a salt stress inducible gene encoding voltage dependent anion channel (VDAC) from pearl millet (*Pennisetum glaucum*). *Plant Physiology and Biochemistry* 44**,** 483-493.

Dodd, A.N., Kudla, J., and Sanders, D. (2010). The language of calcium signaling. *Annual Review of Plant Biology* 61**,** 593-620.

Dubcovsky, J., Maria, G.S., Epstein, E., Luo, M.C., and Dvorak, J. (1996). Mapping of the K^+/Na^+ discrimination locus *Kna1* in wheat. *Theoretical and Applied Genetics* 92**,** 448-454.

Dvorak, J., Noaman, M.M., Goyal, S., and Gorham, J. (1994). Enhancement of the salt tolerance of *Triticum turgidum* L. by the *Kna1* locus transferred from the *Triticum aestivum* L. chromosome 4D by homoeologous recombination. *Theoretical and Applied Genetics* 87**,** 872-877.

El-Hendawy, S.E., Hu, Y., and Schmidhalter, U. (2005). Growth, ion content, gas exchange, and water relations of wheat genotypes differing in salt tolerances. *Australian Journal of Agricultural Research* 56**,** 123-134.

Elshire, R.J., Glaubitz, J.C., Sun, Q., Poland, J.A., Kawamoto, K., Buckler, E.S., and Mitchell, S.E. (2011). A robust, simple genotyping-by-sequencing (GBS) approach for high diversity species. *PLoS ONE* 6**,** e19379.

Elumalai, R.P., Nagpal, P., and Reed, J.W. (2002). A mutation in the Arabidopsis KT2/KUP2 potassium transporter gene affects shoot cell expansion. *The Plant Cell* 14**,** 119-131.

FAO (2019). FAOSTAT. http://www.fao.org/faostat/en/#data/QC. Accessed 26 May 2019.

Flowers, T. (2004). Improving crop salt tolerance. *Journal of Experimental botany* 55**,** 307-319.

Fortmeier, R., and Schubert, S. (1995). Salt tolerance of maize (*Zea mays* L.): the role of sodium exclusion. *Plant Cell & Environment* 18**,** 1041-1047.

Gajdanowicz, P., Michard, E., Sandmann, M., Rocha, M., Corrêa, L.G.G., Ramírez-Aguilar, S.J., Gomez-Porras, J.L., González, W., Thibaud, J.-B., and Van Dongen, J.T. (2011). Potassium (K^+) gradients serve as a mobile energy source in plant vascular tissues. *Proceedings of the National Academy of Sciences* 108**,** 864-869.

Garcia, M., Eckermann, P., Haefele, S., Satija, S., Sznajder, B., Timmins, A., Baumann, U., Wolters, P., Mather, D.E., and Fleury, D. (2019). Genome-wide association mapping of grain yield in a diverse collection of spring wheat (*Triticum aestivum* L.) evaluated in southern Australia. *PLoS ONE* 14**,** e0211730.

Gaxiola, R.A., Yuan, D.S., Klausner, R.D., and Fink, G.R. (1998). The yeast CLC chloride channel functions in cation homeostasis. *Proceedings of the National Academy of Sciences* 95**,** 4046-4050.

Genc, Y., Oldach, K., Gogel, B., Wallwork, H., Mcdonald, G.K., and Smith, A.B. (2013). Quantitative trait loci for agronomic and physiological traits for a bread wheat population grown in environments with a range of salinity levels. *Molecular Breeding* 32**,** 39-59.

Genc, Y., Oldach, K., Verbyla, A.P., Lott, G., Hassan, M., Tester, M., Wallwork, H., and Mcdonald, G.K. (2010). Sodium exclusion QTL associated with improved seedling

growth in bread wheat under salinity stress. *Theoretical and Applied Genetics* 121**,** 877-894.

Genc, Y., Taylor, J., Lyons, G.H., Li, Y., Cheong, J., Appelbee, M., Oldach, K., and Sutton, T. (2019). Bread wheat with high salinity and sodicity tolerance. *Frontiers in Plant Science* 10**,** 1280.

Genc, Y., Taylor, J., Rongala, J., and Oldach, K. (2014). A major locus for chloride accumulation on chromosome 5A in bread wheat. *PLoS ONE* 9**,** e98845

Ghaedrahmati, M., Mardi, M., Naghavi, M.R., Haravan, E.M., Nakhoda, B., Azadi, A., and Kazemi, M. (2014). Mapping QTLs associated with salt tolerance related traits in seedling stage of wheat (*Triticum aestivum* L.). *Journal of Agricultural Science and Technology* 16**,** 1413-1428.

Gierth, M., and Mäser, P. (2007). Potassium transporters in plants – involvement in K^+ acquisition, redistribution and homeostasis. *FEBS Letters* 581**,** 2348-2356.

Gobert, A., Isayenkov, S., Voelker, C., Czempinski, K., and Maathuis, F.J. (2007). The two-pore channel *TPK1* gene encodes the vacuolar K^+ conductance and plays a role in K^+ homeostasis. *Proceedings of the National Academy of Sciences* 104**,** 10726-10731.

Golzarian, M.R., Frick, R.A., Rajendran, K., Berger, B., Roy, S., Tester, M., and Lun, D.S. (2011). Accurate inference of shoot biomass from high-throughput images of cereal plants. *Plant Methods* 7.

Grogan, S.M., Brown-Guedira, G., Haley, S.D., Mcmaster, G.S., Reid, S.D., Smith, J., and Byrne, P.F. (2016). Allelic variation in developmental genes and effects on winter wheat heading date in the US Great Plains. *PLoS ONE* 11**,** e0152852.

Hazzouri, K.M., Khraiwesh, B., Amiri, K.M.A., Pauli, D., Blake, T., Shahid, M., Mullath, S.K., Nelson, D., Mansour, A.L., Salehi-Ashtiani, K., Purugganan, M., and Masmoudi, K. (2018). Mapping of *HKT1;5* gene in barley using GWAS approach and its implication in salt tolerance mechanism. *Frontiers in Plant Science* 9.

Hirsch, R.E., Lewis, B.D., Spalding, E.P., and Sussman, M.R. (1998). A role for the AKT1 potassium channel in plant nutrition. *Science* 280**,** 918-921.

Huang, S.B., Spielmeyer, W., Lagudah, E.S., James, R.A., Platten, J.D., Dennis, E.S., and Munns, R. (2006). A sodium transporter (HKT7) is a candidate for *Nax1*, a gene for salt tolerance in durum wheat. *Plant Physiology* 142**,** 1718-1727.

Isayenkov, S., Isner, J.-C., and Maathuis, F.J. (2011). Rice two-pore K^+ channels are expressed in different types of vacuoles. *The Plant Cell* 23**,** 756-768.

James, R.A., Blake, C., Byrt, C.S., and Munns, R. (2011). Major genes for Na^+ exclusion, *Nax1* and *Nax2* (wheat *HKT1;4* and *HKT1;5*), decrease Na^+ accumulation in bread wheat leaves under saline and waterlogged conditions. *Journal of Experimental Botany* 62**,** 2939-2947.

James, R.A., Blake, C., Zwart, A.B., Hare, R.A., Rathjen, A.J., and Munns, R. (2012). Impact of ancestral wheat sodium exclusion genes *Nax1* and *Nax2* on grain yield of durum wheat on saline soils. *Functional Plant Biology* 39**,** 609-618.

James, R.A., Davenport, R.J., and Munns, R. (2006). Physiological characterization of two genes for Na^+ exclusion in durum wheat, *Nax1* and *Nax2*. *Plant Physiology* 142**,** 1537-1547.

Kaldenhoff, R., and Fischer, M. (2006a). Aquaporins in plants. *Acta Physiologica* 187**,** 169-176.

Kaldenhoff, R., and Fischer, M. (2006b). Functional aquaporin diversity in plants. *Biochimica et Biophysica Acta (BBA)-Biomembranes* 1758**,** 1134-1141.

Kudla, J., Batistič, O., and Hashimoto, K. (2010). Calcium signals: the lead currency of plant information processing. *The Plant Cell* 22**,** 541-563.

Lacombe, B., Pilot, G., Michard, E., Gaymard, F., Sentenac, H., and Thibaud, J.-B. (2000). A shaker-like K^+ channel with weak rectification is expressed in both source and sink phloem tissues of Arabidopsis. *The Plant Cell* 12**,** 837-851.

Lindsay, M.P., Lagudah, E.S., Hare, R.A., and Munns, R. (2004). A locus for sodium exclusion (*Nax1*), a trait for salt tolerance, mapped in durum wheat. *Functional Plant Biology* 31**,** 1105-1114.

Liu, L.-L., Ren, H.-M., Chen, L.-Q., Wang, Y., and Wu, W.-H. (2012). A protein kinase CIPK9 interacts with calcium sensor CBL3 and regulates K^+ homeostasis under low-K^+ stress in *Arabidopsis*. *Plant Physiology***,** pp. 112.206896.

Luan, S. (2009). The CBL–CIPK network in plant calcium signaling. *Trends in Plant Science* 14**,** 37-42.

Luan, S., Kudla, J., Rodriguez-Concepcion, M., Yalovsky, S., and Gruissem, W. (2002). Calmodulins and calcineurin B–like proteins: Calcium sensors for specific signal response coupling in plants. *The Plant Cell* 14**,** S389-S400.

Ma, L., Zhou, E., Huo, N., Zhou, R., Wang, G., and Jia, J. (2007). Genetic analysis of salt tolerance in a recombinant inbred population of wheat (*Triticum aestivum* L.). *Euphytica* 153**,** 109-117.

Martinez-Rodriguez, M.M., Estan, M.T., Moyano, E., Garcia-Abellan, J.O., Flores, F.B., Campos, J.F., Al-Azzawi, M.J., Flowers, T.J., and Bolarin, M.C. (2008). The effectiveness of grafting to improve salt tolerance in tomato when an 'excluder' genotype is used as scion. *Environmental and Experimental Botany* 63**,** 392-401.

Masoudi, B., Mardi, M., Hervan, E.M., Bihamta, M.R., Naghavi, M.R., Nakhoda, B., and Amini, A. (2015). QTL mapping of salt tolerance traits with different effects at the seedling stage of bread wheat. *Plant Molecular Biology Reporter* 33**,** 1790-1803.

Munns, R., James, R.A., Gilliham, M., Flowers, T.J., and Colmer, T.D. (2016). Tissue tolerance: an essential but elusive trait for salt-tolerant crops. *Functional Plant Biology* 43**,** 1103-1113.

Munns, R., James, R.A., and Lauchli, A. (2006). Approaches to increasing the salt tolerance of wheat and other cereals. *Journal of Experimental Botany* 57**,** 1025-1043.

Munns, R., James, R.A., Xu, B., Athman, A., Conn, S.J., Jordans, C., Byrt, C.S., Hare, R.A., Tyerman, S.D., Tester, M., Plett, D., and Gilliham, M. (2012). Wheat grain yield on saline soils is improved by an ancestral Na^+ transporter gene. *Nature Biotechnology* 30**,** 360-U173.

Munns, R., Rebetzke, G.J., Husain, S., James, R.A., and Hare, R.A. (2003). Genetic control of sodium exclusion in durum wheat. *Australian Journal of Agricultural Research* 54**,** 627-635.

Munns, R., and Tester, M. (2008). Mechanisms of salinity tolerance. *Annual Review of Plant Biology* 59**,** 651-681.

Nieves-Cordones, M., Alemán, F., Martínez, V., and Rubio, F. (2014). K^+ uptake in plant roots. The systems involved, their regulation and parallels in other organisms. *Journal of plant physiology* 171**,** 688-695.

Oyiga, B.C., Sharma, R.C., Baum, M., Ogbonnaya, F.C., Leon, J., and Ballvora, A. (2018). Allelic variations and differential expressions detected at quantitative trait loci for salt stress tolerance in wheat. *Plant Cell & Environment* 41**,** 919-935.

Poland, J.A., Brown, P.J., Sorrells, M.E., and Jannink, J.L. (2012). Development of high-density genetic maps for barley and wheat using a novel two-enzyme genotyping-by-sequencing approach. *PLoS ONE* 7.

Quigley, F., Rosenberg, J.M., Shachar-Hill, Y., and Bohnert, H.J. (2001). From genome to function: the *Arabidopsis* aquaporins. *Genome Biology* 3**,** 1-17.

Ragel, P., Ródenas, R., García-Martín, E., Andrés, Z., Villalta, I., Nieves-Cordones, M., Rivero, R.M., Martínez, V., Pardo, J.M., and Quintero, F.J. (2015). The CBL-interacting protein kinase CIPK23 regulates HAK5-mediated high-affinity K^+ uptake in Arabidopsis roots. *Plant Physiology* 169**,** 2863-2873.

Rajendran, K., Tester, M., and Roy, S.J. (2009). Quantifying the three main components of salinity tolerance in cereals. *Plant Cell & Environment* 32**,** 237-249.

Ren, Z.H., Gao, J.P., Li, L.G., Cai, X.L., Huang, W., Chao, D.Y., Zhu, M.Z., Wang, Z.Y., Luan, S., and Lin, H.X. (2005). A rice quantitative trait locus for salt tolerance encodes a sodium transporter. *Nature Genetics* 37**,** 1141-1146.

Rogowsky, P.M., Guidet, F.L.Y., Langridge, P., Shepherd, K.W., and Koebner, R.M.D. (1991). Isolation and characterization of wheat-rye recombinants involving chromosome arm 1ds of wheat. *Theoretical and Applied Genetics* 82**,** 537-544.

Shabala, S. (2017). Signalling by potassium: another second messenger to add to the list? *Journal of Experimental Botany* 68**,** 4003-4007.

Shabala, S., and Cuin, T.A. (2008). Potassium transport and plant salt tolerance. *Physiologia Plantarum* 133**,** 651-669.

Shewry, P.R. (2009). Wheat. *Journal of Experimental Botany* 60**,** 1537-1553.

Shi, S., Li, S., Asim, M., Mao, J., Xu, D., Ullah, Z., Liu, G., Wang, Q., and Liu, H. (2018). The *Arabidopsis* calcium-dependent protein kinases (CDPKs) and their roles in plant growth regulation and abiotic stress responses. *International Journal of Molecular Sciences* 19**,** 1900.

Steinhorst, L., and Kudla, J. (2019). How plants perceive salt. *Nature* 572**,** 318-320.

Suchecki, R., Watson-Haigh, N.S., and Baumann, U. (2017). POTAGE: A visualisation tool for speeding up gene discovery in wheat. *Scientific Reports* 7.

Takahashi, F., Tilbrook, J., Trittermann, C., Berger, B., Roy, S.J., Seki, M., Shinozaki, K., and Tester, M. (2015). Comparison of leaf sheath transcriptome profiles with physiological traits of bread wheat cultivars under salinity stress. *PLoS ONE* 10.

Takahashi, Y., and Tateda, C. (2013). The functions of voltage-dependent anion channels in plants. *Apoptosis* 18**,** 917-924.

Taylor, J., and Butler, D. (2017). R Package ASMap: Efficient genetic linkage map construction and diagnosis. *Journal of Statistical Software* 79**,** 1-29.

Team, R.C. (2018). "R: A language and environment for statistical computing". (Vienna, Austria: R Foundation for Statistical Computing).

Thoday-Kennedy, E.L., Jacobs, A.K., and Roy, S.J. (2015). The role of the CBL–CIPK calcium signalling network in regulating ion transport in response to abiotic stress. *Plant Growth Regulation* 76**,** 3-12.

Tilbrook, J., Schilling, R.K., Berger, B., Garcia, A.F., Trittermann, C., Coventry, S., Rabie, H., Brien, C., Nguyen, M., and Tester, M. (2017). Variation in shoot tolerance mechanisms not related to ion toxicity in barley. *Functional Plant Biology* 44**,** 1194-1206.

Ueda, A., Shi, W., Sanmiya, K., Shono, M., and Takabe, T. (2001). Functional analysis of salt-inducible proline transporter of barley roots. *Plant and Cell Physiology* 42**,** 1282-1289.

Wang, S.C., Basten, C.J., and Zeng, Z.B. (2012). "Windows QTL Cartographer 2.5". (Department of Statistics, North Carolina State University, Raleigh, NC).

Wang, X.-P., Chen, L.-M., Liu, W.-X., Shen, L.-K., Wang, F.-L., Zhou, Y., Zhang, Z., Wu, W.-H., and Wang, Y. (2016). AtKC1 and CIPK23 synergistically modulate AKT1-mediated low-potassium stress responses in Arabidopsis. *Plant Physiology* 170**,** 2264-2277.

Watson-Haigh, N.S., Suchecki, R., Kalashyan, E., Garcia, M., and Baumann, U. (2018). DAWN: a resource for yielding insights into the diversity among wheat genomes. *BMC Genomics* 19**,** 941.

Wei, Q., Guo, Y., Cao, H., and Kuai, B. (2011). Cloning and characterization of an *AtNHX2*-like Na^+/H^+ antiporter gene from *Ammopiptanthus mongolicus* (Leguminosae) and its ectopic expression enhanced drought and salt tolerance in *Arabidopsis thaliana*. *Plant Cell, Tissue and Organ Culture* 105**,** 309-316.

Weinl, S., and Kudla, J. (2009). The CBL-CIPK Ca^{2+}-decoding signaling network: function and perspectives. *New Phytologist* 184**,** 517-528.

Wrigley, C. (2009). "Wheat: a unique grain for the world," in *Wheat: Chemistry and technology*, eds. K. Khan & P.R. Shewry. 4th ed (U.S.A.: AACC International, Inc.), 1-17.

Yokoi, S., Quintero, F.J., Cubero, B., Ruiz, M.T., Bressan, R.A., Hasegawa, P.M., and Pardo, J.M. (2002). Differential expression and function of *Arabidopsis thaliana* NHX Na^+/H^+ antiporters in the salt stress response. *The Plant Journal* 30**,** 529-539.

Figures

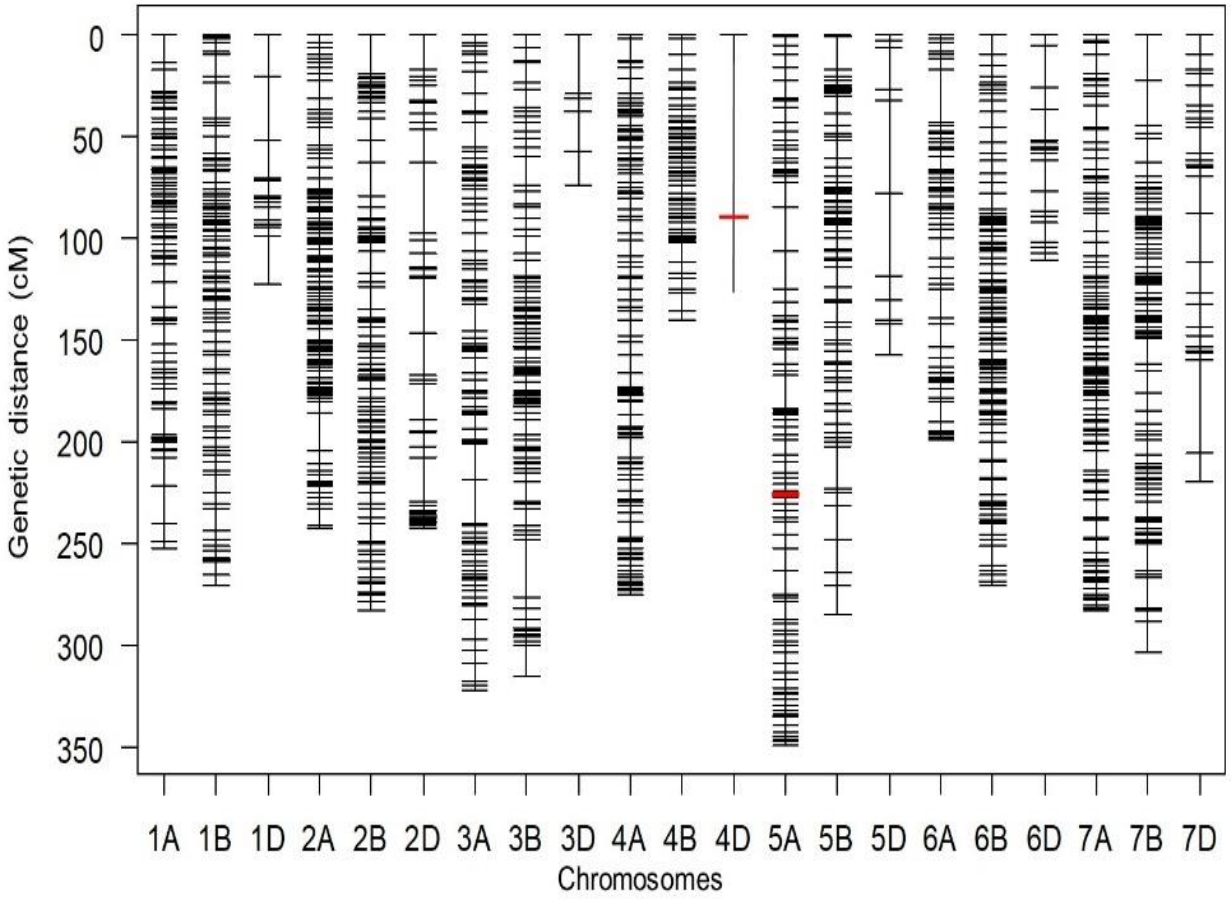

Figure 1: Visual representation of the genetic linkage map of the F_2 Mocho de Espiga Branca × Gladius population showing the chromosomes and the genetic distance (cM). The two markers ch4D-aslsnp-hkt and wMAS000033 were added in addition to the GBS generated SNP markers and are indicated in red on chromosome 4D and 5A, respectively.

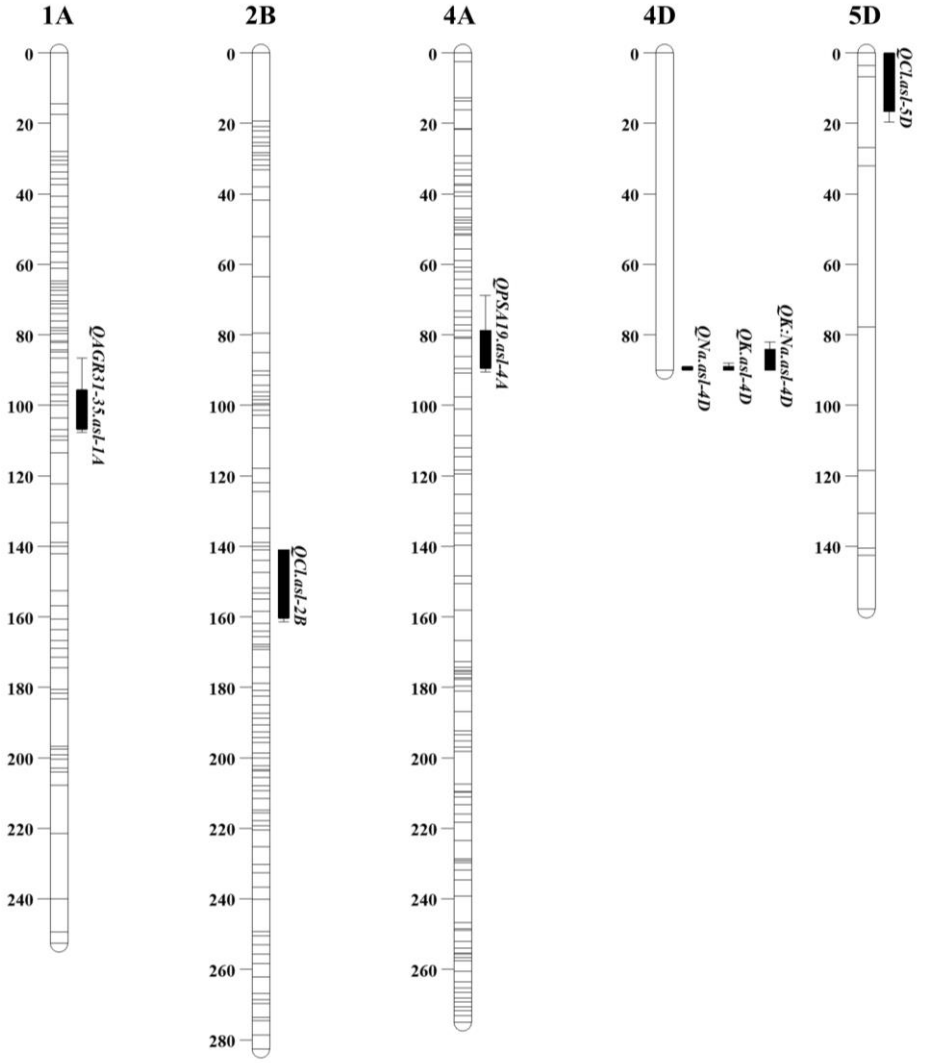

Figure 2: QTL positions detected in composite interval mapping with 1000 permutation at $p \leq 0.05$ for salinity tolerance traits in the Mocho de Espiga Branca × Gladius F_2 population. The vertical QTL bars represent the 1 and 2 LOD drops from the maximum likelihood value. QTL and their positions are indicated for absolute growth rate $AGR_{31\text{-}35}$ (*$QAGR_{31\text{-}35}$.asl-1A*), projected shoot area PSA_{19} (*$QPSA_{19}$.asl-4A*), 4th leaf Na^+ concentration (µmol/g DW) (*QNa.asl-4D*), 4th leaf K^+ concentration (µmol/g DW) (*QK.asl-4D*), 4th leaf K^+:Na^+(*QK:Na.asl-4D*), and 4th leaf Cl^- concentration (µmol/g DW) (*QCl.asl*-2B and *QCl.asl-5D*).

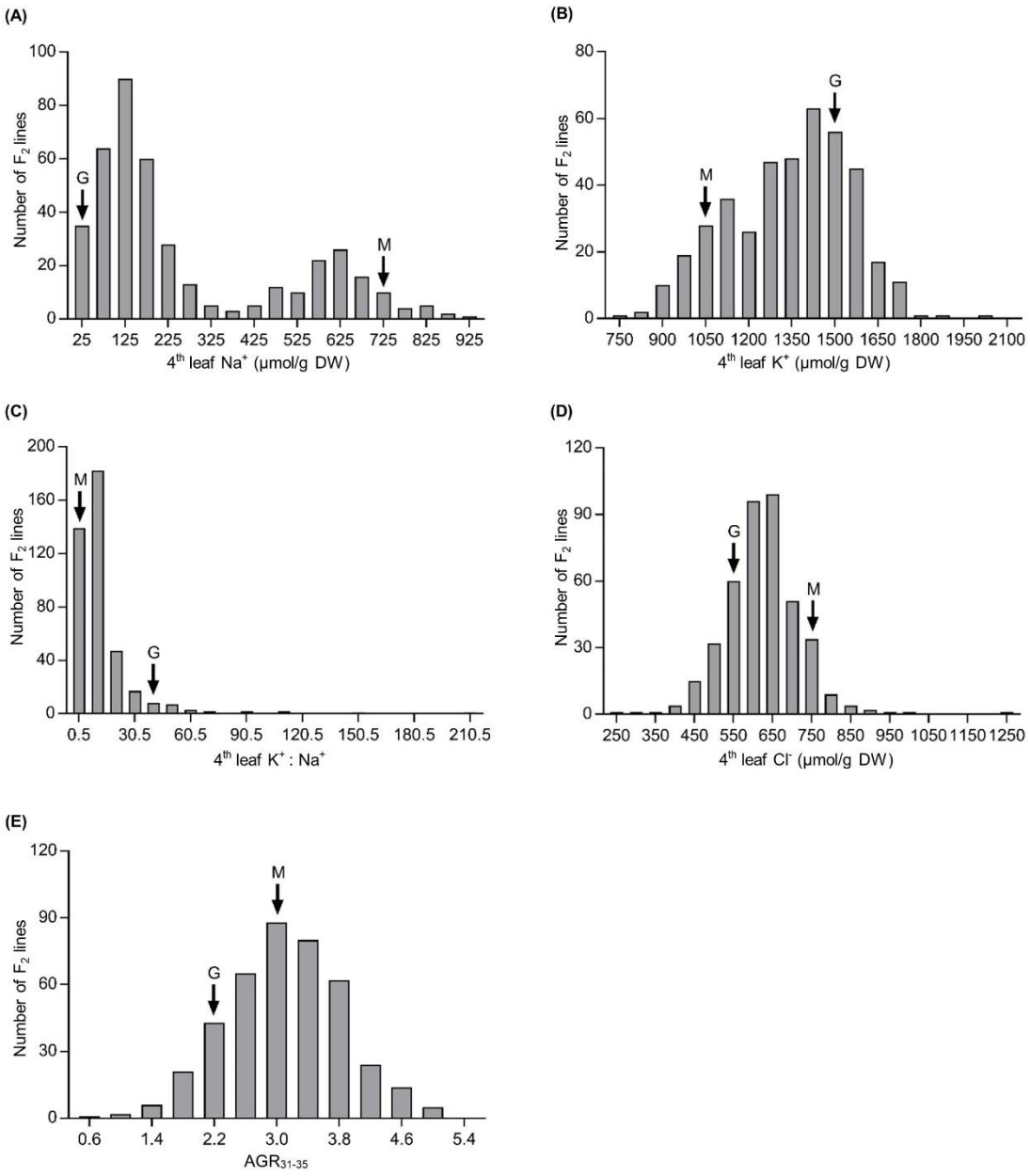

Figure 3: Frequency distribution of the F_2 population for the salinity tolerance sub-traits. **(A)** 4^{th} leaf Na^+ (µmol/g DW). **(B)** 4^{th} leaf K^+ (µmol/g DW). **(C)** 4^{th} leaf K^+:Na^+ (DW). **(D)** 4^{th} leaf Cl^- (µmol/g DW). **(E)** Smoothed absolute growth rate AGR_{31-35} after 12 days in 150 mM NaCl applied at the emergence of 4^{th} leaf. Arrows indicate the trait mean for parents, M = Mocho de Espiga Branca and G = Gladius.

Tables

Table 1. Summary table of the genetic linkage map constructed for the Mocho de Espiga Branca × Gladius F_2 population.

	Chromosome	No. of markers	Length of chromosome (cM)	Ave. spacing between markers (cM)	Max. spacing between marker (cM)
	1A	117	252.6	2.2	18.6
	1B	146	270.4	1.9	17.7
	1D	28	123.3	4.6	31.6
	2A	217	242.6	1.1	19.3
	2B	156	282.6	1.8	19.2
	2D	62	243.0	4.0	34.5
	3A	152	321.9	2.1	20.9
	3B	158	314.9	2.0	28.5
	3D	6	74.1	14.8	29.5
	4A	218	275.0	1.3	10.3
	4B	98	140.1	1.4	9.8
	4D	2	90.1	90.1	90.1
	5A	140	348.7	2.5	21.6
	5B	122	285.1	2.4	21.5
	5D	13	157.8	13.2	45.7
	6A	90	198.8	2.2	26.2
	6B	184	270.5	1.5	9.5
	6D	29	111.4	4.0	20.8
	7A	197	282.7	1.4	10.8
	7B	162	303.5	1.9	23.3
	7D	46	219.8	4.9	45.8
Total	21	2343	4808.7	2.1	90.1

Table 2: The mean ± SEM of the parents Mocho de Espiga Branca and Gladius, and range of the F_2 population (min-max) for plant growth and 4th leaf ion concentrations. The statistical significance between Mocho de Espiga Branca and Gladius is indicated asterisk ($p \leq 0.01$ = **, $p \leq 0.001$ = ***, $p \leq 0.0001$ = ****).

Traits	Mocho de Espiga Branca	Gladius	F_2 population
Na^+ (µmol/g DW)	741.7 ± 20.1 ****	39.7 ± 34.2	7.7 - 945.7
K^+ (µmol/g DW)	967.0 ± 20.0	1499.0 ± 30.0	754.6 - 2018.2
$K^+ : Na^+$	1.3 ± 2.5 ****	37.7 ± 4.2	0.9 - 209.0
Cl^- (µmol/g DW)	757.7 ± 18.1 ***	593.0 ± 30.8	251.0 - 1243.9
PSA_{19} (kpixels)	15.0 ± 0.5 ***	10.5 ± 0.9	4.6 - 24.9
PSA_{22} (kpixels)	20.5 ± 0.7 ***	14.6 ± 1.1	6.1 - 33.8
PSA_{24} (kpixels)	24.8 ± 0.7 ****	17.9 ± 1.3	7.6 - 41.0
PSA_{28} (kpixels)	35.6 ± 1.1 ***	26.1 ± 1.8	12.6 - 62.5
PSA_{31} (kpixels)	46.0 ± 1.4***	33.3 ± 2.4	17.8 - 81.6
PSA_{35} (kpixels)	58.6 ± 1.9 ***	41.9 ± 3.3	25.1 - 102.2
$AGR_{19\text{-}22}$	1.83 ± 0.05***	1.40 ± 0.09	0.52 - 3.10
$AGR_{24\text{-}28}$	2.69 ± 0.09 **	2.07 ± 0.15	1.06 - 5.38
$AGR_{28\text{-}31}$	3.49 ± 0.15 ***	2.39 ± 0.24	1.38 - 6.39
$AGR_{31\text{-}35}$	3.13 ± 0.16 **	2.16 ± 0.28	0.61 - 5.15
$RGR_{19\text{-}22}$	0.11 ± 0.003	0.11 ± 0.005	0.07 - 0.15
$RGR_{24\text{-}28}$	0.09 ± 0.001	0.10 ± 0.002	0.03 - 0.11
$RGR_{28\text{-}31}$	0.09 ± 0.002	0.08 ± 0.004	0.05 - 0.11
$RGR_{31\text{-}35}$	0.06 ± 0.002	0.06 ± 0.003	0.01 - 0.10
Predicted OST	0.88 ± 0.02	0.84 ± 0.03	0.38 - 1.23

Table 3: QTL detected for plant growth and 4th leaf ion concentration in the Mocho de Espiga Branca × Gladius F_2 population using composite interval mapping with 1000 permutation at $p \leq 0.05$. The phenotypic trait with the corresponding QTL detected for the traits are given along with the chromosome, the most significant marker and the marker position on the chromosome, the highest LOD score of the QTL, the allele giving the high phenotypic value, additive effect and phenotypic variation (R^2) explained by the QTL.

Traits	QTL	Chromosome	Marker	Position (cM)	LOD	Additive effect	R^2 (%)
AGR_{31-35}	*$QAGR_{31-35}$.asl-1A*	1A	chr1A_part2:39526696	98.7	4.1	-0.3	4.4
PSA_{19}	*$QPSA_{19}$.asl-4A*	4A	chr4A_part2:125991586	80.5	4.3	-0.7	4.8
Na^+(µmol/g DW)	*QNa.asl-4D*	4D	chr4D_aslsnp	90.0	204.0	666.0	87.2
K^+ (µmol/g DW)	*QK.asl-4D*	4D	chr4D_aslsnp	90.0	77.1	-304.0	57.3
K^+ : Na^+	*QK:Na..asl-4D*	4D	chr4D_aslsnp	90.0	24.7	-10.9	24.4
Cl^- (µmol/g DW)	*QCl.asl-2B*	2B	chr2B_part1:89540368	150.3	5.3	-66.8	6.4
Cl^- (µmol/g DW)	*QCl.asl-5D*	5D	chr5D_part1:63554387	5.6	6.4	17.6	10.8

Table 4: Significant marker ($p \leq 0.001$) intervals detected for plant growth and 4th leaf ion concentration in the Mocho de Espiga Branca × Gladius F_2 population using single marker analysis. The phenotypic traits, chromosome and the intervals containing the significant markers to the corresponding traits are shown along with the most significant marker(s) and its position within the intervals, the significance value (*p*-value) and the phenotypic variation (R^2) explained by the marker.

Traits	Chromosome	No. of significant markers	Chromosome intervals (cM)	Most significant marker	Most significant marker position (cM)	*p*-value	R^2 (%)
AGR_{31-35}	5A	5	233.3-238.8	chr5A_part2:140244196	238.8	0.0006	1.2
				chr5A_part2:140244342	238.8	0.0006	1.2
RGR_{19-22}	1B	5	265.5-270.4	chrUn:314415261	270.4	0.0005	2.4
RGR_{28-31}	4B	47	24.1-73.6	chr4B_part2:45450724	43.8	0.00001	3.4
				chr4B_part2:78847426	43.8	0.00001	4.3
				chr4B_part2:78847457	43.8	0.00001	4.3
RGR_{31-35}	1D	1	79.2	chr1D_part1:420778665	79.2	0.0008	4.2
	4B	13	39.9-46.2	chr4B_part1:254015341	46.2	0.0002	1.8
				chr4B_part2:35164633	46.2	0.0002	0.1
	5A	13	297.7	chr5A_part2:214471250	297.7	0.0007	0.1
				chr5A_part2:214471317	297.7	0.0007	0.1
				chr5A_part2:216085838	297.7	0.0007	2.1
K^+(µmol/g DW)	2A	29	54.3-110.7	chr2A_part1:125947821	98.2	0.0003	0.5
				chr2A_part1:125947705	98.2	0.0003	0.5

Table 5: List of potential candidate genes (gene ID and gene name) for each QTL detected in CIM. The respective Munich Information Center for Protein Sequences (MIPS) annotation hit ID and rice annotation hit ID were given for each gene.

QTL	Chromosome	Gene ID	MIPS annotation hit ID	Rice annotation hit ID	Gene name
$QAGR_{31\text{-}35}$.asl-1A	1A	Traes_1AL_4D668D012	sp|Q0JKV1|AKT1_ORYSJ	LOC_Os03g21390.1	Potassium channel AKT1
		Traes_1AL_792E76B4D	sp|Q38998|AKT1_ARATH	LOC_Os03g42350.1	Potassium channel AKT1
		Traes_1AL_B7757AFDC	sp|Q75HP9|AKT2_ORYSJ	LOC_Os02g29210.2	Potassium channel AKT2
		Traes_1AL_AC6219D99	AT4G23640.1	LOC_Os05g37900.1	Potassium transporter family protein
		Traes_1AL_4FBAF0AAA	sp|Q1HDT3|CHX16_ARATH	LOC_Os07g48650.1	Cation/H^+ antiporter 16
		Traes_1AL_95C7D27A7	sp|Q9M353|CHX20_ARATH	LOC_Os03g31630.1	Cation/H^+ antiporter 20
		Traes_1AL_2D9BC6EE1	AT1G80660.1	LOC_Os05g33644.1	H^+-ATPase 9
		Traes_1AL_4A8B12704	sp|Q08435|PMA1_NICPL	LOC_Os05g37520.2	Plasma membrane ATPase 1
		Traes_1AL_746797AE4	AT5G47100.1	LOC_Os05g30900.1	Calcineurin B-like protein 9
		Traes_1AL_7FE24229E	AT5G04870.1	LOC_Os03g04950.1	Calcium dependent protein kinase 1
		Traes_1AL_C49C8F4AE	AT3G51850.1	LOC_Os05g30870.2	Calcium-dependent protein kinase 13
		Traes_1AL_8D078BE99	AT5G19360.1	LOC_Os01g71000.1	Calcium-dependent protein kinase 34
		Traes_1AL_2A72FFFD6	sp|Q9SZR1|ACA10_ARATH	LOC_Os05g30860.1	Calcium-transporting ATPase 10, plasma membrane-type
		Traes_1AL_F120A5C0D	AT5G53010.1	LOC_Os04g56646.1	Calcium-transporting ATPase, putative
		Traes_1AL_504CDB1731	AT3G43810.1	LOC_Os05g30820.1	Calmodulin 7
		Traes_1AL_80931BE4C	AT1G66400.1	LOC_Os05g30810.1	Calmodulin like 23
$QPSA_{19}$.asl-4A	4A	Traes_4AS_AF4D76704	AT2G40540.1	LOC_Os03g21890.1	potassium transporter 2
		Traes_4AS_46D587139	AT3G05030.1	LOC_Os11g42790.1	sodium hydrogen exchanger 2
		Traes_4AL_3C35261D2	sp|P48768|NAC2_RAT	LOC_Os11g43860.1	Sodium/calcium exchanger 2
		Traes_4AS_F1B3DEB2E	sp|Q5KQN0|CAX2_ORYSJ	LOC_Os03g27960.2	Vacuolar cation/proton exchanger 2
		Traes_4AL_ECCF59611	AT1G54115.1	LOC_Os03g45370.1	cation calcium exchanger 4
		Traes_4AL_0B1EB340A	AT5G55990.1	LOC_Os03g42840.1	calcineurin B-like protein 2
		Traes_4AL_FB1F95CD6	AT1G18890.1	LOC_Os03g48270.1	calcium-dependent protein kinase 1
		Traes_4AL_E0E01F494	AT5G12180.1	LOC_Os11g04170.1	calcium-dependent protein kinase 17
		Traes_4AL_D787CF1CC	AT1G35670.1	LOC_Os11g07040.1	calcium-dependent protein kinase 2

		Traes_4AL_C2ED5E9A0	AT5G21274.1	LOC_Os11g03980.1	calmodulin 6
		Traes_4AL_FA171F7B7	AT5G26240.1	LOC_Os03g48940.3	chloride channel D
		Traes_4AL_0C3D39404	AT5G62670.1	LOC_Os12g44150.1	H^+-ATPase 11
		Traes_4AL_BF403A651	AT2G02040.1	LOC_Os10g02260.2	peptide transporter 2
		Traes_4AL_5B4F878CD	sp|Q7XPY2|PMA1_ORYSJ	LOC_Os04g56160.1	Plasma membrane ATPase
		Traes_4AL_A1A9045D1	AT3G55740.1	LOC_Os07g01090.1	proline transporter 2
QNa.asl-4D	4D	Traes_4DL_3F8034BFD	sp|A2WNZ9|HKT8_ORYSI	LOC_Os01g20160.1	Cation transporter HKT8
QK.asl-4D	4D	Traes_4DL_3F8034BFD	sp|A2WNZ9|HKT8_ORYSI	LOC_Os01g20160.1	Cation transporter HKT8
QK:Na.asl-4D	4D	Traes_4DL_3F8034BFD	sp|A2WNZ9|HKT8_ORYSI	LOC_Os01g20160.1	Cation transporter HKT8
QCl.asl-2B	2B	Traes_2BS_B10700C00	AT4G15755.1	LOC_Os07g47400.1	Calcium-dependent lipid-binding CaLB domain family protein
		Traes_2BS_61278E8A5	AT3G16510.1	LOC_Os07g47400.1	Calcium-dependent lipid-binding CaLB domain family protein
		Traes_2BS_6AECC4811	AT2G27030.3	LOC_Os07g48780.2	Calmodulin 5
		Traes_2BS_6EAAACBDB	AT5G44460.1	LOC_Os07g48340.1	Calmodulin like 43
		Traes_2BS_E5A481317	AT1G54115.1	LOC_Os10g30070.1	Cation calcium exchanger 4
		Traes_2BS_47F79F636	sp|Q7XIW5|CIPKT_ORYSJ	LOC_Os07g48090.1	CBL-interacting protein kinase 29
		Traes_2BS_7BEE046C4	AT2G26980.4	LOC_Os03g20380.7	CBL-interacting protein kinase 3
		Traes_2BS_E67905E6E	AT2G40540.1	LOC_Os07g48130.3	Potassium transporter 2
		Traes_2BS_ECB89174C	AT4G23640.1	LOC_Os07g47350.1	Potassium transporter family protein
		Traes_2BS_3DBC04D39	AT3G05030.1	LOC_Os07g47100.1	Sodium hydrogen exchanger 2
QCl.asl-5D	5D	Traes_5DS_643ED07F6	AT2G37180.1	LOC_Os07g26630.1	Aquaporin-like superfamily protein
		Traes_5DL_448D838B8	AT2G37180.1	LOC_Os02g57720.1	Aquaporin-like superfamily protein
		Traes_5DL_06BF9D1C5	AT2G37180.1	LOC_Os02g44630.3	Aquaporin-like superfamily protein
		Traes_5DS_C968A4E2D	AT4G26570.2	LOC_Os03g42840.1	Calcineurin B-like 3
		Traes_5DS_8471D9E4E	AT5G04870.1	LOC_Os12g30150.1	Calcium dependent protein kinase 1
		Traes_5DS_3D1DB3A71	AT5G04870.1	LOC_Os12g30150.1	Calcium dependent protein kinase 1
		Traes_5DL_14E94E5EE	sp|Q8NE86|MCU_HUMAN	LOC_Os12g02880.1	Calcium uniporter protein, mitochondrial
		Traes_5DL_2184773BC	AT5G47710.1	LOC_Os09g07800.1	Calcium-dependent lipid-binding CaLB domain family protein

Traes_5DL_701598D5F	AT5G12180.1	LOC_Os11g04170.1	Calcium-dependent protein kinase 17
Traes_5DS_51F474DBB	AT5G19450.1	LOC_Os12g12860.1	Calcium-dependent protein kinase 19
Traes_5DS_8C4EC71C0	AT2G31500.1	LOC_Os12g12860.1	Calcium-dependent protein kinase 24
Traes_5DS_69B96465C	AT4G09570.1	LOC_Os12g07230.1	Calcium-dependent protein kinase 4
Traes_5DS_955830536	AT5G53010.1	LOC_Os12g39660.1	Calcium-transporting ATPase
Traes_5DL_761CB8E23	AT5G53010.1	LOC_Os12g04220.1	Calcium-transporting ATPase
Traes_5DL_643823248	AT2G27030.3	LOC_Os11g03980.1	Calmodulin 5
Traes_5DL_90F99AE94	AT1G66400.1	LOC_Os12g04360.1	Calmodulin like 23
Traes_5DL_298BDEE72	AT3G58480.1	LOC_Os12g05420.1	Calmodulin-binding family protein
Traes_5DS_F8172A424	AT4G25800.1	LOC_Os12g36920.1	Calmodulin-binding protein
Traes_5DS_F49283B77	AT4G25800.1	LOC_Os12g36920.1	Calmodulin-binding protein
Traes_5DS_1121EE05F	AT2G18750.1	LOC_Os12g36910.1	Calmodulin-binding protein
Traes_5DS_4A3E02637	AT5G57580.1	LOC_Os12g36110.1	Calmodulin-binding protein
Traes_5DS_7EA171D66	AT3G22930.1	LOC_Os12g41110.1	Calmodulin-like 11
Traes_5DL_FCB8BFE07	AT1G76650.1	LOC_Os12g01400.1	Calmodulin-like 38
Traes_5DL_B669983C4	sp|O04034|CCX5_ARATH	LOC_Os03g08230.1	Cation/calcium exchanger 5
Traes_5DL_C7F1BB6A0	sp|Q9LMJ1|CHX14_ARATH	LOC_Os11g01820.1	Cation/H^+ antiporter 14
Traes_5DL_A3762659F	sp|Q9SIT5|CHX15_ARATH	LOC_Os11g01820.1	Cation/H^+ antiporter 15
Traes_5DS_D50F61EE5	sp|Q9FFR9|CHX18_ARATH	LOC_Os12g42200.1	Cation/H^+ antiporter 18
Traes_5DS_09D7A479D	sp|Q9LUN4|CHX19_ARATH	LOC_Os12g42200.1	Cation/H^+ antiporter 19
Traes_5DL_52119C4D7	AT1G49810.1	LOC_Os09g02214.2	Na^+/H^+ antiporter 2
Traes_5DL_96739D4C9	AT1G49810.1	LOC_Os09g02214.1	Na^+/H^+ antiporter 2
Traes_5DL_D5AE9C6F1	AT1G54370.1	LOC_Os09g11450.2	Sodium hydrogen exchanger 5
Traes_5DL_F6D37B14B	AT1G54370.1	LOC_Os09g11450.1	Sodium hydrogen exchanger 5

Table 6: List of potential candidate genes (gene ID and gene name) within the significant marker ($p \leq 0.001$) intervals detected in SMA. The respective Munich Information Center for Protein Sequences (MIPS) annotation hit ID and rice annotation hit ID were given for each gene.

Traits	Chromosome	Gene ID	MIPS annotation hit ID	Rice annotation hit ID	Gene name
AGR_{31-35}	5A	Traes_5AL_51E31BF07	sp|Q850M0|KCO1_ORYSJ	LOC_Os03g54100.2	Two pore potassium channel a
		Traes_5AL_ACFA5E386	AT5G46050.1	LOC_Os11g17970.1	peptide transporter 3
		Traes_5AL_4477DED49	AT5G01180.1	LOC_Os11g17970.1	peptide transporter 5
RGR_{28-31}	4B	Traes_4BL_DA1CE6B1A	sp|Q9ATM2|SIP12_MAIZE	LOC_Os01g08660.1	Aquaporin SIP1-2
		Traes_4BL_C3F41C738	AT5G18290.1	LOC_Os03g20410.1	Aquaporin-like superfamily protein
		Traes_4BL_FBA9B0C69	AT1G73190.1	LOC_Os03g05290.1	Aquaporin-like superfamily protein
		Traes_4BL_F2CBFEC51	AT1G73190.1	LOC_Os03g05290.1	Aquaporin-like superfamily protein
		Traes_4BS_EBA462C3F	AT4G26570.2	LOC_Os03g42840.1	Calcineurin B-like 3
		Traes_4BL_E5F7EC8AA	AT1G20760.1	LOC_Os03g03830.1	Calcium-binding EF hand family protein
		Traes_4BL_3B8727D00	AT4G38810.2	LOC_Os03g14590.1	Calcium-binding EF-hand family protein
		Traes_4BS_CE48CB0F1	AT4G38810.2	LOC_Os03g14590.2	Calcium-binding EF-hand family protein
		Traes_4BL_2FD6A0AC5	AT1G05150.1	LOC_Os03g15740.1	Calcium-binding tetratricopeptide family protein
		Traes_4BL_BE65A0C40	AT1G50570.1	LOC_Os03g09840.2	Calcium-dependent lipid-binding CaLB domain family protein
		Traes_4BL_16A868FF7	AT3G61050.1	LOC_Os03g14700.1	Calcium-dependent lipid-binding CaLB domain family protein
		Traes_4BS_D7E5E888B	AT5G12180.1	LOC_Os11g04170.1	Calcium-dependent protein kinase 17
		Traes_4BS_9E2145C02	AT1G35670.1	LOC_Os11g07040.1	Calcium-dependent protein kinase 2
		Traes_4BL_9ECEDE4D2	AT1G74740.1	LOC_Os07g38120.1	Calcium-dependent protein kinase 30
		Traes_4BS_B913FA70A	AT3G57530.1	LOC_Os07g38120.1	Calcium-dependent protein kinase 32
		Traes_4BL_68E094E3F	AT3G57530.1	LOC_Os03g59390.1	Calcium-dependent protein kinase 32
		Traes_4BL_46AF42528	AT2G17290.1	LOC_Os03g03660.3	Calcium-dependent protein kinase family protein
		Traes_4BS_73F7EF1B8	sp|O34431|ATCL_BACSU	LOC_Os03g52090.1	Calcium-transporting ATPase
		Traes_4BL_A0A0E8D56	sp|Q08853|ATC_PLAFK	LOC_Os03g17310.1	Calcium-transporting ATPase

		Traes_4BS_E94608B81	AT5G53010.1	LOC_Os03g42020.1	Calcium-transporting ATPase, putative
		Traes_4BL_B4F048033	AT5G53010.1	LOC_Os03g10640.1	Calcium-transporting ATPase, putative
		Traes_4BS_8717122ED	AT2G27030.3	LOC_Os01g17190.1	Calmodulin 5
		Traes_4BL_53CBCD014	AT2G27030.3	LOC_Os07g48780.1	Calmodulin 5
		Traes_4BS_37CDC944F	UniRef90_B6U7V1	LOC_Os11g44920.1	Calmodulin binding protein
		Traes_4BL_F727FA1EC1	AT4G20780.1	LOC_Os03g21380.1	Calmodulin like 42
		Traes_4BS_BFA6CFA7F	UniRef90_G7JLF7	LOC_Os12g01400.1	Calmodulin
		Traes_4BL_6FDCC8F1E	AT3G13600.1	LOC_Os03g07110.2	Calmodulin-binding family protein
		Traes_4BL_84961FD37	AT4G25800.1	LOC_Os03g18960.1	Calmodulin-binding protein
		Traes_4BL_B1A680FE7	UniRef90_Q5VS78	LOC_Os06g01500.2	Calmodulin-binding protein-like
		Traes_4BL_A37F6FD08	sp|Q6NPP4|CMTA2_ARATH	LOC_Os03g09100.1	Calmodulin-binding transcription activator 2
		Traes_4BL_FE3EA0B32	sp|Q7Z624|CMKMT_HUMAN	LOC_Os03g14020.1	Calmodulin-lysine N-methyltransferase
		Traes_4BL_E0ABA8471	AT1G54115.1	LOC_Os03g08230.1	Cation calcium exchanger 4
		Traes_4BS_18D43D3ED	UniRef90_R0B0Y1	LOC_Os03g22550.1	Cation diffusion facilitator family transporter
		Traes_4BL_06DF64691	AT5G22900.1	LOC_Os08g43690.1	Cation/H^+ exchanger 3
		Traes_4BS_B0275259F	AT2G26980.4	LOC_Os12g03810.2	CBL-interacting protein kinase 3
		Traes_4BL_74FCE926F	AT1G01140.3	LOC_Os03g03510.1	CBL-interacting protein kinase 9
		Traes_4BL_F140DE329	AT2G07560.1	LOC_Os03g08560.1	H^+-ATPase 6
		Traes_4BS_E6A1E95AC	AT3G05030.1	LOC_Os11g42790.1	Sodium hydrogen exchanger 2
		Traes_4BS_BB2C84D23	sp|P48768|NAC2_RAT	LOC_Os11g43860.2	Sodium/calcium exchanger 2
		Traes_4BS_0F601AE0D	sp|Q5KQN0|CAX2_ORYSJ	LOC_Os03g27960.2	Vacuolar cation/proton exchanger 2
		Traes_4BL_998689F24	AT2G40540.1	LOC_Os03g21890.1	Potassium transporter 2
		Traes_4BL_C4F6FB884	AT2G40540.1	LOC_Os03g21890.1	Potassium transporter 2
		Traes_4BL_D897F4504	AT2G40540.1	LOC_Os03g21890.1	Potassium transporter 2
		Traes_4BL_0CD383B6E	AT2G40540.1	LOC_Os03g21890.1	Potassium transporter 2
RGR_{31-35}	1D	Traes_1DL_7528A328C	AT1G29230.1	LOC_Os05g43840.1	CBL-interacting protein kinase 18
	4B	Traes_4BL_C3F41C738	AT5G18290.1	LOC_Os03g20410.1	Aquaporin-like superfamily protein
		Traes_4BL_3B8727D00	AT4G38810.2	LOC_Os03g14590.1	Calcium-binding EF-hand family protein

		Traes_4BS_CE48CB0F1	AT4G38810.2	LOC_Os03g14590.2	Calcium-binding EF-hand family protein
		Traes_4BL_2FD6A0AC5	AT1G05150.1	LOC_Os03g15740.1	Calcium-binding tetratricopeptide family protein
		Traes_4BL_BE65A0C40	AT1G50570.1	LOC_Os03g09840.2	Calcium-dependent lipid-binding CaLB domain family protein
		Traes_4BL_16A868FF7	AT3G61050.1	LOC_Os03g14700.1	Calcium-dependent lipid-binding CaLB domain family protein
		Traes_4BL_9ECEDE4D2	AT1G74740.1	LOC_Os07g38120.1	Calcium-dependent protein kinase 30
		Traes_4BS_B913FA70A	AT3G57530.1	LOC_Os07g38120.1	Calcium-dependent protein kinase 32
		Traes_4BL_68E094E3F	AT3G57530.1	LOC_Os03g59390.1	Calcium-dependent protein kinase 32
		Traes_4BL_A0A0E8D56	sp|Q08853|ATC_PLAFK	LOC_Os03g17310.1	Calcium-transporting ATPase
		Traes_4BL_B4F048033	AT5G53010.1	LOC_Os03g10640.1	Calcium-transporting ATPase, putative
		Traes_4BL_53CBCD014	AT2G27030.3	LOC_Os07g48780.1	Calmodulin 5
		Traes_4BL_F727FA1EC1	AT4G20780.1	LOC_Os03g21380.1	Calmodulin like 42
		Traes_4BL_84961FD37	AT4G25800.1	LOC_Os03g18960.1	Calmodulin-binding protein
		Traes_4BL_B1A680FE7	UniRef90_Q5VS78	LOC_Os06g01500.2	Calmodulin-binding protein-like
		Traes_4BL_FE3EA0B32	sp|Q7Z624|CMKMT_HUMAN	LOC_Os03g14020.1	Calmodulin-lysine N-methyltransferase
		Traes_4BS_18D43D3ED	UniRef90_R0B0Y1	LOC_Os03g22550.1	Cation diffusion facilitator family transporter
		Traes_4BL_06DF64691	AT5G22900.1	LOC_Os08g43690.1	Cation/H^+ exchanger 3
		Traes_4BL_998689F24	AT2G40540.1	LOC_Os03g21890.1	Potassium transporter 2
		Traes_4BL_C4F6FB884	AT2G40540.1	LOC_Os03g21890.1	Potassium transporter 2
		Traes_4BL_D897F4504	AT2G40540.1	LOC_Os03g21890.1	Potassium transporter 2
		Traes_4BL_0CD383B6E	AT2G40540.1	LOC_Os03g21890.1	Potassium transporter 2
		Traes_4BS_0F601AE0D	sp|Q5KQN0|CAX2_ORYSJ	LOC_Os03g27960.2	Vacuolar cation/proton exchanger 2
	5A	Traes_5AL_4DA57EEF6	sp|Q94920|VDAC_DROME	LOC_Os03g04460.1	Voltage-dependent anion-selective channel
		Traes_5AL_0CC44448F	AT4G15740.1	LOC_Os01g27190.1	Calcium-dependent lipid-binding CaLB domain family protein
K^+ (µmol/g DW)	2A	Traes_2AL_542E74269	sp|Q0JKV1|AKT1_ORYSJ	LOC_Os07g07910.1	Potassium channel AKT1
		Traes_2AL_166405256	sp|Q9M8S6|SKOR_ARATH	LOC_Os04g36740.1	Potassium channel SKOR
		Traes_2AS_35F9CBE17	AT1G60160.1	LOC_Os07g32530.1	Potassium transporter family protein

Traes_2AS_B1279EDF6	AT1G60160.1	LOC_Os07g32530.1	Potassium transporter family protein
Traes_2AL_CF1233942	AT1G60160.1	LOC_Os03g37830.1	Potassium transporter family protein
Traes_2AL_7ADC58E67	AT1G60160.1	LOC_Os07g01214.1	Potassium transporter family protein
Traes_2AL_987F244D2	AT1G60160.1	LOC_Os04g32920.4	Potassium transporter family protein
Traes_2AL_1BAAB97A3	AT1G60160.1	LOC_Os02g31910.2	Potassium transporter family protein
Traes_2AL_D66EA2EB5	AT1G30270.1	LOC_Os07g05620.2	CBL-interacting protein kinase 23
Traes_2AS_73898140B	AT4G11610.1	LOC_Os07g30020.1	C2 calcium/lipid-binding plant phosphoribosyl transferase family protein
Traes_2AL_2E02A8028	AT5G04870.1	LOC_Os07g06740.1	Calcium dependent protein kinase
Traes_2AS_7922A7AD21	AT5G39670.1	LOC_Os07g43800.1	Calcium-binding EF-hand family protein
Traes_2AS_A2BA027FD	sp|Q9H9S4|CB39L_HUMAN	LOC_Os07g39630.1	Calcium-binding protein 39-like
Traes_2AS_75618D6FF	UniRef90_G7I3N1	LOC_Os03g27790.1	Calcium-binding protein
Traes_2AS_B5A77CE31	AT1G23140.1	LOC_Os07g31720.1	Calcium-dependent lipid-binding CaLB domain family protein
Traes_2AS_A17B8569B	AT3G17980.1	LOC_Os07g31830.1	Calcium-dependent lipid-binding CaLB domain family protein
Traes_2AL_7E647D11D	AT3G17980.1	LOC_Os07g01780.1	Calcium-dependent lipid-binding CaLB domain family protein
Traes_2AL_FB7F81E82	AT1G48590.2	LOC_Os07g01780.1	Calcium-dependent lipid-binding CaLB domain family protein
Traes_2AS_0A03EAE04	AT1G50570.1	LOC_Os07g39620.2	Calcium-dependent lipid-binding CaLB domain family protein
Traes_2AS_C0704A2F51	AT1G50570.1	LOC_Os07g39620.2	Calcium-dependent lipid-binding CaLB domain family protein
Traes_2AS_6757FEF7C	AT2G17890.1	LOC_Os07g42770.1	Calcium-dependent protein kinase 16
Traes_2AS_6EE3793BB	AT2G17890.1	LOC_Os07g22710.4	Calcium-dependent protein kinase 16
Traes_2AS_8540A96D1	AT2G17890.1	LOC_Os07g22710.4	Calcium-dependent protein kinase 16
Traes_2AS_99DB98818	AT2G17890.1	LOC_Os07g22710.3	Calcium-dependent protein kinase 16
Traes_2AS_6DA49285E	AT5G19450.1	LOC_Os07g38120.1	Calcium-dependent protein kinase 19
Traes_2AS_FACC395EF	AT1G50700.1	LOC_Os07g33110.2	Calcium-dependent protein kinase 33
Traes_2AS_6DBCC813D	AT1G66410.2	LOC_Os10g25010.1	Calmodulin 4
Traes_2AL_07405FB60	AT4G20780.1	LOC_Os04g41540.1	Calmodulin like 42

	Traes_2AS_A3907B42D	AT3G13600.1	LOC_Os07g43970.1	Calmodulin-binding family protein
	Traes_2AL_C59AC8444	AT2G18750.1	LOC_Os04g36660.1	Calmodulin-binding protein
	Traes_2AS_506D953C1	sp|Q6NPP4|CMTA2_ARATH	LOC_Os07g43030.1	Calmodulin-binding transcription activator 2
	Traes_2AS_2C3FC2736	sp|Q8GSA7|CMTA3_ARATH	LOC_Os03g27080.1	Calmodulin-binding transcription activator 3
	Traes_2AL_773EA7A5A	sp|Q9FYG2|CMTA4_ARATH	LOC_Os04g31900.1	Calmodulin-binding transcription activator 4
	Traes_2AS_4C4190DEB	sp|O23463|CMTA5_ARATH	LOC_Os07g30774.1	Calmodulin-binding transcription activator 5
	Traes_2AL_E80950527	AT5G49890.1	ChrSy.fgenesh.mRNA.37	Chloride channel C
	Traes_2AL_3F769FE10	AT2G39890.1	LOC_Os03g44230.1	Proline transporter 1

Supplementary Figures

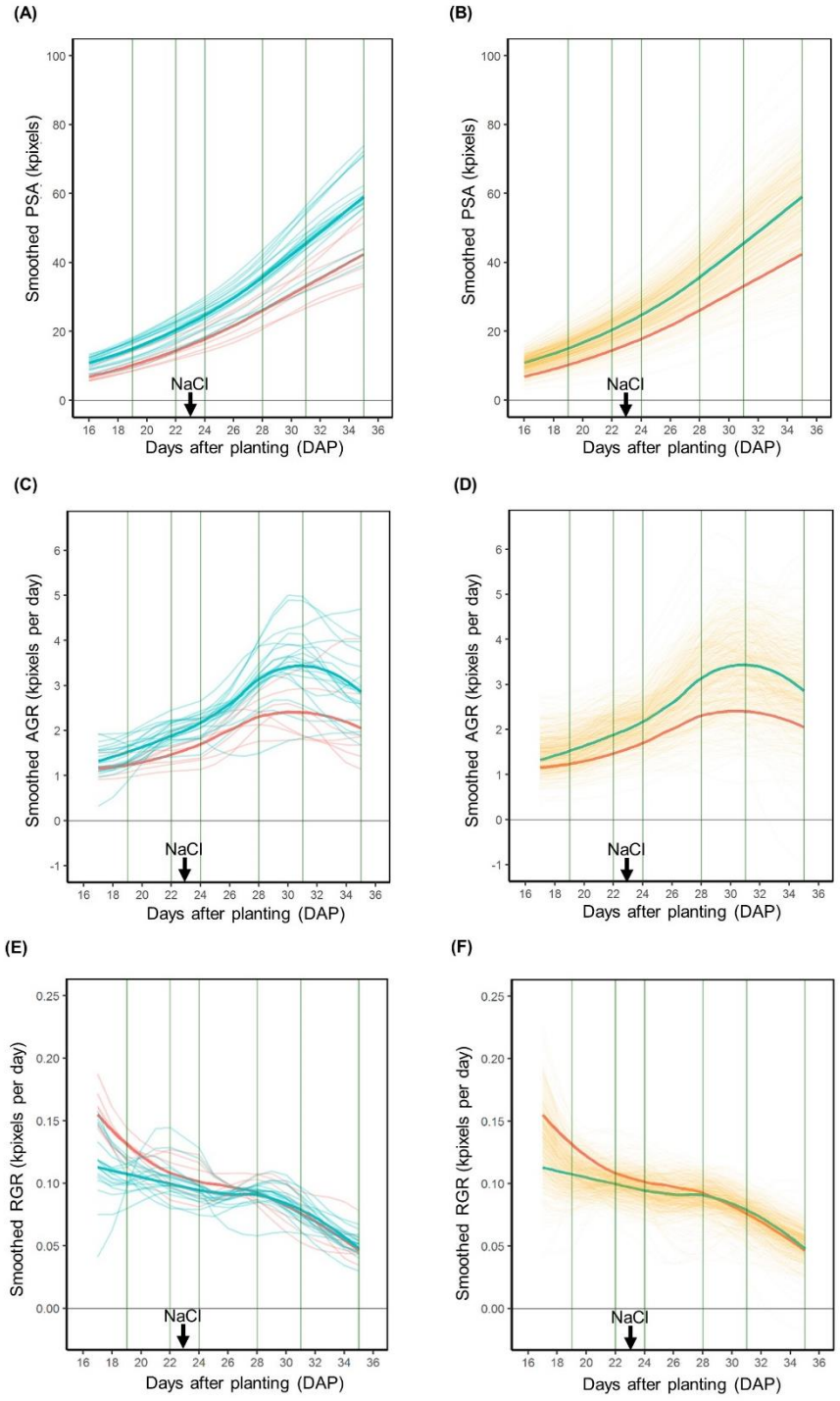

Supplementary Figure 1: Plant growth response before and after 150 mM NaCl treatment. **(A)** Smoothed projected shoot area (PSA) of the parent Mocho de Espiga Branca (in blue) and Gladius (in red). **(B)** Smoothed PSA of the F_2 population (in orange). **(C)** Smoothed absolute growth rate (AGR) calculated based on the PSA of the parents Mocho de Espiga Branca (in blue) and Gladius (in red). **(D)** Smoothed AGR calculated based on the PSA of the F_2 population

(in orange). **(E)** Smoothed relative growth rate (RGR) calculated based on the PSA of the parents Mocho de Espiga Branca (in blue) and Gladius (in red). **(F)** Smoothed RGR calculated based on the PSA of the F_2 population (in orange). The stress was applied 23 DAP shown in black arrow and the intervals selected for the growth analysis are shown in green with the corresponding post salt stress days shown. The thick blue and red lines indicate the mean value of the parents, Mocho de Espiga Branca and Gladius, respectively.

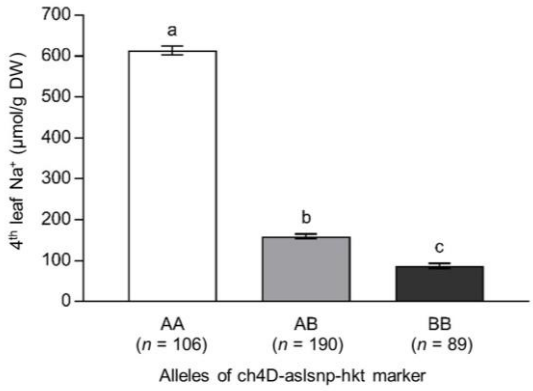

Supplementary Figure 2: The genotyping of Mocho de Espiga Branca × Gladius F_2 population using the tsl2SALTY-4D marker and the allele segregation for the 4th leaf Na^+ concentration. AA indicates the allele from Mocho de Espiga Branca; AB indicates heterozygous allele; BB indicates the allele from Gladius; and the number (*n*) of lines segregated with the alleles are also given. A different letter indicates significant difference between the 4th leaf Na^+ concentrations for each marker alleles (one-way ANOVA followed by Tukey's post hoc test, $p \leq 0.05$).

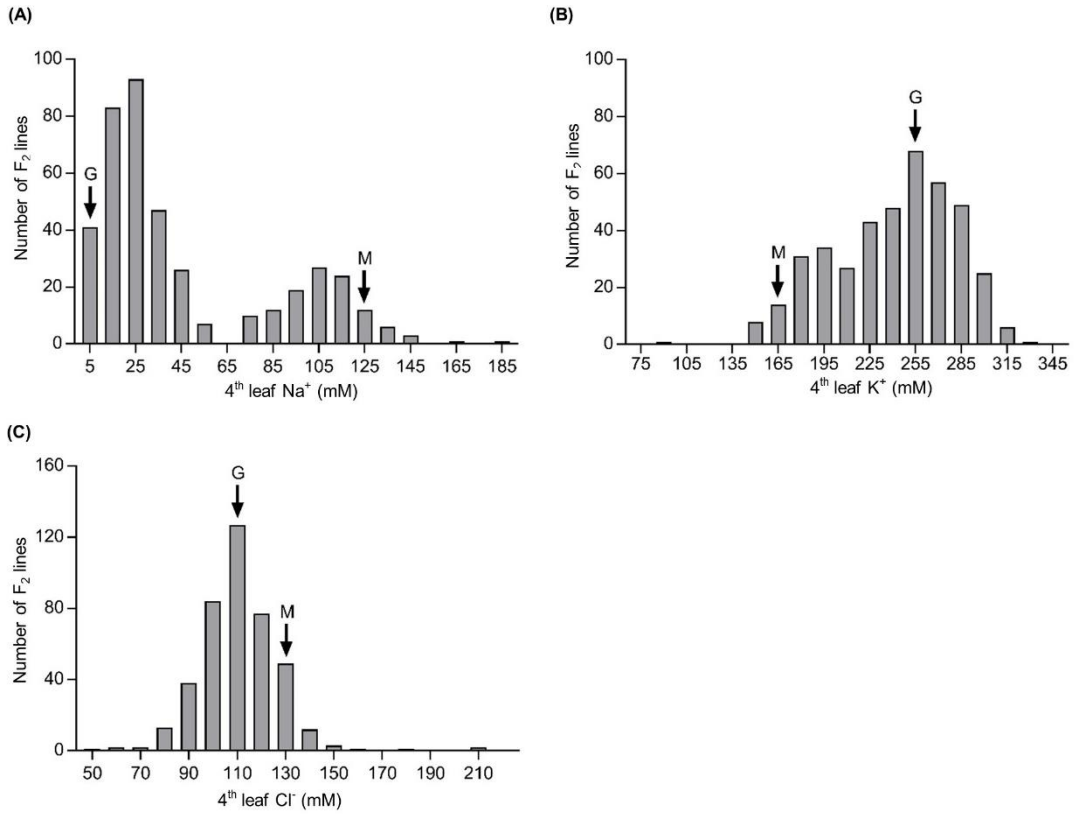

Supplementary Figure 3: Frequency distribution of the F_2 population of Mocho de Espiga Branca × Gladius. The 4th leaf (mM) **(A)** Na^+, **(B)** K^+, **(C)** Cl^- concentration after 12 days in 150 mM NaCl applied at the emergence of 4th leaf. Arrows indicate the trait mean for parents, M = Mocho de Espiga Branca and G = Gladius.

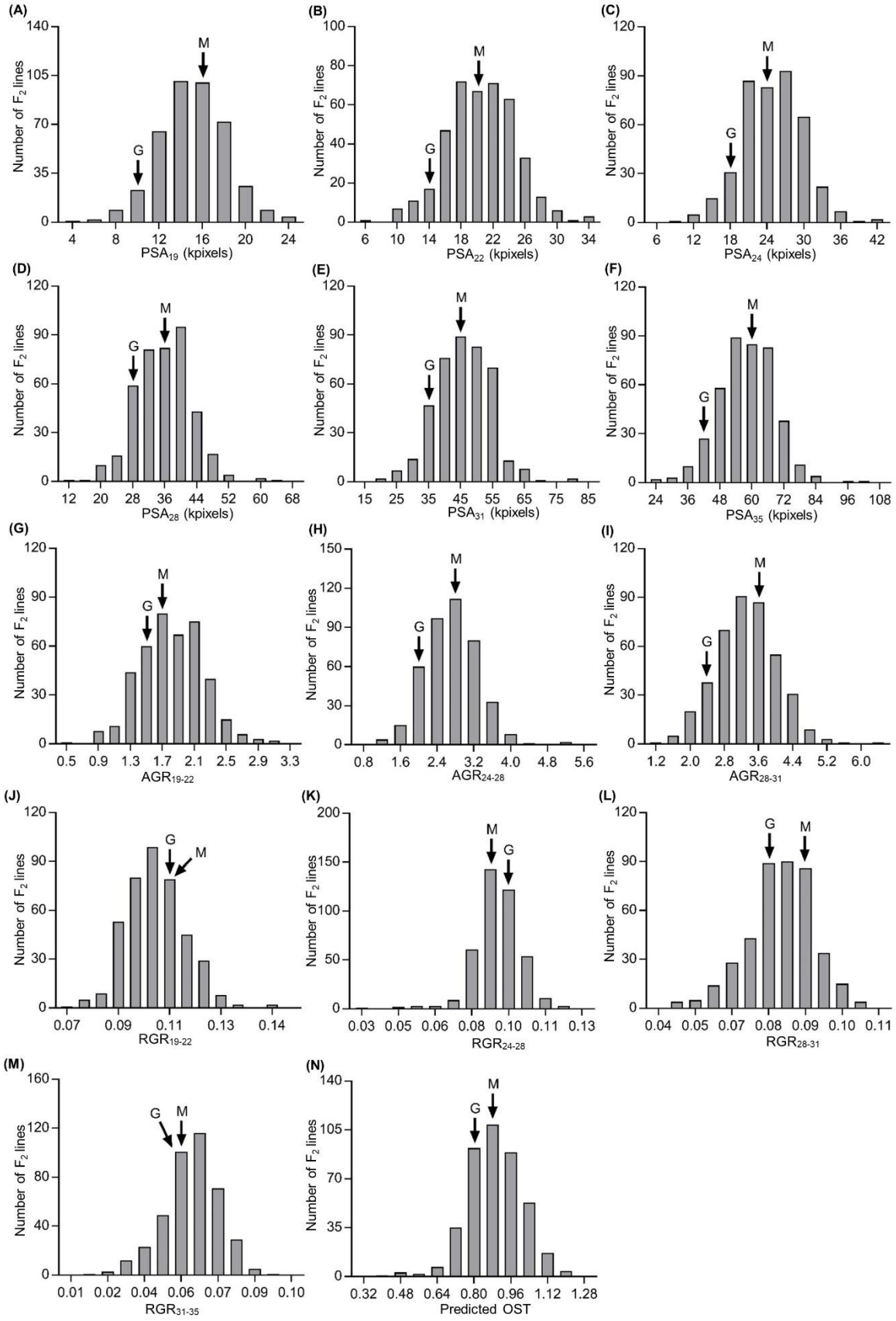

Supplementary Figure 4: Frequency distribution of the F_2 population for the smoothed projected shoot area (PSA), smoothed absolute growth rate (AGR) and smoothed relative growth rate (RGR). Salt stress as applied at the emergence of 4th leaf, 23 days after planting

(DAP). **(A)** Smoothed PSA_{19}. **(B)** Smoothed PSA_{22}. **(C)** Smoothed PSA_{24}. **(D)** Smoothed PSA_{28}. **(E)** Smoothed PSA_{31}. **(F)** Smoothed PSA_{35}. **(G)** Smoothed $AGR_{19\text{-}22}$. **(H)** Smoothed $AGR_{24\text{-}28}$. **(I)** Smoothed $AGR_{28\text{-}31}$. **(J)** Smoothed $AGR_{31\text{-}35}$. **(K)** Smoothed $RGR_{19\text{-}22}$. **(L)** Smoothed $RGR_{24\text{-}28}$. **(M)** Smoothed $RGR_{28\text{-}31}$. **(N)** Predicted osmotic tolerance (OST). The subscript after the smoothed PSA, AGR or RGR indicated the days after planting. Arrows indicate the trait mean for parents, M = Mocho de Espiga Branca and G = Gladius.

Supplementary Tables

Supplementary Table 1: The mean ± SEM of the parent Mocho de Espiga Branca and Gladius, and the range of the F_2population (min-max) for 4th leaf ion concentration. The statistical significance between Mocho de Espiga Branca and Gladius is indicated asterisk ($p \leq 0.01$ = **, $p \leq 0.001$ = ***, $p \leq 0.0001$ = ****).

Traits	Mocho de Espiga Branca	Gladius	F_2 population
Na^+ (mM)	126.6 ± 3.3 ****	7.4 ± 5.6	2.4 - 186.9
K^+ (mM)	165.4 ± 3.2 ****	267.0 ± 5.5	87.1 - 324.3
Cl^- (mM)	129.4 ± 3.4 **	106.6 ± 5.7	52.4 - 214.7

Appendix Files

Full list of genes identified by Composite Interval Mapping (CIM) and Single Marker Analysis (SMA) in this study are provided in the Appendix File 1 and Appendix File 2, respectively, in separate excel workbooks submitted with this thesis.

Chapter 4 - Understanding the role of five known compatible solutes in salinity tolerance of a bread wheat landrace Mocho de Espiga Branca

Statement of Authorship

Title of Paper	Understanding the role of five known compatible solutes in a bread wheat landrace Mocho de Espiga Branca
Publication Status	☐ Published ☐ Accepted for Publication ☐ Submitted for Publication ☑ Unpublished and Unsubmitted w ork w ritten in manuscript style
Publication Details	Although this chapter is written and formatted as a manuscript, this work is not intended to be submitted for publication.

Principal Author

Name of Principal Author (Candidate)	Chana (Chana Borjigin)
Contribution to the Paper	Contributed to the experimental design, conducted the hydroponic experiment and ion concentration measurement, assisted compatible solute extraction, analysed and interpreted the data and wrote manuscript.
Overall percentage (%)	85%
Certification:	This paper reports on original research I conducted during the period of my Higher Degree by Research candidature and is not subject to any obligations or contractual agreements with a third party that would constrain its inclusion in this thesis. I am the primary author of this paper.
Signature	Date 04/11/2019

Co-Author Contributions

By signing the Statement of Authorship, each author certifies that:

i. the candidate's stated contribution to the publication is accurate (as detailed above);
ii. permission is granted for the candidate in include the publication in the thesis; and
iii. the sum of all co-author contributions is equal to 100% less the candidate's stated contribution.

Name of Co-Author	Rhiannon K. Schilling
Contribution to the Paper	Conceived the work, contributed to the experimental design, interpreted the work and contributed to supervision, reviewed and commented on the manuscript.
Signature	Date 04/11/2019

Name of Co-Author	Lukasz Kotula
Contribution to the Paper	Conducted compatible solute extraction and assisted data analysis.
Signature	Date 04.11.2019

Name of Co-Author	Gregory R. Cawthray		
Contribution to the Paper	Performed HPLC quantification and data analysis.		
Signature		Date	4th November 2019

Name of Co-Author	Allison S. Pearson		
Contribution to the Paper	Conceived the work, contributed to the experimental design, interpreted the work and contributed to supervision, reviewed and commented on the manuscript.		
Signature		Date	12/11/2019

Name of Co-Author	Stuart J. Roy		
Contribution to the Paper	Conceived the work, contributed to the experimental design, interpreted the work and contributed to supervision, reviewed and commented on the manuscript.		
Signature		Date	13/11/2019

Understanding the role of five known compatible solutes in salinity tissue tolerance of a bread wheat landrace Mocho de Espiga Branca

Running title: Role of compatible solutes in salinity tissue tolerance of Mocho de Espiga Branca

Chana Borjigin[1], Rhiannon K. Schilling[1], Lukasz Kotula[2,3], Gregory R. Cawthray[4], Allison S. Pearson[1,5], Stuart J. Roy[1,6,*]

[1]School of Agriculture, Food and Wine, The University of Adelaide, PMB 1, Glen Osmond, South Australia 5064, Australia

[2]School of Agriculture and Environment, The University of Western Australia, 35 Stirling Highway, Crawley, Western Australia 6009, Australia

[3]ARC Industrial Transformation Research Hub on Legumes for Sustainable Agriculture, The University of Western Australia, 35 Stirling Highway, Crawley, Western Australia 6009, Australia

[4]School of Biological Sciences, The University of Western Australia, 35 Stirling Highway, Crawley, Western Australia 6009, Australia

[5]ARC Centre of Excellence in Plant Energy Biology, The University of Adelaide, PMB 1, Glen Osmond, South Australia 5064, Australia

[6]ARC Industrial Transformation Research Hub for Wheat in a Hot and Dry Climate, The University of Adelaide, PMB1, Glen Osmond, South Australia 5064, Australia

*Corresponding author:

Stuart J. Roy E-mail: stuart.roy@adelaide.edu.au

Abstract

Osmotic adjustment is important for maintaining cell turgor and volume which helps to maintain plant growth under salinity stress. Organic solutes, such as glycine betaine, proline and sugars, are known osmolytes which contribute to osmotic adjustment in salt stressed plants. A Portuguese bread wheat landrace was previously identified with a high leaf Na^+ concentration whilst maintaining a similar growth as the Australian bread wheat cultivars Gladius and Scout. We examined the concentrations of five known organic osmolytes (glycine betaine, proline, sucrose, glucose and fructose) in the 4th leaf of Mocho de Espiga Branca, Gladius and Scout in response to salinity using high-performance liquid chromatography (HPLC) quantification. The concentrations of all detected solutes in Mocho de Espiga Branca were found to be the same as Gladius and Scout following exposure to salinity, suggesting that glycine betaine, proline, sucrose, glucose and fructose are not responsible for any enhanced osmotic adjustment in Mocho de Espiga Branca compared to Gladius or Scout.

Introduction

Salinity is a major abiotic constraint that results in a reduction in cereal growth and productivity (Schachtman and Munns 1992; Colmer *et al.* 2005; Munns *et al.* 2006; Munns and Tester 2008). During prolonged salinity stress, Na^+ and Cl^- can accumulate to high concentrations in plant leaves, which adversely affects plant cell function and metabolic processes, ultimately resulting in reduced growth or plant death (Yeo *et al.* 1991; Fricke and Peters 2002; Colmer *et al.* 2005; Munns and Tester 2008). Salinity tolerance mechanisms in plants have been well documented and tissue tolerance, which is the capacity of a plant to maintain growth while containing high concentrations of leaf Na^+ and Cl^-, is one of the key mechanisms (Flowers and Colmer 2008; Munns and Tester 2008; Shabala 2013; Munns *et al.* 2016).

Compartmentation of Na^+ into the cell vacuole is considered an important sub trait of tissue tolerance (Yeo and Flowers 1983; Munns and Tester 2008). Previous studies have shown that the salinity tolerance of barley (*Hordeum vulgare*) is correlated with the sequestration of Na^+ into the vacuole of leaf cells (Wu *et al.* 2015). As the cytoplasmic Na^+ concentration increases, osmotic adjustment is required to balance the osmotic pressure within the subcellular compartments in order to maintain cell turgor (Greenway and Munns 1980; Munns and Tester 2008; Munns *et al.* 2016). This process is generally achieved by an increased accumulation of K^+ or organic solutes, such as the low molecular weight amino acids glycine betaine and proline, or sugars such as sucrose, glucose and fructose that can be present in the cell without causing adverse effects on metabolic activities (Colmer et al. 1995; Ashraf and Foolad 2007; Munns and Tester 2008; Munns *et al.* 2016; Sami et al. 2016). Many studies have suggested a link between an increased level of organic solutes and the salinity tolerance of many cereal crops including bread wheat (*Triticum aestivum*) (Colmer *et al.* 1995), rice (*Oryza sativa*) (Garcia *et al.* 1997) and barley (Widodo *et al.* 2009).

A Portuguese bread wheat landrace, Mocho de Espiga Branca, was previously identified with up to a 6-fold higher leaf Na^+ concentration whilst maintaining similar shoot growth as two Australian bread wheat cultivars in a controlled glasshouse under saline conditions (Chapter 2). In chapter 2, a single nucleotide polymorphism (SNP) in HKT1;5-D was discovered to be associated with high concentrations of leaf Na^+ in Mocho de Espiga Branca. However, it remained unknown as to Mocho de Espiga Branca was able to maintain growth whilst containing these high concentrations of leaf Na^+ (tissue tolerance) and whether there are any differences in the type or concentration of organic solutes in Mocho de Espiga Branca compared to Gladius and Scout. Improving our understanding of the tissue tolerance mechanism in Mocho de Espiga Branca would provide a greater insight into the control of tissue tolerance in bread wheat. In the present study, the concentration of five organic solutes reported to correlate with osmotic adjustment in plants under salinity stress were tested to investigate whether these solutes are associated with the improved tissue tolerance of Mocho de Espiga Branca compared to Gladius and Scout.

Materials and methods

Plant materials and growth conditions

A bread wheat landrace Mocho de Espiga Branca and two cultivars Gladius and Scout were used in this study. A fully supported 80 L hydroponics system as previously described (Genc *et al.* 2007) was used to grow plants under two NaCl treatments (0 and 150 mM) in a glasshouse at the Australian Plant Phenomics Facility (The Plant Accelerator®, University of Adelaide, Australia; latitude: -34.971366°, longitude: 138.639758°) between April and May 2018. The hydroponic system was equipped with a trolley fitted with two trays each containing 42 tubes filled with polycarbonate pellets with the trays connected to a tank containing 80 L of a modified Hoagland solution (mM): NH_4NO_3 (0.2); KNO_3 (5.0); $Ca(NO_3)_2{\cdot}4H_2O$ (2.0); $MgSO_4{\cdot}7H_2O$ (2.0); KH_2PO_4 (0.1); $Na_2Si_3O_7$ (0.5); NaFe(III)EDTA (0.05); $MnCl_2{\cdot}4H_2O$ (0.005); $ZnSO_4{\cdot}7H_2O$ (0.01); $CuSO_4{\cdot}5H_2O$ (0.0005) and $Na_2MoO_3{\cdot}2H_2O$ (0.0001). Uniform sized seeds from each genotype were surface-sterilized using ultraviolet (UV) light for 2 min and germinated in petri dishes on moist filter paper for 4 days at room temperature before transplanting. Seedlings from three cultivars were completely randomised in 28 blocks in each treatment. NaCl was applied to the 150 mM treatment at the emergence of the 4^{th} leaf by adding 116.88 g NaCl twice daily in 25 mM increments until a final concentration of 150 mM was reached. 3.8 g of supplemental $CaCl_2{\cdot}2H_2O$ was added into the 150 mM NaCl treatment tanks at each 25 mM NaCl increment in order to maintain constant Ca^{2+} activity. The plants were irrigated by the nutrient solution in a 20 min flood and drain cycle and the complete nutrient solution and salinity treatment was replaced every 7 days. The pH of the solution was maintained between 6.5 and 7.0 throughout the experiment using a 3.2% HCl solution and a portable waterproof specific Ion–pH–mV–Temperature meter (Model WP-90, TPS Pty Ltd, Australia).

Plant sampling

After 21 days of NaCl treatment, 20 plants from each cultivar were sampled from each treatment to determine shoot and root biomass, 4th leaf and root ion (Na^+, K^+ and Cl^-) concentration and 4th leaf organic solute concentration (glycine betaine, proline, sucrose, fructose and glucose). The 4th leaf of each plant was cut into two equal parts along the mid vein using a scalpel blade, with the fresh weight (FW) of each half recorded. One half of the leaf was dried in an oven at 60 °C for 2 days and the dry weight (DW) measured for ion analysis, whilst the other leaf half was placed in a 10 mL tube and frozen in liquid nitrogen to be stored at -80 °C for organic solute analyses. The roots from the 150 mM treatments were rinsed in 10 mM $CaSO_4$ solution and blotted on paper towel to remove external traces of NaCl from the hydroponic nutrient solution before sampling. The roots and the remaining shoot were separated, the fresh weight recorded and then dried in the oven before measuring the dry weight.

On the same sampling day, the 4th leaf from another three plants from each cultivar in each treatment was harvested to determine osmolality in the leaf tissue. The leaf was cut in half as described previously, with one half of the leaf placed in a 10 mL tube, snap frozen in liquid nitrogen and stored at -80 °C for the purpose of osmolality measurement. The other half was dried in an oven as described previously for the purpose of ion analysis to determine whether the ion concentrations in each cultivar were consistent between replicates in each treatment.

Root and leaf Na^+, K^+ and Cl^- concentration analysis

The dried roots were digested in 10 mL of 1% HNO_3 (v/v), and the dried half of the 4th leaf was digested in 5 mL of 1% HNO_3 (v/v) at 85 °C for 4 hours in a SC154 HotBlock® (Environmental Express, Inc., South Carolina, US). Na^+ and K^+ concentrations in the root and leaf tissue digests were measured using a flame photometer (Model 420; Sherwood Scientific Ltd., Cambridge, UK), and Cl^- concentration in the digests were measured using a chloride analyzer (Model 926; Sherwood Scientific Ltd).

Organic solute extraction

Organic solutes in the frozen half of the 4th leaf were extracted as described in Fan *et al.* (1993) and Colmer *et al.* (2000). The leaf material was freeze-dried overnight in a freeze-dryer (Model ALPHA 1-2 LDplus, Martin Christ Gefriertrocknungsanlagen GmbH, Germany) and the dry weight was recorded for each sample. To have sufficient dry material for organic solute extraction, five leaves from each genotype were combined into a single tube before grinding on a Geno/Grinder® (Model 2010, SPEX® SamplePrep LLC., USA) for 2 min at 1000 ×g. 100 mg of well mixed tissue powder was weighed and transferred into a labelled centrifuge tube and 3 mL of 5% (w/v) perchloric acid (PCA) was added into the tube. The tube was kept on ice to prevent the sample from oxidation, and the samples were vortexed until there were no clumps of sample remaining in the tube. The sample was then centrifuged at 27300 ×g for 30 min at 4 °C (Model Avanti JXN-26, Beckman Coulter Inc., USA), and the supernatant was transferred to a new tube. The residual pellet was re-suspended in 3 mL of 5% (w/v) PCA, vortexed thoroughly, and centrifuged at 27300 ×g for 30 min at 4 °C. The supernatant collected from the extraction was neutralised using 5 M of K_2CO_3 until a pH of 3.2-3.5 was reached. The neutralized sample was transferred into a clean centrifuge tube and centrifuged at 27300 ×g for 30 min at 4 °C before collecting the extract in a new tube. Each tube was weighed before and after transferring the neutralized sample to record the weight of the extract. The extract was stored at -20 °C until quantification of the organic solutes.

High-Performance Liquid Chromatography (HPLC) quantification

A HPLC system (Waters Corporation, Milford, MA, USA) was used to quantify the glycine betaine, proline, sucrose, fructose and glucose concentration in the organic solutes extract of the 4th leaf (Supplementary Figure 1). The HPLC system consisted of a 600E pump, 717 auto-sampler, 996 photodiode array detector (PDA) and Millennium Chromatography Manager software equipped with a Sugar-Pak column (300 mm length × 6.5 mm diameter) (Waters Corporation). The Sugar-Pak column was held at 90 ± 0.5 ºC and separation was achieved using

a mobile phase of 5.0 mg/L Ca-EDTA at 0.6 mL/min following the established protocol by Naidu (1998). The PDA output at 195 nm was used for quantification, with a scanning range of 190-300 nm to compare spectral properties of peaks with that of the standards.

All compounds (glycine betaine, L-proline, sucrose, D-glucose, D-fructose, sorbitol and mannitol) used as standard solutions were purchased from Sigma-Aldrich (St Louis, MO, USA) and were of analytical grade quality. Sorbitol and mannitol were included in the mixed standard solution as part of the experimental routine, as these solutes are sometimes detected in samples (Naidu 1998). Standards were calibrated by measuring the peak area on the chromatogram and plotting against the amount of analyte injected. Retention times of the standards were used to identify analytes in the sample extracts with the PDA spectral data and peak purity used to confirm organic solutes. Empower™ 2 software (Waters Corporation, MA, USA) was used for data acquisition and processing. Typical sample injections were 20 µL with a runtime of 30 min per sample and a standard was analysed every 10 samples to check for any detector drift of the HPLC system. The lower detection limits for the five organic compounds analysed were 75 µM for glycine betaine, 100 µM for sucrose, 170 µM for fructose, 210 µM for glucose and 125µM for proline.

Measurement of leaf sap osmolality

For measuring leaf osmolality, the frozen half of the 4th leaf harvested from the three additional plants of each cultivar under each treatment was used. The frozen leaf was thawed, transferred into a 5 mL syringe barrel, which had filter paper placed at the bottom of the barrel, and the cell sap (not tissue fragments) was pushed to pass through the syringe to a 1.5 mL collection tube. The syringe with the leaf sample and collection tube were placed in a 50 mL centrifuge tube, and the leaf sap was collected by centrifuging the tube at 2590 ×g rpm for 15 min (Model ROTANTA 460-R, Hettich Zentrifugen, Germany). 20 µL of 4× diluted leaf sap was used for osmolality measurements on a micro-osmometer (Model 210, Fiske Associates Inc, USA). The

osmometer was calibrated with 50 and 850 mmol/kg osmolality standards (Wescor, Inc.), and the calibration was checked after every sixth measurement.

Estimated contribution of various solutes to leaf sap osmotic potential ($\psi_{\pi\text{-sap}}$)

Osmotic potential (ψ_π) of a given solute was calculated as $\psi_\pi = - nRT/V$ following Colmer *et al.* (1995), where *n* is the number of solute molecules; *R* is the universal gas constant, *T* is temperature in °*K*, *V* is volume in L. Osmotic co-efficient of the ions (Na^+, Cl^- and K^+) were assumed to equal 0.92 at 25 °C as salt does not fully dissociate at high concentrations (Short and Colmer 1999). The $\psi_{\pi\text{-sap}}$ of the plants in 0 and 150 mM NaCl treatments was calculated based on the leaf sap osmolality measured from the three additional plants sampled from each cultivar in each treatment. The ψ_π of the leaf ions and organic solutes was calculated based on the concentrations obtained from the leaf blade of 20 plants sampled from each treatment for the ions and organic solutes analysis. The differences in the contribution of a given solute to the leaf sap $\psi_{\pi\text{-sap}}$ in 0 and 150 mM NaC1-treated leaf blade was calculated by subtracting the value in 0 mM NaCl from that in the corresponding 150 mM NaC1-treated leaf blade of each cultivar.

Statistical analysis

Microsoft® Office Excel 2016 was used for randomising the three cultivars within each of the 28 blocks in each treatment. Prism 7 for Windows (version 7.02; GraphPad Software, Inc.) was used for graphing. The data were statistically analysed using a two-way analysis of variance (ANOVA) in GenStat® 15th edition for Windows (version 15.3.09425; VSN International Ltd, UK), and Tukey's multiple comparison test was performed to determine the means of the data that were significantly different between the cultivars and treatments at a probability level of $p \leq 0.05$.

Results

Mocho de Espiga Branca accumulated similar shoot and root biomass to Australian cultivars

Mocho de Espiga Branca had a total shoot biomass of 0.48 ± 0.03 g DW/plant in 150 mM NaCl treatment which was similar to Gladius (0.41 ± 0.05 g DW/plant) and Scout (0.46 ± 0.03 g DW/plant) (Figure 1a). No significant difference was observed in the total root biomass of Mocho de Espiga Branca (0.07 ± 0.005 g DW/plant) and Scout (0.06 ± 0.004 g DW/plant) at 150 NaCl, whilst Gladius (0.05 ± 0.01 g DW/plant) had significantly less total root biomass than Mocho de Espiga Branca (Figure 1b).

Mocho de Espiga Branca accumulated high leaf Na^+ concentration

The 4th leaf Na^+ concentration was up to 3.9-fold higher in Mocho de Espiga Branca (2072.9 ± 142.4 µmol/g DW) than Gladius (782.4 ± 114.2 µmol/g DW) and Scout (536.5 ± 84.3 µmol/g DW) in 150 mM NaCl, while the Na^+ concentration was similar in the 4th leaf of all three cultivars at 0 mM NaCl (Figure 2a). The K^+ concentration in the 4th leaf of Mocho de Espiga Branca (287.3 ± 8.1 µmol/g DW) was 64% and 66% less than Gladius and Scout respectively at 150 mM NaCl, while the K^+ concentration in Mocho de Espiga Branca (1186.2 ± 28.0 µmol/g DW) was 9% and 2% less than Gladius and Scout respectively in 0 mM NaCl (Figure 2b). The 4th leaf Cl^- concentration of Mocho de Espiga Branca (2580.7 ± 195.9 µmol/g DW) was significantly higher than Gladius (2007.2 ± 255.8 µmol/g DW) and Scout (1262.0 ± 142.1 µmol/g DW) at 150 mM NaCl, whilst the concentration was similar in all three cultivars at 0 mM NaCl (Figure 2c).

Mocho de Espiga Branca had less root Na^+ (1033.0 ± 29.1 µmol/g DW) compared to Gladius (1297.5 ± 35.3 µmol/g DW) and Scout (1208.8 ± 30.3 µmol/g DW) at 150 mM NaCl (Figure 2d). There was no significant difference in the root Na^+ concentration of all three cultivars at 0 mM NaCl (Figure 2d). Root K^+ concentration in Mocho de Espiga Branca (535.3 ± 19.9 µmol/g

DW) was similar to Gladius (486.6 ± 15.7 µmol/g DW) and Scout (598.7 ± 16.0 µmol/g DW) at 150 mM NaCl, while the concentration in Mocho de Espiga Branca (1293.8 ± 27.3 µmol/g DW) was significantly less than Gladius (1401.8 ± 26.0 µmol/g DW) and Scout (1499.8 ± 40.0 µmol/g DW) in 0 mM NaCl (Figure 2e). Mocho de Espiga Branca had a significantly higher root Cl^- concentration at 425.1 ± 12.9 µmol/g DW compared to Gladius (348.3 ± 21.3 µmol/g DW) and Scout (299.4 ± 14.2 µmol/g DW) in 150 mM NaCl, whereas the concentration in all three cultivars was similar at 0 mM NaCl (Figure 2f).

Organic solutes concentrations were similar between the cultivars

The 4th leaf glycine betaine in Mocho de Espiga Branca (29.0 ± 5.6 µmol/g DW), Gladius (29.4 ± 6.1 µmol/g DW) and Scout (19.9 ± 4.7 µmol/g DW) was increased up to 2.7-fold at 150 mM NaCl compared to 0 mM NaCl. However, there were no significant difference in the glycine betaine concentration between all three cultivars at either NaCl treatment (Figure 3a). The 4th leaf fructose concentration in all three cultivars was higher in 150 mM compared to 0 mM NaCl, with no significant difference observed between the cultivars at either treatment (Figure 3b). The sucrose concentration in the 4th leaf of Mocho de Espiga Branca (24.0 ± 10.1 µmol/g DW), Gladius (20.8 ± 5.8 µmol/g DW) and Scout (21.9 ± 4.0 µmol/g DW) was reduced 50-54% in 150 mM compared to 0 mM NaCl, however, there were no significant differences between all three cultivars within each treatment (Figure 3c). The 4th leaf glucose concentration in Mocho de Espiga Branca and Gladius was similar in 0 and 150 mM NaCl treatments (Figure 3d). In the HPLC quantification, no glucose was detected in Scout above the minimum glucose detection limits of 210 µM at 0 mM NaCl and glucose was only detected from two Gladius and one Scout plant out of four replicates tested for each cultivar at 150 mM NaCl (Figure 3d). No proline was detected above the proline detection limits (125 µM) in the quantification from the 4th leaf of all three cultivars at any treatment except for one Gladius sample which had 9.4 µmol/g DW proline in 150 mM NaCl.

Mocho de Espiga Branca has high leaf sap osmolality

The 150 mM NaCl treatment induced an increase in osmolality of the 4th leaf sap in all three cultivars compared to 0 mM NaCl treatment. The osmolality of Mocho de Espiga Branca (773.0 ± 157.0 mOsmol/kg) was significantly higher than Gladius (484.0 ± 13.0 mOsmol/kg) and Scout (493.0 ± 19.0 mOsmol/kg) at 150 mM NaCl, while no significant difference was observed for the leaf sap osmolality between all three cultivars at 0 mM NaCl.

Contributions of the organic solutes to the leaf sap $\psi_{\pi\text{-sap}}$ were similar between cultivars

The 4th leaf sap $\psi_{\pi\text{-sap}}$ was similar in all three cultivars in 0 mM NaCl, while more negative $\psi_{\pi\text{-sap}}$ value was found in Mocho de Espiga Branca (-1.9 MPa) compared to Gladius (-1.2 MPa) and Scout (-1.2 MPa) in the 150 mM NaCl treatment (Table 1).

The total contribution of the selected solutes accounted for approximately half of the $\psi_{\pi\text{-sap}}$ in all three cultivars at 0 mM NaCl (Table 2) with K^+ contributing the most (38.9 – 41.9%) among the solutes in all three cultivars (Table 2). In the 150 mM NaCl treatment, the total contribution of the selected solutes to the $\psi_{\pi\text{-sap}}$ was increased to 105% in Mocho de Espiga Branca, 121% in Gladius and 88.7% in Scout (Table 2). The contributions of Na^+ and Cl^- to the $\psi_{\pi\text{-sap}}$ in 150 mM NaCl increased the most out of each solute, while K^+ contribution declined in all three cultivars compared to those in 0 mM NaCl (Table 2).

Among cultivars, the contribution of Na^+ to the $\psi_{\pi\text{-sap}}$ in Mocho de Espiga Branca (43.2%) at 150 mM NaCl was higher than Gladius (26.0%) and Scout (17.8%), while the K^+ contribution in Mocho de Espiga Branca (5.9%) was lower than both Gladius (24.8%) and Scout (27.9%) (Table 2). Cl^- contribution to the $\psi_{\pi\text{-sap}}$ in Mocho de Espiga Branca (53.5%) at 150 mM NaCl was higher than Scout (41.1%) but lower than Gladius (66.2%) (Table 2). Although changes were found between the contributions of organic solutes to $\psi_{\pi\text{-sap}}$ in response to NaCl treatment,

the values were similar between the cultivars (Table 2). Overall, compared to the contributions of selected organic solutes, Na^+, K^+ and Cl^- made greater contributions to the $\psi_{\pi\text{-sap}}$ of all three cultivars in 150 mM NaCl (Table 2).

Discussion

Mocho de Espiga Branca accumulated up to 3.9-fold greater Na^+ and had a 64-66% decrease in K^+ concentration in the 4th leaf compared to Gladius and Scout at 150 mM NaCl. Mocho de Espiga Branca was also able to maintain a similar shoot biomass in response to the salinity stress even with this high concentration of leaf Na^+. Although changes were observed for the accumulation of five organic solutes (glycine betaine, proline, sucrose, glucose and fructose) tested in this study between 0 and 150 mM NaCl treatment, there were no significant differences in the concentration of these in Mocho de Espiga Branca when compared to Gladius and Scout.

In all cultivars, the glycine betaine concentration in the 4th leaf increased up to 2.7 fold under salinity (Figure 3a). This finding is in agreement with a previous study and supports the concept that increasing salinity induces the accumulation of glycine betaine in wheat (Colmer *et al.* 1995). Previously it has been shown that the salinity tolerance of an amphiploid from a cross between Chinese Spring × *L. elongatum* is correlated with the accumulation of higher glycine betaine along with lower Na^+ and higher K^+ concentrations in the youngest leaf blade in 200 mM NaCl (Colmer *et al.* 1995). However, the results of this study showed that the concentrations of glycine betaine in the 4th leaf of Mocho de Espiga Branca is similar to Gladius and Scout, even though it had higher Na^+ and lower K^+ in the leaf (Figure 2a, 2b and 3a). This lack of difference in glycine betaine under high salinity between cultivars indicates that it is unlikely that glycine betaine is an important osmolyte in the osmotic adjustment of the 4th leaf of Mocho de Espiga Branca.

Although previously a positive linear correlation was found between leaf proline and Na^+ concentrations in bread wheat (Colmer *et al.* 1995), in this study no proline was detected above the detection limits in any cultivars at any treatment except for one Gladius plant at 150 mM NaCl. In bread wheat, proline has been shown to progressively decrease from the older leaves to younger leaves and it is also highly dependent on the level of salinity that the plant is exposed

(Colmer *et al.* 1995). Similar results were reported in durum wheat, where the proline was detected predominantly in older leaves and tended to accumulate at the early stage of stress onset (Carillo *et al.* 2008). The lack of proline detection in Mocho de Espiga Branca, Gladius and Scout in this study may be due to the fact that only the 4th leaf was sampled for the analysis and it occurred later during the salinity stress which had only one level of 150 mM NaCl. In addition, genetic variation in the amount of stress-induced proline accumulation between cultivars within a plant species exists as reviewed by Ashraf and Foolad (2007). It is, therefore, difficult to draw a conclusion for the role of proline in salinity tolerance in Mocho de Espiga Branca from one tissue (4th leaf) and one time-point of sampling (21 days of NaCl treatment). Future studies could examine the proline concentration in each individual leaf of the plant at several stages during stress in order to understand the proline distribution and its contribution to salinity tolerance in Mocho de Espiga Branca compared to other bread wheat cultivars.

The concentration of sucrose in the 4th leaf of Mocho de Espiga Branca, Gladius and Scout was significantly decreased at 150 mM NaCl compared to 0 mM NaCl (Figure 3c). This decrease in sucrose in response to salinity could be due to the stress-induced inhibition of sucrose synthesis or the hydrolysis of elevated sucrose as a result of reduced usage of the assimilates in the plant (Munns *et al.* 2016; Sami *et al.* 2016). The decrease in sucrose concentration may also be a result of sucrose being mobilised to other plant sinks, such as younger leaves and roots, which require more energy under stress (Kebrom *et al.* 2012; Mason *et al.* 2014). An increase in fructose concentration in the 4th leaf of all cultivars under 150 mM NaCl (Figure 3b) may be an indication of greater hydrolysis of sucrose. In contrast, the 4th leaf glucose concentration was stable in both the 0 mM and 150 mM NaCl treatment in all three cultivars (Figure 3 d). However, it should be noted that a lack of replication of glucose measurements makes it difficult to be conclusive of this response and it is not possible to determine if glucose has a role in osmotic adjustment for any of the cultivars tested.

Although the concentration of all four detected organic solutes (glycine betaine, fructose, sucrose and glucose) in the 4th leaf of Mocho de Espiga Branca, Gladius and Scout responded upon salinity treatment which is in agreement with previous studies, due to there was no significant differences between the cultivars it is not clear what organic solute may be responsible to balancing the higher Na^+ concentration in the 4th leaf of Mocho de Espiga Branca. Alternate organic solutes, such as trehalose and raffinose (Hill *et al*, 2013), may be contributing to the tissue tolerance of Mocho de Espiga Branca and this could be further investigated by analysing a wider range of metabolites in Mocho de Espiga Branca, Gladius and Scout under control and saline conditions in the future.

It has previously been proposed that the Na^+ ion may not have an important role in osmotic adjustment of wheat plants under salinity due to the Na^+ exclusion mechanism (Munns *et al.* 2016). However, in this study, although the total estimated contributions of the selected solutes in Mocho de Espiga Branca and Gladius exceeded 100%, most likely due to the difference in sample preparation method between the measurement of solute concentrations and leaf sap osmolality, Na^+ had a greater contribution to the leaf sap $\psi_{\pi\text{-sap}}$ in Mocho de Espiga Branca compared to Gladius and Scout at 150 mM NaCl (Table 1). This suggests that Mocho de Espiga Branca may be an exception and could possibly be a bread wheat using high leaf Na^+ concentrations to regulate osmotic adjustment similar to some halophytic plants such as *Limonium latifolium* (Gagneul *et al.* 2007). Mocho de Espiga Branca (and perhaps bread wheat in general) may have the potential to accumulate a high concentration of Na^+ in the cytoplasm without damaging functional processes in the cell. The limiting concentration to which Na^+ can be accumulated in the cytoplasm would be worth revisiting in future studies, using Mocho de Espiga Branca and advances in cellular imaging technologies. These technologies could help to determine the actual limit to which Na^+ accumulation can be tolerated in cellular compartments as this still remains unknown due to the complexity of isolation (Munns *et al.* 2016).

When the cytoplasmic Na^+ exceeds the allowed limits, excessive Na^+ is transported to other cellular compartments such as the vacuole, chloroplast and mitochondria (Flowers *et al.* 2015). Compartmentalising Na^+ into the vacuole is considered an important tissue tolerance mechanism (Munns and Tester 2008; Munns *et al.* 2016). This process is achieved through tonoplast Na^+/H^+ antiporters which import Na^+ from the cytoplasm into the vacuole in order to maintain lower cytoplasmic Na^+ and export the H^+ into the cytoplasm in order to balance cation homeostasis in the cytoplasm (Munns *et al.* 2016). In halophytic plants the chloroplast is reported to be able to regulate similar concentrations of Na^+ that is present in the cytosol under salinity (Flowers and Colmer 2015). It is possible that Mocho de Espiga Branca is able to maintain cell turgor using this ability to effectively distribute the excessive Na^+ within the cell compartments to maintain its growth.

As one of the most salt tolerant cereal plants, barley accumulates high concentrations of Na^+ in the leaf and previous studies have shown that barley is able to maintain higher concentrations of K^+ and lower Na^+ in the mesophyll cells than in epidermal cells (Fricke *et al.* 1996; James *et al.* 2006). In chickpea, the ability to exclude Na^+ from the mesophyll cell and partition this into epidermal cells was also reported to be associated with the maintenance of photosynthesis and salinity tolerance (Kotula *et al.* 2019). It is possible that Mocho de Espiga Branca may have a similar tolerance mechanisms as barley or chickpea with more efficient compartmentalisation of Na^+ into epidermal cells in order to avoid damaging photosynthetic process and to maintain growth under salinity. The ability of Mocho de Espiga Branca to compartmentalise Na^+ into cell vacuoles should be measured in future studies.

In conclusion, the organic solutes tested in Mocho de Espiga Branca were found to respond similarly to Gladius and Scout following exposure to salinity, suggesting these organic solutes are not contributing to the ability of Mocho de Espiga Branca to maintain growth under salt concentrations to any greater extent than these two cultivars. In future studies, quantitative

detection of Na^+, K^+ and Cl^- concentration in Mocho de Espiga Branca in different cells, such as epidermal and mesophyll cells, and in different intracellular compartments, such as the cytoplasm and vacuole, should be investigated in order to understand cellular ion distribution. Analysis of a wider range of metabolites could also be measured to determine the role of other plant metabolites present in Mocho de Espiga Branca in response to salinity compared to Gladius and Scout.

Acknowledgments

This study was funded by the Grains Research and Development Corporation (GRDC): Project UA00145, UA00151, and the GRDC and the International Wheat Yield Partnership (IWYP): Projects IWYP39/ACP0009; IWYP60/ANU00027. The Plant Accelerator®, Australian Plant Phenomics Facility, is funded under the National Collaborative Research Infrastructure Strategy (NCRIS). The authors thank Prof. Timothy Colmer (University of Western Australia, Perth, Australia) for providing experimental facilities to extract and quantify the organic solute, and discussion on the data analysis. We also thank The Plant Accelerator® for assisting with the glasshouse experiments. CB thanks the China Scholarship Council and the University of Adelaide Joint Postgraduate Scholarships Program for her PhD stipend.

Author Contributions

CBo contributed to the experimental design, conducted the hydroponic experiment and ion concentration measurement, assisted compatible solute extraction, analysed and interpreted the work and wrote manuscript; RKS conceived the work, contributed to the experimental design, interpreted the work and contributed to supervision, reviewed and commented on the manuscript; LK conducted compatible solute extraction and assisted data analysis; GRC performed HPLC quantification and analysed the data; ASP conceived the work, contributed to the experimental design, interpreted the work and contributed to supervision, reviewed and commented on the manuscript; SJR conceived the work, contributed to the experimental design, interpreted the work and contributed to supervision, reviewed and commented on the manuscript.

References

Ashraf, M, Foolad, M (2007) Roles of glycine betaine and proline in improving plant abiotic stress resistance. *Environmental and Experimental Botany* **59**, 206-216.

Carillo, P, Mastrolonardo, G, Nacca, F, Parisi, D, Verlotta, A, Fuggi, A (2008) Nitrogen metabolism in durum wheat under salinity: accumulation of proline and glycine betaine. *Functional Plant Biology* **35**, 412-426.

Colmer, TD, Corradini, F, Cawthray, GR, Otte, ML (2000) Analysis of dimethylsulphoniopropionate (DMSP), betaines and other organic solutes in plant tissue extracts using HPLC. *Phytochemical Analysis* **11**, 163-168.

Colmer, TD, Epstein, E, Dvorak, J (1995) Differential solute regulation in leaf blades of various ages in salt-sensitive wheat and a salt-tolerant wheat x *lophopyrum-elongatum* (host) A. Love amphiploid. *Plant Physiology* **108**, 1715-1724.

Colmer, TD, Munns, R, Flowers, TJ (2005) Improving salt tolerance of wheat and barley: future prospects. *Australian Journal of Experimental Agriculture* **45**, 1425-1443.

Fan, TWM, Colmer, TD, Lane, AN, Higashi, RM (1993) Determination of metabolites by H-NMR and GC - analysis for organic osmolytes in crude tissue-extracts. *Analytical Biochemistry* **214**, 260-271.

Flowers, TJ, Colmer, TD (2008) Salinity tolerance in halophytes. *New Phytologist* **179**, 945-963.

Flowers, TJ, Colmer, TD (2015) Plant salt tolerance: adaptations in halophytes. *Annals of Botany* **115**, 327-331.

Flowers, TJ, Munns, R, Colmer, TD (2015) Sodium chloride toxicity and the cellular basis of salt tolerance in halophytes. *Annals of Botany* **115**, 419-431.

Fricke, W, Leigh, RA, Tomos, AD (1996) The intercellular distribution of vacuolar solutes in the epidermis and mesophyll of barley leaves changes in response to NaCl. *Journal of Experimental Botany* **47**, 1413-1426.

Fricke, W, Peters, WS (2002) The biophysics of leaf growth in salt-stressed barley. A study at the cell level. *Plant Physiology* **129**, 374-388.

Gagneul, D, Aïnouche, A, Duhazé, C, Lugan, R, Larher, FR, Bouchereau, A, (2007) A reassessment of the function of the so-called compatible solutes in the halophytic Plumbaginaceae Limonium latifolium. *Plant Physiology* **144**, 1598-1611.

Garcia, AB, Engler, J, Iyer, S, Gerats, T, Van Montagu, M, Caplan, AB (1997) Effects of osmoprotectants upon NaCl stress in rice. *Plant Physiology* **115**, 159-169.

Genc, Y, McDonald, GK, Tester, M (2007) Reassessment of tissue Na^+ concentration as a criterion for salinity tolerance in bread wheat. *Plant Cell & Environment* **30**, 1486-1498.

Greenway, H, Munns, R (1980) Mechanisms of salt tolerance in non-halophytes. *Annual Review of Plant Physiology and Plant Molecular Biology* **31**, 149-190.

Hill, CB, Jha, D, Bacic, A, Tester, M, Roessner, U (2013) Characterization of ion contents and metabolic responses to salt stress of different *Arabidopsis AtHKT1;1* genotypes and their parental strains. *Molecular Plant* **6**, 350-368.

James, RA, Munns, R, Von Caemmerer, S, Trejo, C, Miller, C, Condon, T (2006) Photosynthetic capacity is related to the cellular and subcellular partitioning of Na^+, K^+ and Cl^- in salt-affected barley and durum wheat. *Plant Cell & Environment* **29**, 2185-2197.

Kebrom, TH, Chandler, PM, Swain, SM, King, RW, Richards, RA, Spielmeyer, W (2012) Inhibition of tiller bud outgrowth in the *tin* mutant of wheat is associated with precocious internode development. *Plant Physiology* **160**, 308-318.

Kotula, L, Clode, PL, Jimenez, JDLC, Colmer, TD (2019) Salinity tolerance in chickpea is associated with the ability to 'exclude' Na^+ from leaf mesophyll cells. *Journal of Experimental Botany* **70**, 4991-5002.

Mason, MG, Ross, JJ, Babst, BA, Wienclaw, BN, Beveridge, CA (2014) Sugar demand, not auxin, is the initial regulator of apical dominance. *Proceedings of the National Academy of Sciences* **111**, 6092-6097.

Munns, R, James, RA, Gilliham, M, Flowers, TJ, Colmer, TD (2016) Tissue tolerance: an essential but elusive trait for salt-tolerant crops. *Functional Plant Biology* **43**, 1103-1113.

Munns, R, James, RA, Lauchli, A (2006) Approaches to increasing the salt tolerance of wheat and other cereals. *Journal of Experimental Botany* **57**, 1025-1043.

Munns, R, Tester, M (2008) Mechanisms of salinity tolerance. *Annual Review of Plant Biology* **59**, 651-681.

Naidu, BP (1998) Separation of sugars, polyols, proline analogues, and betaines in stressed plant extracts by high performance liquid chromatography and quantification by ultra violet detection. *Australian Journal of Plant Physiology* **25**, 793-800.

Sami, F, Yusuf, M, Faizan, M, Faraz, A, Hayat, S (2016) Role of sugars under abiotic stress. *Plant Physiology and Biochemistry* **109**, 54-61.

Schachtman, DP, Munns, R (1992) Sodium accumulation in leaves of triticum species that differ in salt tolerance. *Australian Journal of Plant Physiology* **19**, 331-340.

Shabala, S (2013) Learning from halophytes: physiological basis and strategies to improve abiotic stress tolerance in crops. *Annals of Botany* **112**, 1209-1221.

Short, DC, Colmer, TD (1999) Salt Tolerance in the Halophyte *Halosarcia pergranulata* subsp. *pergranulata*. *Annals of Botany* **83**, 207-213.

Widodo, Patterson, JH, Newbigin, E, Tester, M, Bacic, A, Roessner, U (2009) Metabolic responses to salt stress of barley (*Hordeum vulgare* L.) cultivars, Sahara and Clipper, which differ in salinity tolerance. *Journal of Experimental Botany* **60**, 4089-4103.

Wu, HH, Shabala, L, Zhou, MX, Stefano, G, Pandolfi, C, Mancuso, S, Shabala, S (2015) Developing and validating a high-throughput assay for salinity tissue tolerance in wheat and barley. *Planta* **242**, 847-857.

Yeo, A, Flowers, T (1983) Varietal differences in the toxicity of sodium ions in rice leaves. *Physiologia Plantarum* **59**, 189-195.

Yeo, A, Lee, Λ-S, Izard, P, Boursier, P, Flowers, T (1991) Short-and long-term effects of salinity on leaf growth in rice (*Oryza sativa* L.). *Journal of Experimental Botany* **42**, 881-889.

Figures

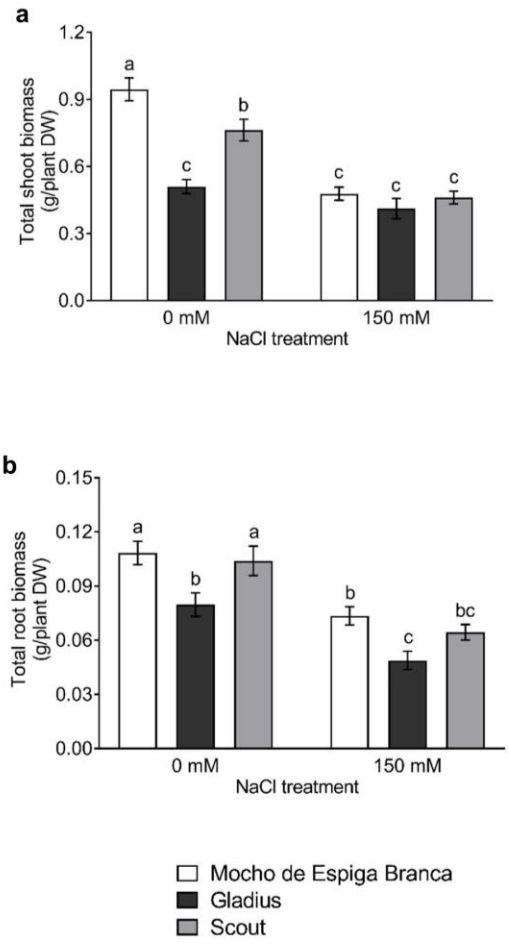

Figure 1: Shoot and root biomass of Mocho de Espiga Branca, Gladius and Scout at 0 and 150 mM NaCl. Plant shoot and root biomass were determined 21 days after treatment with 0 and 150 mM NaCl. **a,** Total shoot biomass. **b,** Total root biomass. Data presented as the mean ± standard error of the mean (SEM), where n = 20. Bars showing different letters indicated significant differences determined by two-way ANOVA with Tukey's multiple comparison test at $p \leq 0.05$.

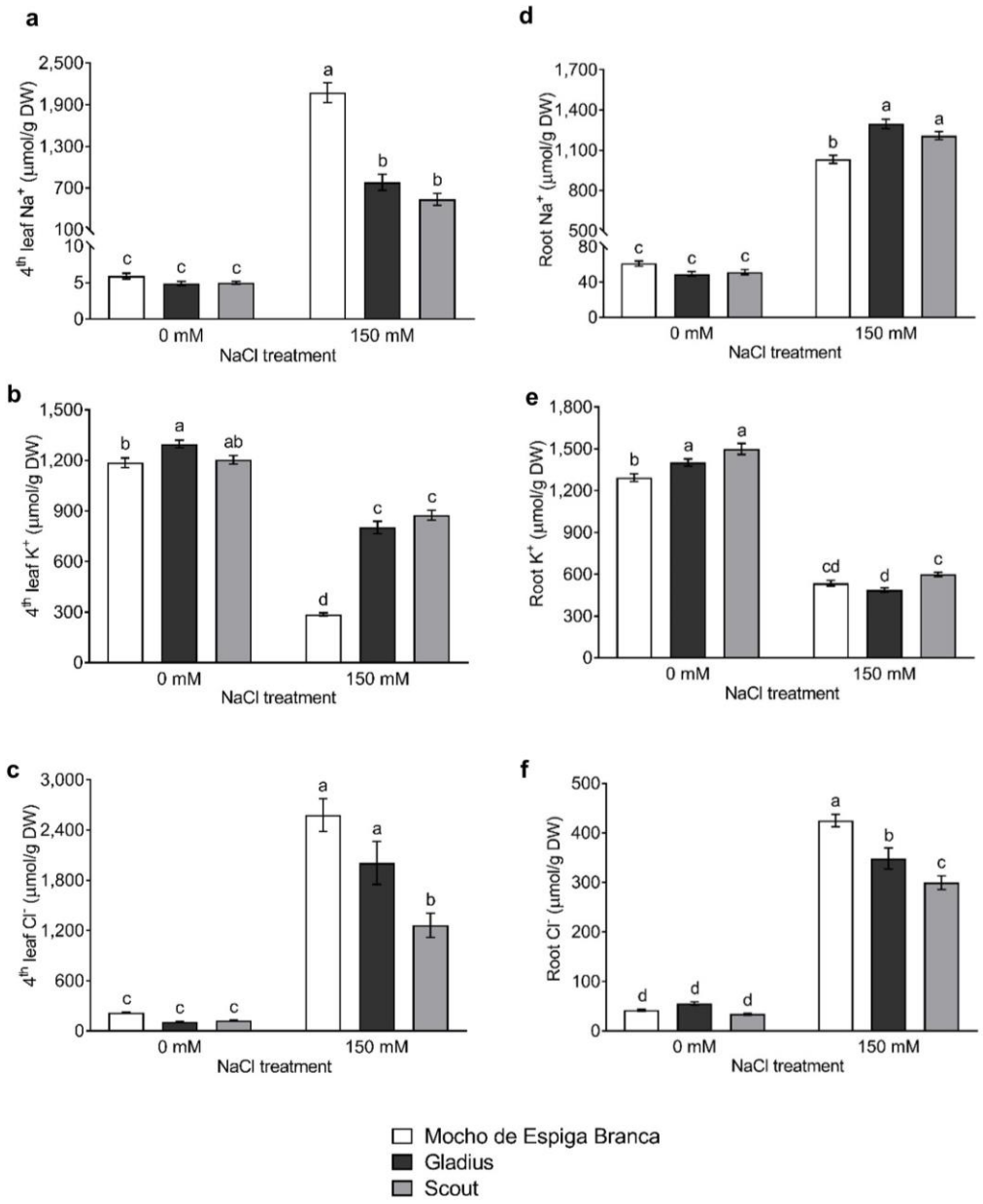

Figure 2: Ion concentrations of the 4th leaf and root from Mocho de Espiga Branca, Gladius and Scout at 0 and 150 mM NaCl. 4th leaf **a,** Na^+; **b,** K^+ and **c,** Cl^- concentration; Root **d,** Na^+; **e,** K^+ and **f,** Cl^- concentration determined 21 days after treatment with 0 and 150 mM NaCl Data presented as the mean ± SEM (n = 20). Bars showing different letters indicated significant differences determined by two-way ANOVA with Tukey's multiple comparison test at $p \leq 0.05$.

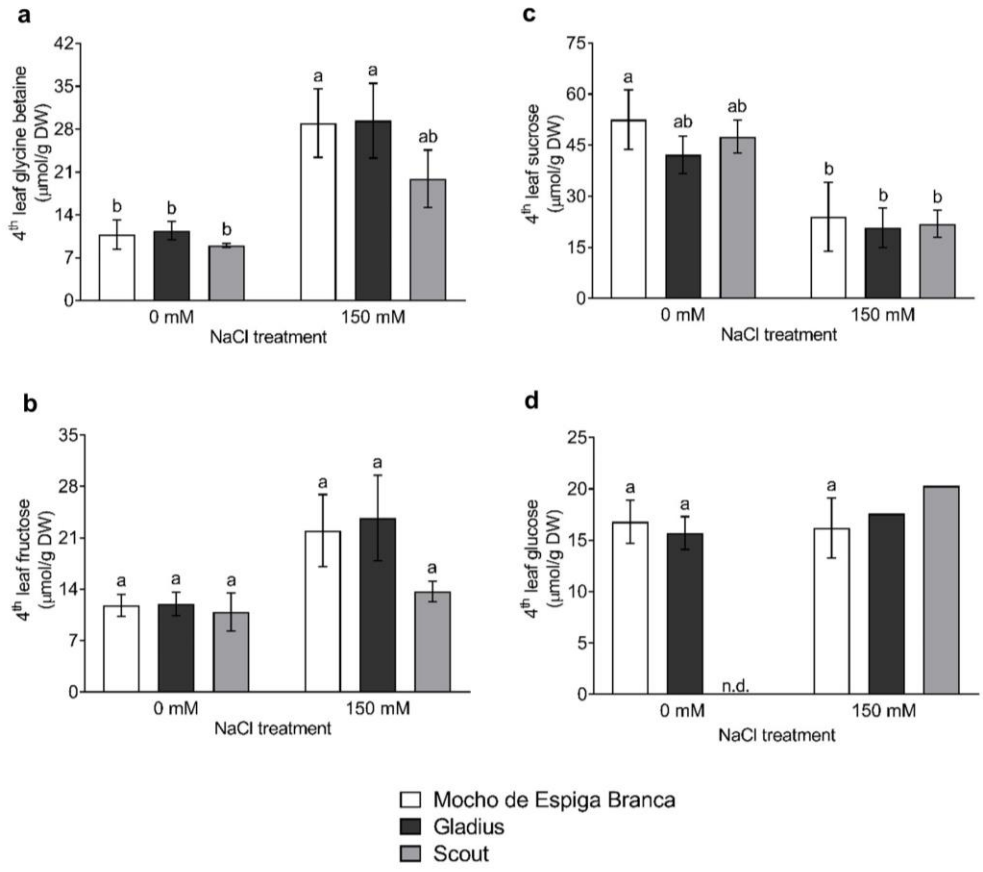

Figure 3: The 4th leaf organic solutes concentration in Mocho de Espiga Branca, Gladius and Scout at 0 and 150 mM NaCl. 4th leaf **a,** glycine betaine; **b,** sucrose; **c,** fructose; **d,** glucose determined 21 days after treatment with 0 and 150 mM NaCl. Data presented as the mean ± SEM (n = 5, except for glucose concentration in Gladius where n = 2 and in Scout where n = 1 at 150 mM; n.d. = not detected above the detection limits in the HPLC quantification). Bars showing different letters indicated significant differences determined by two-way ANOVA with Tukey's multiple comparison test at $p \leq 0.05$.

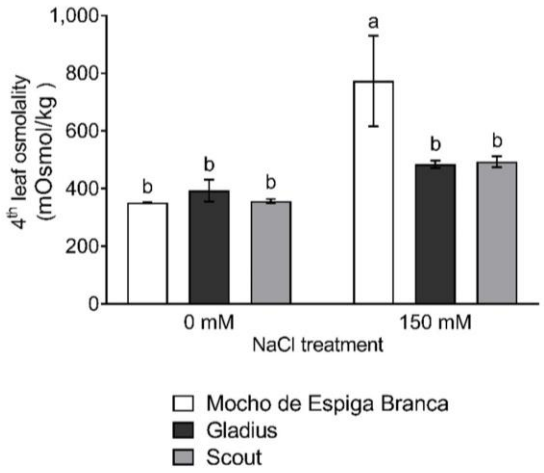

Figure 4: Osmolality of the 4th leaf sap in Mocho de Espiga Branca, Gladius and Scout at 0 and 150 mM NaCl. Data presented as the mean ± SEM (n = 3). Bars showing different letters indicated significant differences determined by two-way ANOVA with Tukey's multiple comparison test at $p \leq 0.05$.

Tables

Table 1: Osmotic potential (ψ_π) of leaf sap and the selected solutes at 0 and 150 mM NaCl treatment. Data presented as the mean ± SEM (n = 20 for ψ_π of ions; n = 3 - 5 for ψ_π of organic solutes except for $\psi_{\pi\text{-glucose}}$ in Gladius where n = 2 and in Scout where n = 1 at 150 mM; n.d. = not detected above the detection limits in the HPLC quantification).

Treatments	Cultivars	ψ_π-sap	ψ_π-Na+	ψ_π-K+	ψ_π-Cl-	ψ_π-glycinebetaine	ψ_π-sucrose	ψ_π-fructose	ψ_π-glucose
0 mM NaCl	Mocho de Espiga Branca	-0.87 ± 0.01	-0.002 ± 0.0001	-0.34 ± 0.01	-0.06 ± 0.003	-0.003 ± 0.001	-0.02 ± 0.003	-0.004 ± 0.001	-0.005 ± 0.001
	Gladius	-0.97 ± 0.1	-0.001 ± 0.0001	-0.38 ± 0.01	-0.03 ± 0.003	-0.004 ± 0.001	-0.01 ± 0.002	-0.004 ± 0.001	-0.01 ± 0.0004
	Scout	-0.89 ± 0.02	-0.002 ± 0.0001	-0.37 ± 0.01	-0.04 ± 0.002	-0.003 ± 0.0001	-0.02 ± 0.001	-0.003 ± 0.001	n.d.
150 mM NaCl	Mocho de Espiga Branca	-1.9 ± 0.4	-0.82 ± 0.07	-0.11 ± 0.004	-1.02 ± 0.09	-0.01 ± 0.002	-0.01 ± 0.004	-0.01 ± 0.002	-0.01 ± 0.001
	Gladius	-1.2 ± 0.03	-0.31 ± 0.06	-0.30 ± 0.01	-0.79 ± 0.13	-0.01 ± 0.002	-0.01 ± 0.002	-0.01 ± 0.002	-0.01
	Scout	-1.2 ± 0.05	-0.21 ± 0.04	-0.33 ± 0.02	-0.49 ± 0.06	-0.01 ± 0.002	-0.01 ± 0.001	-0.01 ± 0.001	-0.01

Table 2: Estimated contributions of the selected solute to the leaf sap $\psi_{\pi\text{-sap}}$ at 0 and 150 mM NaCl. The contribution of each solute to the leaf sap $\psi_{\pi\text{-sap}}$ is determined as the ψ_{π} of each solute at each NaCl treatment relative to the leaf sap $\psi_{\pi\text{-sap}}$ at the respective NaCl treatment shown in Table 1.

Treatments	Cultivars	Contributions of the selected solutes to $\psi_{\pi\text{-sap}}$ (%)							Total contributions of the selected solutes to $\psi_{\pi\text{-sap}}$ (%)
		Na^+	K^+	Cl^-	Glycine betaine	Sucrose	Fructose	Glucose	
0 mM NaCl	Mocho de Espiga Branca	0.2	39.5	7.4	0.4	1.8	0.4	0.6	50.3
	Gladius	0.1	38.9	3.2	0.4	1.4	0.4	0.5	44.9
	Scout	0.2	41.9	4.3	0.3	1.7	0.4	ND	48.8
150 mM NaCl	Mocho de Espiga Branca	43.2	5.9	53.5	0.6	0.5	0.5	0.3	105
	Gladius	26.0	24.8	66.2	1.1	0.7	0.8	1.2	121
	Scout	17.8	27.9	41.1	0.7	0.7	0.5	0.7	88.7

Supplementary Figures

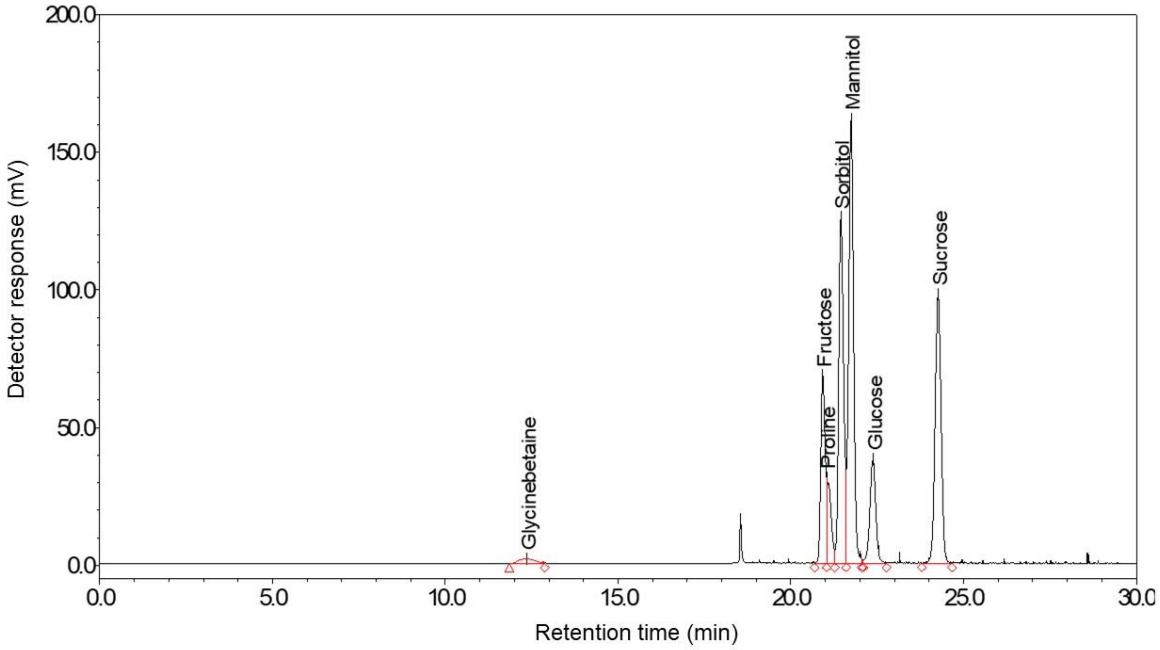

Supplementary Figure 1: Separation of a mixed standard solution containing glycine betaine, proline, sucrose, fructose, glucose, sorbitol and mannitol. The retention times (min) of the glycine betaine, proline, sucrose, fructose and glucose used to identify the corresponding solutes from the 4th leaf organic solute extracts based on the detector response (mV). Sorbitol and mannitol were included in the mixed standard solution as an experimental routine as these two solutes sometimes could be detected as part of solute adjustment and interfere the detection of the solutes of interest having closer retention time.

Chapter 5 - General discussion

Review of thesis aims

Shoot Na^+ exclusion was previously established as a major determinant of salinity tolerance in bread wheat (Colmer *et al.* 2005; Munns *et al.* 2006; Genc *et al.* 2010; Roy *et al.* 2014; Hanin *et al.* 2016; Ismail and Horie 2017). Shoot Na^+ exclusion enables bread wheat to reduce root-to-shoot Na^+ transport by retrieving Na^+ from the xylem (Byrt *et al.* 2007; Byrt *et al.* 2014). Although Na^+ exclusion is sometimes positively correlated with improved performance of bread wheat under salinity (Chhipa and Lal 1995; Ashraf and O'leary 1996; Ashraf and Khanum 1997), this relationship is not always found to occur (Chhipa and Lal 1995; Ashraf and O'leary 1996; Ashraf and Khanum 1997; Genc *et al.* 2007; Genc *et al.* 2019). Despite this, shoot Na^+ exclusion is frequently cited as the most important salt tolerance mechanism for bread wheat and other mechanisms such as tissue tolerence has received less attention (Colmer *et al.* 2005; Munns *et al.* 2006; Munns and Tester 2008; Ismail and Horie 2017). A Portuguese landrace, Mocho de Espiga Branca, was identified with up to 10× leaf Na^+ concentration and yet maintained similar growth compared to bread wheat cultivars Gladius and Scout under salinity, suggesting the importance of salinity tolerance mechanisms other than shoot Na^+ exclusion in bread wheat. Better uunderstanding of the genetics controlling the salinity tolerance of Mocho de Espiga Branca may provide opportunities to identify novel alleles playing key roles in salinity tolerance of bread wheat. Introducing these novel alleles into elite cultivars would enhance the salinity tolerance. Therefore, the aim of this PhD project was to address the following three questions:

1. How does Mocho de Espiga Branca accumulate a high leaf Na^+ concentration? (Chapter 2)
2. What are the potential genomic regions responsible for salinity tolerance traits in Mocho de Espiga Branca? (Chapter 3)
3. Can the tissue tolerance trait in Mocho de Espiga Branca be physiologically dissected? (Chapter 4)

Summary of the main findings

In this PhD study, a naturally occurring single nucleotide substitution in the *TaHKT1;5-D* gene resulted in an amino acid variation L190P in an important Na^+ transporter TaHKT1;5-D, and this variation was identified to be responsible for the high shoot Na^+ concentration in Mocho de Espiga Branca (Chapter 2). Genomic regions significantly associated with salinity tolerance were detected on chromosomes 1A, 1D, 4B and 5A for plant growth traits (PSA, AGR and RGR), and on chromosome 2A, 2B, 4D and 5D for leaf ion (Na^+, K^+ and Cl^-) concentrations (Chapter 3). Potential candidate genes within the detected QTL regions were identified, including those that encoded Na^+/H^+ antiporters, K^+ channels, Na^+/Ca^{2+} transporter, H^+-ATPase, calcineurin B-like proteins (CBLs), CBL-interacting protein kinases (CIPK) and calcium-transporting ATPase (Chapter 3). Further investigation of organic solutes known to be important in plant osmotic adjustment showed that glycine betaine, proline, sucrose, glucose and fructose are not likely responsible for any enhanced osmotic adjustment in Mocho de Espiga Branca under salinity compared to Gladius and Scout (Chapter 4).

Implications of thesis findings

Studies have reported the importance of shoot Na^+ exclusion associated with a candidate protein TaHKT1;5-D in reducing shoot Na^+ concentrations in bread wheat (Byrt *et al.* 2007; Byrt *et al.* 2014). However, accumulating high concentrations of Na^+ in the shoot due to the presence of impaired TaHKT1;5-D appeared to not affect the overall salinity tolerance in Mocho de Espiga Branca compared to Gladius and Scout (Chapter 2). This finding supports findings in a previous PhD thesis in which reducing *TaHKT1;5-D* transcript levels in bread wheat resulted in significantly greater leaf Na^+ concentrations in T_3 RNAi 1 lines, with the plant biomass and growth rate not affected by the lack of TaHKT1;5-D expression compared to its null segregants (Krishnan 2013). In a recent study, a bread wheat germplasm WM#293 was reported as having higher relative and absolute grain yield in high Na^+ conditions than the other bread wheat tested in the study (Genc *et al.* 2019). Collectively, these findings may imply that bread wheat is able

to tolerate salinity with limited Na^+ exclusion at the root and high shoot Na^+ concentrations, indicating that there must be mechanisms other than Na^+ exclusion that play important role in salinity tolerance in bread wheat.

Salinity tolerance mechanisms other than Na^+ exclusion in bread wheat

Growth maintenance of plants that accumulate high leaf Na^+ concentrations under saline conditions usually rely on tissue tolerance mechanisms (Flowers and Colmer 2008; Munns and Tester 2008; Shabala and Mackay 2011; Adolf *et al.* 2013; Flowers and Colmer 2015; Munns *et al.* 2016). Therefore, tissue tolerance mechanisms may have important roles in salinity tolerance in Mocho de Espiga Branca. The mechanisms could involve intracellular compartmentation of toxic ions, accumulation of high concentrations of compatible solutes in the cytoplasm, the ability to use inorganic solutes as cheap osmolytes and effective intercellular ion partitioning under stress (Munns and Tester 2008).

Intracellular compartmentation of toxic ions

Intracellular Na^+ sequestration in vacuoles has been reported to be important in plants to avoid damage in leaf metabolism when Na^+ is accumulated to a high concentration (Munns and Tester 2008; Roy *et al.* 2014; Munns *et al.* 2016). Na^+ sequestration is achieved by facilitating the inward flow of Na^+ into vacuoles by tonoplast Na^+/H^+ exchangers through the maintenance of an electrochemical difference across the tonoplast (Tester and Davenport 2003; Apse and Blumwald 2007; Plett and Møller 2010; Ismail and Horie 2017). In this PhD study, several *NHXs* were shortlisted as potential candidates for both plant growth and leaf ion accumulation traits (Chapter 3). This may indirectly imply the importance of effectively storing elevated Na^+ into the vacuoles in order to maintain regular metabolic processes in bread wheat under salinity stress. Cryo-scanning electron microscopy with energy-dispersive X-ray microanalysis (SEM-EDX) has been used to successfully quantify vacuolar Na^+, K^+ and Cl^- concentrations in leaf cells from salt-treated barley (James *et al.* 2006), durum wheat (James *et al.* 2006) and chickpea

(Kotula *et al.* 2019). In future studies, these approaches can be applied to detect the vacuolar Na^+ concentration in bread wheat cultivars including Mocho de Espiga Branca to examine the ability of vacuolar Na^+ compartmentation of the plant under salinity.

Accumulation of high concentrations of compatible solutes in cytoplasm

Increased vacuolar Na^+ concentrations increases the osmotic potential of other subcellular compartments including the cytosol and therefore requires accumulation of compatible solutes in the cytoplasm to balance the osmotic pressure (Munns and Tester 2008; Munns *et al.* 2016). Compatible solutes synthesized by plants for osmotic adjustment are small, electrically neutral, soluble organic compounds that are non-toxic to metabolic activities at high concentrations (Munns 2005). Some compatible solutes such as glycine betaine and proline could also act as osmoprotectants in the plants to stabilize soluble or membrane proteins in order to maintain plant growth under salinity stress (Munns 2005). Five well-known compatible solutes (glycine betaine, proline, sucrose, glucose and fructose) involved in osmotic adjustment under saline conditions were tested in this study but had no significant extra contribution in Mocho de Espiga Branca when compared to Gladius and Scout (Chapter 4). However, these results do not rule out other organic osmolytes, such as mannitol and trehalose that could contribute to osmotic adjustment in plant under salt stress.

In future research, a broader suite of salt-induced metabolites in Mocho de Espiga Branca could be analysed by the application of an untargeted method using liquid or gas chromatography–mass spectrometry (LC or GC-MS). Previously, metabolites were analysed using untargeted a GC-MS approach in two barley genotypes that differed in salt tolerance (Widodo *et al.* 2009). A total of 72 known compounds were detected in the leaf extract and the landrace Sahara with higher salt tolerance despite having a higher leaf Na^+ concentration appeared to accumulate greater levels of metabolites involved in cellular protection in the leaf compared to the less tolerant cultivar Clipper (Widodo *et al.* 2009). Therefore, analysis of a broader range of

metabolites in salt-treated Mocho de Espiga Branca could allow the identification of compatible solutes potentially involved in osmotic adjustment, as well as osmoprotectants that may play an important role in Na^+ tissue tolerance in bread wheat.

Accumulation of inorganic solutes for osmotic adjustment

Compared to the osmotic adjustment of bread wheat using organic solutes, the high leaf Na^+ in Mocho de Espiga Branca itself could be the cheapest osmolytes (Chapter 4), as synthesizing organic solutes is an energy demanding process which is accompanied by a growth penalty (Munns and Tester 2008; Munns *et al.* 2016; Asif *et al.* 2019; Munns *et al.* 2019a; Munns *et al.* 2019b; Tyerman *et al.* 2019). For instance, 3.5 moles of ATP is required to accumulate one mole of Na^+, whereas 41 moles of ATP is required for proline, 50 moles for glycine betaine and 52 moles for sucrose (Raven 1985). In Mocho de Espiga Branca, Na^+ is present at a high concentration in the leaf compared to Gladius, which may have allowed Mocho de Espiga Branca to primarily use Na^+ for the osmotic adjustment at a sub-toxic level in order to minimise the plant growth reduction rather than synthesize organic solutes (Chapter 2, 3, 4). To avoid Na^+ toxicity to cell metabolism, the elevated Na^+ needs to be carefully regulated to keep cytosolic Na^+ at a low concentration (Munns and Tester 2008). Although studies have shown that Na^+ concentration above 80 mM started to inhibit the activity of enzymes involved in cellular metabolism or photosynthesis *in vitro*, no direct measurement of cytosolic Na^+ concentration has been conducted to examine the situation in bread wheat leaf cells to date (Greenway and Osmond 1972; Osmond and Greenway 1972; Flowers and Dalmond 1992).

In Mocho de Espiga Branca (and potentially bread wheat in general), Na^+ maybe present at a relatively high concentration in the cytoplasm without having a negative impact on cell metabolism, however, how much Na^+ in the cytoplasm is toxic to cell metabolism and where the excessive Na^+ can be intracellularly stored in bread wheat remains unkown and needs to be thoroughly investigated. Although direct measurement of cytoplasmic Na^+ concentration is

challenging due to the difficulties to isolate the cytoplasmic compartments, indirect measurement have been conducted (Kronzucker and Britto 2011; Munns *et al.* 2016). For example, in a study on six bread wheat genotypes with contrasting salinity tolerance, cytosolic Na^+ concentrations have been indirectly quantified in different root cells using the CoroNa Green fluorescent dye imaging approach and it was found that cytosolic Na^+ levels in root meristem were significantly higher in salt tolerant than sensitive genotypes at 100 mM NaCl (Wu *et al.* 2015). In the future studies, this approach can be used to determine the variation in the cytosolic Na^+ concentration in leaf cells from bread wheat under salt stress and investigate its linkage to salinity tolerance.

Intercellular partitioning of Na^+, K^+ and Cl^- ions

Bread wheat could be capable of effective partitioning of Na^+, K^+ and Cl^- into different cell types and thereby maintaining ion homeostasis and photosynthetic capacity of the leaf under salt stress. Among cereals, barley is considered the most salt tolerant plant and is able to maintain growth despite accumulating high concentration of leaf Na^+ under saline conditions (Munns and Tester 2008). A study using cryo-scanning electron microscopy with energy-dispersive X-ray microanalysis (SEM-EDX) in salt-treated barley showed that the vascular Na^+ concentration was similar in mesophyll and epidermal cells, Cl^- was at high concentrations in the epidermis, and K^+ was high in mesophyll cells (James *et al.* 2006). Using the same analytical technique, a recent work in chickpea reported that the salinity tolerant genotype Genesis 836 had greater Na^+ exclusion from leaf mesophyll cells and Na^+ compartmentation in leaf epidermal compared to the salinity sensitive genotype Rupali (Kotula *et al.* 2019). However, no similar work has been reported in bread wheat.

In this PhD study, Mocho de Espiga Branca and Gladius showed similar ion partitioning patterns at the tissue level where both cultivars tended to store more Na^+ and Cl^- in the leaf sheath than in the leaf blade (Chapter 2). However, there may be differences in partitioning of

those ions at intercellular level between the two cultivars, allowing Mocho de Espiga Branca to maintain growth with a high leaf Na^+ concentration. A number of genes encoding proteins involved in ion homeostasis in plants under stress were shortlisted as potential candidates associated with salinity tolerance in Mocho de Espiga Branca (Chapter 3). Therefore, it is possible for bread wheat to effectively partition the Na^+, Cl^- and K^+ into different cell types in order to maintain plant photosynthesis and cell functions under salinity stress. Use of the same technique applied in barley and chickpea would allow understanding the intercellular Na^+, K^+ and Cl^- partitioning preference of bread wheat under salinity stress.

How can genetic control of Na^+ tissue tolerance be better detected in bread wheat?

Investigation of representative traits and development of an advanced mapping population

A list of genes was shortlisted as potential candidates associated with salinity tolerance in the QTL analysis while using a Mocho de Espiga Branca × Gladius F_2 population and phenotyping the population for 19 salinity tolerance sub-traits (Chapter 3). However, the phenotypic traits being measured in this study might not be the best sub traits to measure that represent the Na^+ tissue tolerance trait in bread wheat. Other phenotypic traits, for example vacuolar ion concentrations, could be investigated in the F_2 population using analytical techniques such as cryo-scanning electron microscopy (SEM) X-ray microanalysis or CoroNa Green florescent dye as previously mentioned if a high-throughput option is available in the future.

Once the best method for measuring tissue tolerance has been developed, advanced mapping populations such as recombinant inbred lines (RILs) and near-isogenic lines (NILs) can be developed for QTL analysis in order to detect narrower genomic regions associated with Na^+ tissue tolerance. Using conventional breeding it can take several years to generate RIL and NIL mapping populations, however, with the use of speed breeding six generations of wheat can now be grown in a year to speed up germplasm development (Watson *et al.* 2018). This is achieved by growing plants under extended photoperiod to accelerate the growth rate and

germinate the immature seed to obtain the next generation faster than traditional breeding (Watson *et al.* 2018). Speed breeding has been successfully applied in many plant species including bread wheat and for different traits including plant height and diseases resistance (Alahmad *et al.* 2018; Ghosh *et al.* 2018). Therefore, it is possible to use this approach to generate advanced mapping populations, which together with fine mapping will greatly speed up the detection of candidate genes tightly linked to the QTLs identified for Na^+ tissue tolerance in Mocho de Espiga Branca.

Use of mutational studies to identify genetics controlling Na^+ tissue tolerance mechanisms

This study identified a SNP in *TaHKT1;5-D* that is responsible for the high leaf Na^+ concentration in Mocho de Espiga Branca under salinity and developed a CAPS marker tsl2SALTY-4D tightly linked to this SNP (Chapter 2). Therefore, it is now possible to introduce the high leaf Na^+ phenotype into bread wheat accessions by altering the targeted SNP site in *TaHKT1;5-D* gene using genome editing technologies such as clustered regularly interspaced short palindromic repeats (CRISPR-Cas9) (Mao *et al.* 2013; Shan *et al.* 2013; Sander and Joung 2014; Liang *et al.* 2017), transcription activator-like effector-based nucleases (TALEN) (Bedell *et al.* 2012; Gaj *et al.* 2013; Ma *et al.* 2017) and zinc-finger nucleases (ZFN) (Wood *et al.* 2011; Gaj *et al.* 2013). The use of these technologies would enable efficient introduction of the SNP in the *TaHKT1;5-D* gene into a set of bread wheat accessions and generate plants with high leaf Na^+ concentrations and diverse growth performance under saline conditions. Phenotyping this set of bread wheat accessions for salinity tolerance and genotyping the accessions using a next-generation sequencing (NGS) platform for SNP discovery would allow performing a genome wide association analysis (GWAS) to identify SNP markers and potential candidate genes associated with Na^+ tissue tolerance in bread wheat. However, the limitation of genome editing technologies is currently the introduction of additional modifications to the targeted alleles as the core of these technologies is based on bringing genetic modifications by inducing target DNA double-strand breaks to activate the cellular DNA repair mechanisms (Gaj *et al.* 2013).

Alternatively, a Targeting Induced Local Lesions IN Genomes (TILLING) population could be generated for selecting plants that carry the SNP site resulting high leaf Na^+ concentration and the alleles potentially responsible for improved growth performance under saline condition (Gilchrist *et al.* 2006; Mejlhede *et al.* 2006; Kurowska *et al.* 2011). For instance, using ethyl methane sulphonate (EMS) treatment to the seeds from elite bread wheat cultivar, it is possible to develop a TILLING population M_1 which contains plants with a high frequency of point mutations distributed randomly in the genome. Growing M_2 plants and genotyping them using the marker tsl2SALTY-4D developed in this study (Chapter 2) would allow the identification of plants carrying the allele resulting in the high leaf Na^+ concentration. Growing the selected M_3 plants would enable phenotyping the population for salinity tolerance sub-traits such as plant growth or yield under salinity and performing a GWAS analysis as mentioned previously would provide SNP markers and potential candidates associated with Na^+ tissue tolerance in bread wheat. The mutated plants from a TILLING population are not considered genetically modified organisms (GMO) and the mutations are stable compared to other gene editing approaches (Kurowska *et al.* 2011). Therefore, the beneficial alleles or genes detected in the GWAS analysis could be backcrossed to elite cultivars to generate Na^+ tissue tolerant bread wheat in the future.

Future directions

Use of advances in functional genomics for investigating Na^+ tissue tolerance mechanisms in Mocho de Espiga Branca

Although this study shortlisted many potential expressed genes for salinity tolerance in Mocho de Espiga Branca, the database used for the gene identification was not originally generated from salt-treated plants (Chapter 3). In future studies, a transcriptomic approach such as RNA-sequencing (RNA-seq) could be applied to investigate gene expression in Mocho de Espiga Branca subjected to salt stress. However, this approach should be used with care, as gene expression does not directly imply the protein being encoded by the gene will be functional

(Chapter 2). In this study, no significant difference in *TaHKT1;5-D* expression was found between Mocho de Espiga Branca and Gladius (Chapter 2). The functional difference in the TaHKT1;5-D transporter between the two cultivars was revealed from the whole gene sequencing and the subsequent electrophysiological studies and protein modelling. Therefore, incorporating the RNA-seq analysis with whole genome sequencing of Mocho de Espiga Branca should be considered in the future studies. This will enable the researchers to compare both the expression and sequence of the potential genes responsible for salinity tolerance including Na^+ tissue tolerance in Mocho de Espiga Branca.

Use of evolutionary studies

In this study, among more than 70 bread wheat accessions Mocho de Espiga Branca was identified as being the only cultivar which carries the TaHKT1;5-D L190P variation and accumulates a significantly higher leaf Na^+ under salinity stress (Chapter 2). Recently a research group identified that more than 45% of modern cultivated barley accessions carry HvHKT1;5 P189 which is likely to be the major determinant of the high shoot and grain Na^+ in barley (Houston *et al*., unpublished). This could raise an opposite assumption to modern bread wheat cultivars in which the TaHKT1;5-D L190P variation somehow was lost in the breeding practices with preference to selecting cultivars accumulating low Na^+ in the shoot. Similar to barley, it would be interesting to study the evolution of TaHKT1;5-D L190P variation across many bread wheat accessions, which could potentially provide more information from an evolutionary perspective to answer the question why Mocho de Espiga Branca carries TaHKT1;5-D L190P variation and is able to tolerate high shoot Na^+ under salinity stress.

Translation of the Na^+ tissue tolerance trait in bread wheat from the laboratory to farm

The ultimate aim of studying salinity tolerance of any cereal plants including bread wheat in both the laboratory and glasshouse is to translate research findings to practical outcomes, such as increase grain yields in saline paddocks. Often saline agricultural land not only contains

salinity but also contains multiple other biotic and abiotic stresses, such as sodicity and drought (Rengasamy 2010; Asif *et al.* 2019). To develop a Na^+ tissue tolerant bread wheat cultivar using Mocho de Espiga Branca there is the need to develop germplasm containing the TaHKT1;5-D L190P variant that is also tolerant of these other multiple constraints and to evaluate this under field conditions.

Concluding remarks

In this PhD study, the detection of an impaired Na^+ transporter TaHKT1;5-D responsible for the increased shoot Na^+ concentration in Mocho de Espiga Branca highlighted that mechanisms other than Na^+ exclusion are also important in the salinity tolerance of bread wheat. Overall, the identification of the TaHKT1;5-D variant in Mocho de Espiga Branca linked to the high leaf Na^+ concentration of this landrace and the development of a CAPS genetic marker to track the SNP variation of *TaHKT1;5-D* developed in this PhD will accelerate the development of more elite salt tolerant bread wheat cultivars in the future. Furthermore, the detailed genetic and physiological dissection of salinity tolerance traits in Mocho de Espiga Branca will help to progress research towards increasing our understanding of tissue tolerance in bread wheat.

References

Adolf, VI, Jacobsen, SE, Shabala, S (2013) Salt tolerance mechanisms in quinoa (*Chenopodium quinoa* Willd.). *Environmental and Experimental Botany* **92**, 43-54.

Alahmad, S, Dinglasan, E, Leung, KM, Riaz, A, Derbal, N, Voss-Fels, KP, Able, JA, Bassi, FM, Christopher, J, Hickey, LT (2018) Speed breeding for multiple quantitative traits in durum wheat. *Plant Methods* **14**, 36.

Apse, MP, Blumwald, E (2007) Na^+ transport in plants. *FEBS Letters* **581**, 2247-2254.

Ashraf, M, Khanum, A (1997) Relationship between ion accumulation and growth in two spring wheat lines differing in salt tolerance at different growth stages. *Journal of Agronomy and Crop Science* **178**, 39-51.

Ashraf, M, O'leary, J (1996) Responses of some newly developed salt-tolerant genotypes of spring wheat to salt stress: 1. Yield components and ion distribution. *Journal of Agronomy and Crop Science* **176**, 91-101.

Asif, MA, Pearson, AS, Schilling, RK, Roy, SJ (2019) Opportunities for developing salt-tolerant wheat and barley varieties. *Annual Plant Reviews* **2**, 1-61.

Bedell, VM, Wang, Y, Campbell, JM, Poshusta, TL, Starker, CG, Krug II, RG, Tan, W, Penheiter, SG, Ma, AC, Leung, AY (2012) *In vivo* genome editing using a high-efficiency TALEN system. *Nature* **491**, 114-118.

Byrt, CS, Platten, JD, Spielmeyer, W, James, RA, Lagudah, ES, Dennis, ES, Tester, M, Munns, R (2007) HKT1;5-like cation transporters linked to Na^+ exclusion loci in wheat, *Nax2* and *Kna1*. *Plant Physiology* **143**, 1918-1928.

Byrt, CS, Xu, B, Krishnan, M, Lightfoot, DJ, Athman, A, Jacobs, AK, Watson-Haigh, NS, Plett, D, Munns, R, Tester, M, Gilliham, M (2014) The Na^+ transporter, TaHKT1;5-D, limits shoot Na^+ accumulation in bread wheat. *The Plant Journal* **80**, 516-526.

Chhipa, B, Lal, P (1995) Na^+/K^+ ratios as the basis of salt tolerance in wheat. *Australian Journal of Agricultural Research* **46**, 533-539.

Colmer, TD, Munns, R, Flowers, TJ (2005) Improving salt tolerance of wheat and barley: future prospects. *Australian Journal of Experimental Agriculture* **45**, 1425-1443.

Flowers, T, Dalmond, D (1992) Protein synthesis in halophytes: the influence of potassium, sodium and magnesium in vitro. *Plant and Soil* **146**, 153-161.

Flowers, TJ, Colmer, TD (2008) Salinity tolerance in halophytes. *New Phytologist* **179**, 945-963.

Flowers, TJ, Colmer, TD (2015) Plant salt tolerance: adaptations in halophytes. *Annals of Botany* **115**, 327-331.

Gaj, T, Gersbach, CA, Barbas III, CF (2013) ZFN, TALEN, and CRISPR/Cas-based methods for genome engineering. *Trends in Biotechnology* **31**, 397-405.

Genc, Y, McDonald, GK, Tester, M (2007) Reassessment of tissue Na^+ concentration as a criterion for salinity tolerance in bread wheat. *Plant Cell & Environment* **30**, 1486-1498.

Genc, Y, Oldach, K, Verbyla, AP, Lott, G, Hassan, M, Tester, M, Wallwork, H, McDonald, GK (2010) Sodium exclusion QTL associated with improved seedling growth in bread wheat under salinity stress. *Theoretical and Applied Genetics* **121**, 877-894.

Genc, Y, Taylor, J, Lyons, GH, Li, Y, Cheong, J, Appelbee, M, Oldach, K, Sutton, T (2019) Bread wheat with high salinity and sodicity tolerance. *Frontiers in Plant Science* **10**, 1280.

Ghosh, S, Watson, A, Gonzalez-Navarro, OE, Ramirez-Gonzalez, RH, Yanes, L, Mendoza-Suárez, M, Simmonds, J, Wells, R, Rayner, T, Green, P (2018) Speed breeding in growth chambers and glasshouses for crop breeding and model plant research. *Nature Protocols* **13**, 2944–2963.

Gilchrist, EJ, Haughn, GW, Ying, CC, Otto, SP, Zhuang, J, Cheung, D, Hamberger, B, Aboutorabi, F, Kalynyak, T, Johnson, L (2006) Use of Ecotilling as an efficient SNP discovery tool to survey genetic variation in wild populations of *Populus trichocarpa*. *Molecular Ecology* **15**, 1367-1378.

Greenway, H, Osmond, C (1972) Salt responses of enzymes from species differing in salt tolerance. *Plant Physiology* **49**, 256-259.

Hanin, M, Ebel, C, Ngom, M, Laplaze, L, Masmoudi, K (2016) New insights on plant salt tolerance mechanisms and their potential use for breeding. *Frontiers in Plant Science* **7**, 1787.

Ismail, AM, Horie, T (2017) Genomics, physiology, and molecular breeding approaches for improving salt tolerance. *Annual Review of Plant Biology* **68**, 405-434.

James, RA, Munns, R, Von Caemmerer, S, Trejo, C, Miller, C, Condon, T (2006) Photosynthetic capacity is related to the cellular and subcellular partitioning of Na^+, K^+ and Cl^- in salt-affected barley and durum wheat. *Plant Cell & Environment* **29**, 2185-2197.

Kotula, L, Clode, PL, Jimenez, JDLC, Colmer, TD (2019) alinity tolerance in chickpea is associated with the ability to 'exclude' Na^+ from leaf mesophyll cells. *Journal of Experimental Botany* **70**, 4991-5002.

Krishnan, M (2013) Cell type-specific manipulation of salt tolerance genes in wheat and barley. PhD thesis, The University of Adelaide.

Kronzucker, HJ, Britto, DT (2011) Sodium transport in plants: a critical review. *New Phytologist* **189**, 54-81.

Kurowska, M, Daszkowska-Golec, A, Gruszka, D, Marzec, M, Szurman, M, Szarejko, I, Maluszynski, M (2011) TILLING-a shortcut in functional genomics. *Journal of Applied Genetics* **52**, 371.

Liang, Z, Chen, K, Li, T, Zhang, Y, Wang, Y, Zhao, Q, Liu, J, Zhang, H, Liu, C, Ran, Y (2017) Efficient DNA-free genome editing of bread wheat using CRISPR/Cas9 ribonucleoprotein complexes. *Nature Communications* **8**, 14261.

Ma, J, Xiang, H, Donnelly, DJ, Meng, F-R, Xu, H, Durnford, D, Li, X-Q (2017) Genome editing in potato plants by agrobacterium-mediated transient expression of transcription activator-like effector nucleases. *Plant Biotechnology Reports* **11**, 249-258.

Mao, Y, Zhang, H, Xu, N, Zhang, B, Gou, F, Zhu, J-K (2013) Application of the CRISPR–Cas system for efficient genome engineering in plants. *Molecular Plant* **6**, 2008-2011.

Mejlhede, N, Kyjovska, Z, Backes, G, Burhenne, K, Rasmussen, SK, Jahoor, A (2006) EcoTILLING for the identification of allelic variation in the powdery mildew resistance genes mlo and Mla of barley. *Plant Breeding* **125**, 461-467.

Munns, R (2005) Genes and salt tolerance: bringing them together. *New Phytologist* **167**, 645-663.

Munns, R, Day, DA, Fricke, W, Watt, M, Arsova, B, Barkla, BJ, Bose, J, Byrt, CS, Chen, Z-H, Foster, KJ, Gilliham, M, Henderson, SW, Jenkins, CLD, Kronzucker, HJ, Miklavcic, SJ, Plett, D, Roy, SJ, Shabala, S, Shelden, MC, Soole, KL, Taylor, NL, Tester, M, Wege, S, Wegner, LH, Tyerman, SD (2019a) Energy costs of salt tolerance in crop plants. *New Phytologist. doi.org/10.1111/nph.15864*.

Munns, R, James, RA, Gilliham, M, Flowers, TJ, Colmer, TD (2016) Tissue tolerance: an essential but elusive trait for salt-tolerant crops. *Functional Plant Biology* **43**, 1103-1113.

Munns, R, James, RA, Lauchli, A (2006) Approaches to increasing the salt tolerance of wheat and other cereals. *Journal of Experimental Botany* **57**, 1025-1043.

Munns, R, Passioura, JB, Colmer, TD, Byrt, CS (2019b) Osmotic adjustment and energy limitations to plant growth in saline soil. *New Phytologist. doi: 10.1111/nph.15862.*

Munns, R, Tester, M (2008) Mechanisms of salinity tolerance. *Annual Review of Plant Biology* **59**, 651-681.

Osmond, C, Greenway, H (1972) Salt responses of carboxylation enzymes from species differing in salt tolerance. *Plant Physiology* **49**, 260-263.

Plett, DC, Møller, IS (2010) Na^+ transport in glycophytic plants: what we know and would like to know. *Plant Cell & Environment* **33**, 612-626.

Raven, JA (1985) Regulation of pH and generation of osmolarity in vascular plants: a cost-benefit analysis in relation to efficiency of use of energy, nitrogen and water. *New Phytologist* **101**, 25-77.

Rengasamy, P (2010) Soil processes affecting crop production in salt-affected soils. *Functional Plant Biology* **37**, 613-620.

Roy, SJ, Negrão, S, Tester, M (2014) Salt resistant crop plants. *Current Opinion in Biotechnology* **26**, 115-124.

Sander, JD, Joung, JK (2014) CRISPR-Cas systems for editing, regulating and targeting genomes. *Nature Biotechnology* **32**, 347-355.

Shabala, S, Mackay, A (2011) Ion transport in halophytes. In 'Plant Responses to Drought and Salinity Stress: Developments in a Post-Genomic Era.' (Ed. I Turkan.) Vol. 57 pp. 151-199. (Academic Press Ltd-Elsevier Science Ltd: London)

Shan, Q, Wang, Y, Li, J, Zhang, Y, Chen, K, Liang, Z, Zhang, K, Liu, J, Xi, JJ, Qiu, J-L (2013) Targeted genome modification of crop plants using a CRISPR-Cas system. *Nature Biotechnology* **31**, 686-688.

Tester, M, Davenport, R (2003) Na^+ tolerance and Na^+ transport in higher plants. *Annals of Botany* **91**, 503-527.

Tyerman, SD, Munns, R, Fricke, W, Arsova, B, Barkla, BJ, Bose, J, Bramley, H, Byrt, C, Chen, ZH, Colmer, TD, Cuin, T, Day, DA, Foster, KJ, Gilliham, M, Henderson, SW, Horie, T, Jenkins, CLD, Kaiser, BN, Katsuhara, M, Plett, D, Miklavcic, SJ, Roy, SJ, Rubio, F, Shabala, S, Shelden, M, Soole, K, Taylor, NL, Tester, M, Watt, M, Wege, S, Wegner, LH, Wen, ZY (2019) Energy costs of salinity tolerance in crop plants. *New Phytologist* **221**, 25-29.

Watson, A, Ghosh, S, Williams, MJ, Cuddy, WS, Simmonds, J, Rey, MD, Hatta, MAM, Hinchliffe, A, Steed, A, Reynolds, D, Adamski, NM, Breakspear, A, Korolev, A, Rayner, T, Dixon, LE, Riaz, A, Martin, W, Ryan, M, Edwards, D, Batley, J, Raman, H, Carter, J, Rogers, C, Domoney, C, Moore, G, Harwood, W, Nicholson, P, Dieters, MJ,

DeLacy, IH, Zhou, J, Uauy, C, Boden, SA, Park, RF, Wulff, BBH, Hickey, LT (2018) Speed breeding is a powerful tool to accelerate crop research and breeding. *Nature Plants* **4**, 23-29.

Widodo, Patterson, JH, Newbigin, E, Tester, M, Bacic, A, Roessner, U (2009) Metabolic responses to salt stress of barley (*Hordeum vulgare* L.) cultivars, Sahara and Clipper, which differ in salinity tolerance. *Journal of Experimental Botany* **60**, 4089-4103.

Wood, AJ, Lo, T-W, Zeitler, B, Pickle, CS, Ralston, EJ, Lee, AH, Amora, R, Miller, JC, Leung, E, Meng, X (2011) Targeted genome editing across species using ZFNs and TALENs. *Science* **333**, 307-307.

Wu, HH, Shabala, L, Liu, XH, Azzarello, E, Zhou, M, Pandolfi, C, Chen, ZH, Bose, J, Mancuso, S, Shabala, S (2015) Linking salinity stress tolerance tissue-specific Na^+ sequestration in wheat roots. *Frontiers in Plant Science **6***, 71.